Studies of Bacterial and Insect Cytochromes P450 in Degradation of Pesticides

by

Nicole Gkaleni

B.Sc., Technological Educational Institute of Peloponnese, 2017

Thesis Submitted in Partial Fulfillment of the

Requirements for the Degree of

Master of Science

in the

Department of Chemistry

Faculty of Science

© Nicole Gkaleni 2021

SIMON FRASER UNIVERSITY

Summer 2021

Declaration of Committee

Name:	**Nicole Gkaleni**
Degree:	**Master of Science (Chemistry)**
Title:	***Studies of Bacterial and Insect Cytochromes P450 in Degradation of Pesticides***

Committee: **Chair: Paul Li**
Professor, Chemistry

Erika Plettner
Supervisor
Professor, Chemistry

Leah Bendell
Committee Member
Professor, Biological Sciences

Tim Storr
Committee Member
Professor, Chemistry

George Agnes
Examiner
Professor, Chemistry

Abstract

Cytochromes P450 is a group of heme-containing enzymes with diverse catalytic activity that can be used for the biodegradation of environmental chemicals. Cytochrome P450$_{cam}$ (CYP101A1) from the soil bacterium *Pseudomonas putida* is known for hydroxylating camphor. Here, I have investigated the dehalogenation ability of two P450$_{cam}$ mutants, ES6 (G120S) and ES7 (V247F/D297N/K314E), in comparison to the wild-type (WT) enzyme. Six hexachlorinated persistent organic pollutants (POP), namely endosulfan (ES), ES diol, ES lactone, ES ether, ES sulfate and heptachlor, were tested since they are similarly structured to the native substrate. The mutated enzymes were capable of converting the selected substrates to phenols and o-quinones, which were detected using a colorimetric assay with 4-aminoantipyrine (4-AAP). Kinetic studies and statistical analysis were carried out and it was found that both ES6 and ES7 are significantly more active than the WT, with the highest activity noticed against ES ether and heptachlor.

The western honey bee, *Apis mellifera*, is a vital pollinator of the ecosystem, however, its being threatened by the ectoparasitic mite, *Varroa destructor*. This pest is becoming immune towards commercially available pesticides, thus, new control agents have been previously synthesized that showed miticidal effects. Fortunately, insect cytochromes P450 are known to be responsible for the metabolism of such xenobiotics. Here, I have tested the ability of three potent dialkoxybenzene compounds, namely 1-allyloxy-4-propoxybenzene (**3c**{*3,6*}), 1,4-dipropoxybenzene (**3c**{*3,3*}) and 1,4-diallyloxybenzene (**3c**{*6,6*}), to get degraded by honey bee cytochromes P450. The formation of the dealkylated products was detected in abdomen extracts using a colorimetric assay with 4-aminoantipyrine (4-AAP). Kinetic studies and statistical analysis showed a downregulation of detectable P450 activity in the treated vs. the untreated extracts. Gas chromatography-mass spectrometry (GC-MS) quantitative assays were carried out and three dealkylated products were found, hydroquinone (HQ), 1-hydroxy-4-propoxybenzene (**2c**{*3*}) and 1-hydroxy-4-allyloxybenzene (**2c**{*6*}).

Keywords: Cytochrome P450; biodegradation; persistent organic pollutant; enzyme kinetics; *Apis mellifera*; *Varroa destructor*

Dedicated to my sister and parents for always believing in me.

Acknowledgements

First and foremost, I would like to acknowledge and sincerely thank my supervisor, Dr. Erika Plettner, for giving me the opportunity to work with her, as without her guidance and mentorship, this would not have been possible. I appreciate tremendously the trust she had in me that made me challenge myself every single day and helped me become a better researcher.

I want to extent my gratitude towards my supervisory committee, Dr. Tim Storr and Dr. Leah Bendell, for being kind and supporting, and mostly for their helpful suggestions that contributed to improving my work. I am also thankful towards our graduate assistant, Natalie Fournier, for always being there to answer every question regarding my studies at Simon Fraser University, and thesis assistant, Anise Ladha, for helping me put together this thesis.

From my group members, I acknowledge Dr. Abdul Rehman for providing me with the mutated enzymes, and most importantly, Priyadarshini Balaraman for giving me the wild-type enzyme, training me, and assisting me whenever I needed some extra help. Additionally, I want to thank Dr. Mailyn Terrado and Soniya Dawdani for their thoughtful comments and willingness to assist me despite working on different projects. Moreover, I would like to acknowledge Dr. Govardhana Pinnelli for providing me with the styrene maleic acid, and especially thank Dr. Jorge Macias-Samano for not only giving me fresh bees to work with, but for his useful life advice, smiles and words of encouragement throughout this journey. I also want to express my appreciation towards Ashna Aulakh, for her support, companionship and understanding, but mostly for her spontaneity, that made this experience so much better.

I wish to express my gratitude towards my family and especially my parents, Georgios Gkalenis and Lygeri Kaymenou, and my sister, Marianna Gkaleni, for always checking up on me to make sure I was doing okay and cheering me up. Finally, I am beyond grateful to all my dear friends, for keeping me company despite the time difference, and particularly Athina Magklara, my best friend, who was by my side whenever I really needed to talk to someone.

Table of Contents

List of Tables

List of Figures

List of Acronyms

2c{*3*}	1-hydroxy-4-propoxy benzene
2c{*6*}	1-hydroxy-4-allyloxy benzene
3c{*1,1*}	1,4-dimethoxybenzene
3c{*3,3*}	1,4-dipropoxybenzene
3c{*3,6*}	1-allyloxy-4-propoxybenzene
3c{*6,6*}	1,4-diallyloxybenzene
4-AAP	4-Aminoantipyrine
ABC	ATP-binding cassette transporter
AchE	Acetylcholine esterase
AcOH	Acetic acid
AEBSF	4-(2-aminoethyl)benzenesulfonyl fluoride
ANOVA	Analysis of variance
APS	Ammonium persulfate
BSA	Bovine serum albumin
CL	Confidence level
CO	Carbon monoxide
COE	Carboxylesterase
Cpd I	Compound I
Cpdd 0	Compound 0
CPR	Cytochrome P450 reductase
CYP	Cytochrome P450
Cys	Cysteine
DDT	Dichlorodiphenyltrichloroethane
DEET	N,N-Diethyl-3-methylbenzamide
DNA	Deoxyribonucleic acid
E. coli	*Escherichia coli*
EDTA	Ethylenediaminetetraacetic acid
ES	Endosulfan

ET	Electron transport
EtOAc	Ethyl acetate
EtOH	Ethanol
FAD	Flavin adenine dinucleotide
FdR	Ferredoxin reductase
FDR	False discovery rate
FdX	Ferredoxin
FMN	Flavin mononucleotide
G6P	Glucose-6-phosphate
G6PDH	Glucose-6-phosphate dehydrogenase
GC-MS	Gas chromatography – mass spectrometry
GST	Glutathione S-transferase
Hex	Hexane
His	Histidine
HQ	Hydroquinone
HRP	Horseradish peroxidase
IPTG	Isopropyl β-D-1-thiogalactopyranoside
kDa	kilodalton
LB	Luria-Bertani
LIC	Ligation-independent cloning vector
Mb	Mega bases
m-CPBA	meta-chloroperoxybenzoic acid
MeOH	Methanol
MOE	Molecular operating environment
NAD^+	Nicotinamide adenine dinucleotide - oxidized
NADH	Nicotinamide adenine dinucleotide - reduced
$NADP^+$	Nicotinamide adenine dinucleotide phosphate - oxidized
NADPH	Nicotinamide adenine dinucleotide phosphate - reduced
NMR	Nuclear magnetic resonance

NMWL	Nominal molecular weight limit
P. putida	*Pseudomonas putida*
PCR	Polymerase chain reaction
PDB	Protein data band
PdR	Putidaredoxin reductase
PdX	Putidaredoxin
PMSF	Phenylmethylsulfonyl fluoride
PTFE	Tissue Grinder Potter-Elvehjem
RCSB	Research collaboratory for structural bioinformatics
RNA	Ribonucleic acid
rpm	Rounds per minute
S.E.	Standard error
SDS-PAGE	Sodium dodecyl sulphate - Polyacrylamide gel electrophoresis
SeSaM	Sequence saturated mutagenesis
SMA	Styrene maleic acid
SOC	Super optimal broth
SRS	Substrate recognition region
T. ni	*Trichoplusia ni*
TEMED	N,N,N′,N′-Tetramethylethylenediamine
Tris	Tris(hydroxymethyl)aminomethane
UGT	Uridine 5'-diphospho-glucuronosyltransferase
UV-Vis	Ultraviolet-visible spectroscopy
WT	Wild-type
δ-ALA	δ-Aminolevulinic acid

Chapter 1.

Introduction

1.1. Introduction to Cytochromes P450

Cytochromes P450 (CYP450s) are hemoproteins responsible for catalyzing a diverse range of reactions. They belong to the large superfamily of oxidoreductases and are part of the subclass of oxygenases, specifically, the sub-category of monooxygenases. All CYP450s have as a prosthetic group an iron porphyrin (heme) located in their active site (distal side) and a conserved cysteine thiolate ligand (proximal side). Cytochromes P450 are versatile enzymes with enormous biocatalytic potential and can accept a broad range of substrates. They usually act as terminal monooxygenases in various reactions and are known for transferring an oxygen atom into the substrate in the presence of molecular dioxygen, forming a hydroxylated product and resulting in the concomitant reduction and release of the other oxygen as water (Montellano, 2005). The earliest reference on these enzymes dates back to the 1940s, where R. T. Williams described through *in vivo* studies on animals that they were responsible for the metabolism of xenobiotics (Williams, 1947).

Their name was coined in the 1960s when T. Omura and R. Sato reported that the reduced form of the hemoprotein which absorbs at 420 nm, exhibits a 450 nm peak when it is saturated with carbon monoxide (Omura & Sato, 1964). In their abbreviation (P450), P stands for pigment since they have a heme, and 450 relates to their aforementioned characteristic so-called Soret peak at 450 nm.

1.1.1. Cytochrome P450 classification systems

Cytochromes P450 catalyze multiple reactions, thus, a systematic nomenclature is being used based on their structural homology instead of the reactions they catalyze. The genes of this family are abbreviated as CYP, a number is then added which designates the particular family that involves proteins with > 40% sequence identity (e.g CYP101). Then, a letter is used to indicate the subfamily based on a > 55% sequence identity (e.g

1

CYP101A), and finally, a number is added to the end designating the particular gene/protein (e.g. CYP101A1) (McDonnell & Dang, 2013; Nelson, 2009). According to the Cytochrome P450 Engineering Database (CYPED), as of 2021, there are 317 CYP superfamilies, 1701 homologous subfamilies, and 52675 sequences, and the number of sequences keeps growing every year (IBTB, 2021).

The various families of these proteins are known to have < 20% sequence conservation with their general fold and topography, as well as the monooxygenase reaction, being conserved in all of them. However, their substrate recognition regions (SRS) are highly flexible, enabling them to have great catalytic potential (Gotoh, 1992). To perform those various chemical reactions, the majority needs a redox partner source for transferring the redox equivalents. Thus, another way to classify P450s is through their Electron Transport (ET) system (Degtyarenko & Kulikova, 2001; McLean et al., 2005). According to the bibliography, different classification systems categorize P450s from three up to ten types. There are at least five major classes, thus, only these will be discussed here along with their "subclasses" (Hannemann et al., 2007; Li et al., 2020; Munro et al., 2007; Roberts et al., 2002; Sakaki, 2012; Urlacher & Girhard, 2012; L.-H. Xu & Du, 2018).

Class I contains most bacterial and mitochondrial P450 systems (Figure 1.1, Ia, Ib). It is composed of three common elements: 1) a FAD-containing reductase (FdR) which is responsible for transferring electrons from NAD(P)H to 2) an iron-sulfur ferredoxin (FdX) and finally to 3) cytochrome P450. The most notable example of a bacterial system is cytochrome P450$_{cam}$ (CYP101A1) from *Pseudomonas putida* (Tyson et al., 1972), and of a mitochondrial system is cytochrome P450$_{scc}$ (CYP11A1) (Hannemann et al., 2007).

Class II contains microsomal P450s from eukaryotic organisms (Figure 1.1, II). It consists of two common elements: 1) a NAD(P)H cytochrome P450 reductase (CRP) containing FMN and FAD and 2) cytochrome P450. Examples involve mammalian, plant, fungal, and insect P450s such as CYP2C5 (rabbit) (Munro et al., 2007). However, there is an exemption of a prokaryotic cytochrome P450$_{sca}$ (CYP105A3) found in the bacterium *Streptomyces carbophilus* (Hannemann et al., 2007).

The Class III systems do not depend on redox partners; they are self-sufficient and contains two elements that are fused, 1) a CPR and 2) a cytochrome P450 which is linked to it through its C-terminus domain (Figure 1.1, III). This class is represented by cytochrome P450BM3 (CYP102A1) from *Bacillus megaterium* (Whitehouse et al., 2012).

Class IV is also self-sufficient and contains fusion systems that consist of "two" components, 1) an FMN-Fe_2S_2 flavin-ferredoxin reductase which is linked to 2) cytochrome P450 (Figure 1.1, IV). One of the first reported systems here is the bacterial cytochrome P450$_{rhf}$ (CYP116B2) from *Rhodococcus sp.* (Roberts et al., 2002).

Class V involves a special case of P450s that are self-sufficient and consist of a single component, cytochrome P450 (Figure 1.1, Va, Vb). These can be cytosolic soluble P450s such as cytochrome P450$_{nor}$ (CYP55A1) from *Fusarium oxysporum* where the electrons are transferred directly to the heme domain from NADH (Daiber et al., 2008), or membrane-bound, such as cytochrome P450$_{TxA}$ (Hsu et al., 1999).
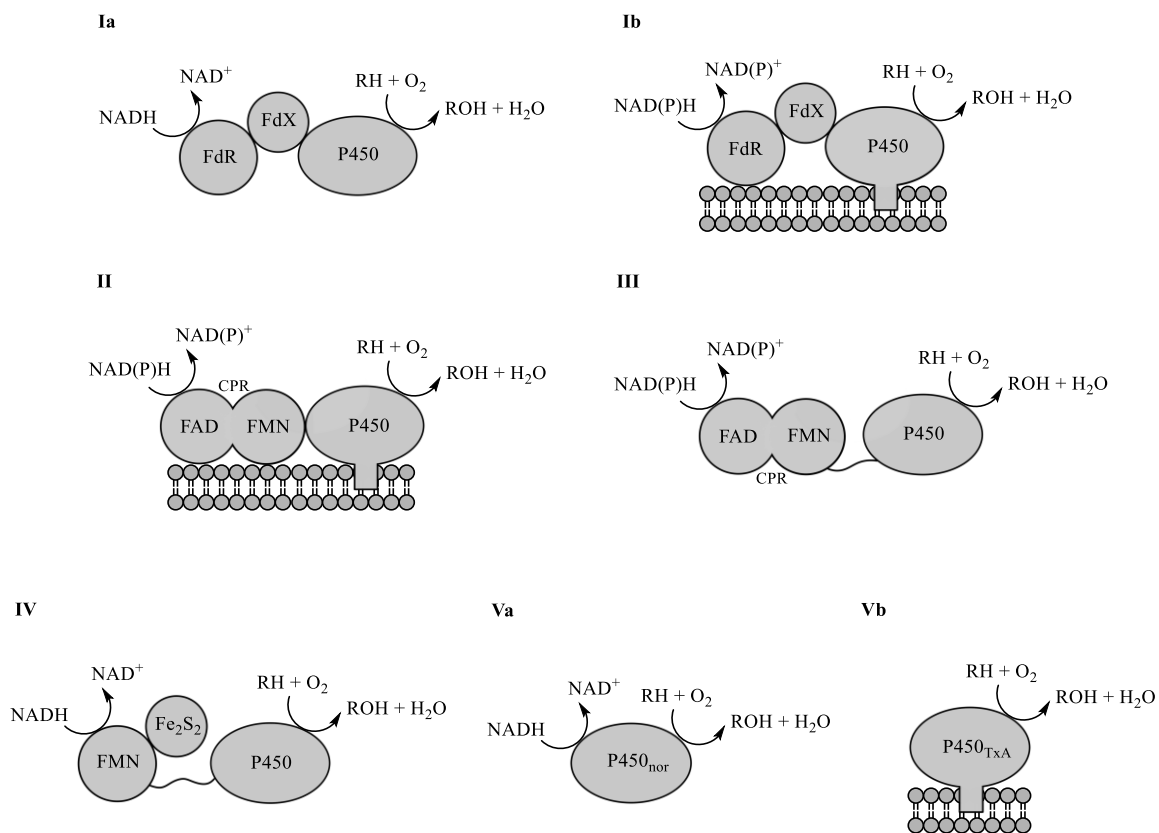
Figure 1.1. **Ia) Class I bacterial P450 with the whole system being soluble; Ib) Class I mitochondrial P450 where only FdX is soluble, and the other components are membrane-bound; II) Class II membrane-bound microsomal P450s; III) Class III self-sufficient soluble CPR-P450 fusion system; IV) Class IV self-sufficient soluble FMN/Fe₂S₂-P450 fusion system; Va) Class V self-sufficient singular P450s with soluble, NADH-dependant system; Vb) Class V self-sufficient singular P450s, membrane-bound.**

1.1.2. The catalytic cycle of cytochrome P450

The catalytic cycle of cytochrome P450 consists of multiple steps (Figure 1.2), starting from the resting state of the enzyme in its ferric form (Fe^{3+}) **1** which is coordinated by an axially bound water molecule (distal side) as its sixth ligand, the thiol of a conserved cysteine residue. This state is characterized as low spin since the iron d-orbital splitting energy is high, the five electrons of the ferric 3d-shell pair up in the lower orbitals instead of going into the higher ones. So, in the final complex, there will be one unpaired electron, thus, the spin will be S=1/2 (Schaller, 2006). In that state, the heme is known for having a trough between 390 to 410 nm in the UV/visible spectrum, and a peak between 425-435

nm (Jefcoate, 1978). The water molecule is then displaced by the substrate (R-H), resulting in a penta-coordinated ferric species (Fe^{3+}) **2**. This causes an electron reorganization as the system shifts to a high spin state where the iron d-orbital splitting energy is low, causing the electrons to go into the higher orbitals this time. As a result, the system ends up with five unpaired electrons and a spin of $S=5/2$ (Schaller, 2006). This ligand-induced shift from the low spin state to the high is known as the Type I spectral shift, with the heme showing a trough at approximately 420 nm and a peak around 385 nm (Jefcoate, 1978). A single electron is then delivered by the redox partner proteins, reducing the ferric iron (Fe^{3+}) to a ferrous state (Fe^{2+}) **3**, which in turn binds to molecular dioxygen (O_2) and forms a ferric-superoxo intermediate **4**. Another electron is delivered again by the redox partners, helping the reduction of the dioxygen to give a ferric-peroxo intermediate **5** which is consecutively protonated, leading to a ferric-hydroperoxo complex **6** that is referred as Compound 0 (**Cpd 0**) (Davydov et al., 2001). A second protonation results in the cleavage of the oxygen-oxygen bond of **6** and release of water, forming the ferryl-oxo species **7** that is referred as Compound I (**Cpd I**) (Montellano, 2005). Cpd I is basically a radical cation that is considered the most reactive intermediate in the catalytic cycle (Rittle & Green, 2010) and is identified by its characteristic Soret peak at around 370 nm and a porphyrin π-cation band at 690 nm (Luthra et al., 2011). An oxygen rebound mechanism follows (Groves et al., 1978; Groves & McClusky, 1976) that involves radical recombination by abstraction of a hydrogen from the substrate to form **8** which shows a Soret peak at around 415-425 nm (Groves et al., 1978). The substrate is then oxidized leading to the release of the hydroxylated product (R-OH) **9**. Finally, as the product dissociates, the enzyme reverts to its initial resting state **1** as a water molecule binds to it, and the catalytic cycle goes on again.

Nevertheless, the catalytic cycle is not a linear process and can be hindered by three uncoupling pathways which are unproductive in terms of substrate turnover (Denisov et al., 2005). These are: a) oxidase pathway, where during the radical reaction, **7** can utilize two reducing equivalents from NAD(P)H and FdR forming two water molecules instead of oxygenating the substrate, b) peroxidase pathway, during which the hydroperoxide anion of **6** is released forming H_2O_2, and c) autoxidation pathway, which results in the production of a superoxide anion from **4**. All these pathways lead back to the high spin state **2** but

synthesized oxidants such as *meta*-chloroperoxybenzoic acid (*m*-CPBA), can be used to prevent this by generating Cpd I without the need of NAD(P)H or redox partners (Jung, 2011).
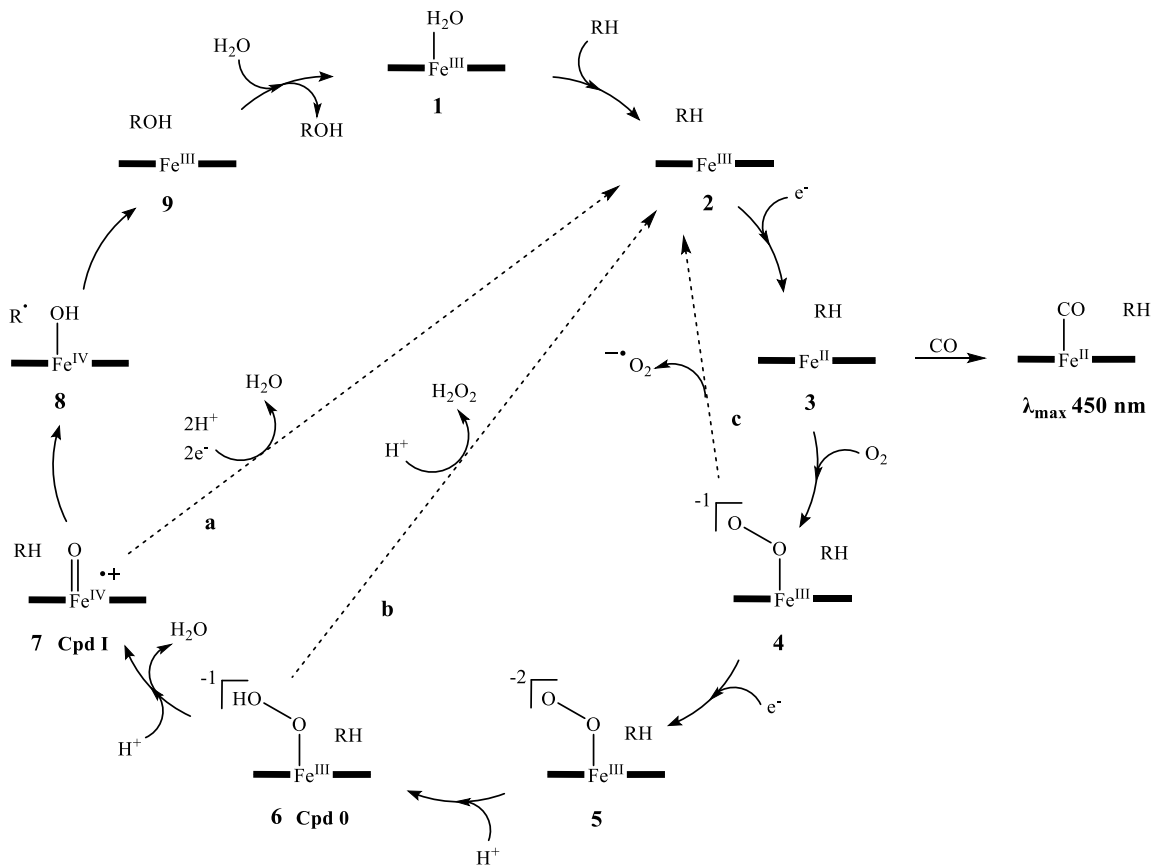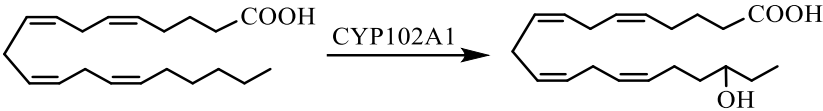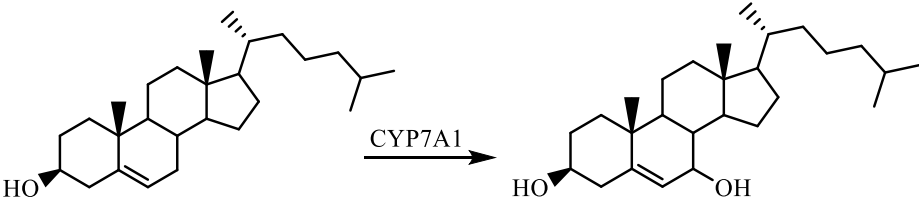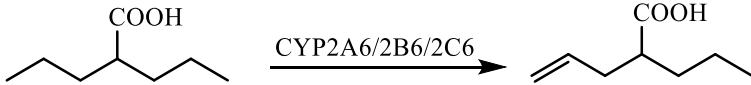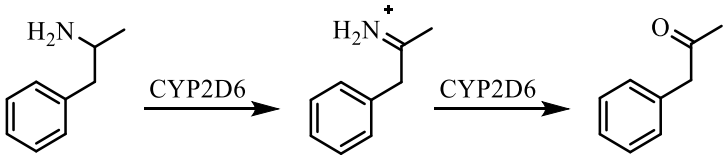
Figure 1.2. **Cytochrome P450 catalytic cycle. The different species depicted are 1-9. RH is the substrate (ROH oxidized) and the Fe atom with the bold horizontal lines is the heme moiety. The electrons (e⁻) are supplied from the redox partners. Cpd refers to Compound 0 and I. The uncoupling reactions are shown as a) oxidase, b) peroxidase and c) autooxidation pathway. CO is the carbon monooxide.**
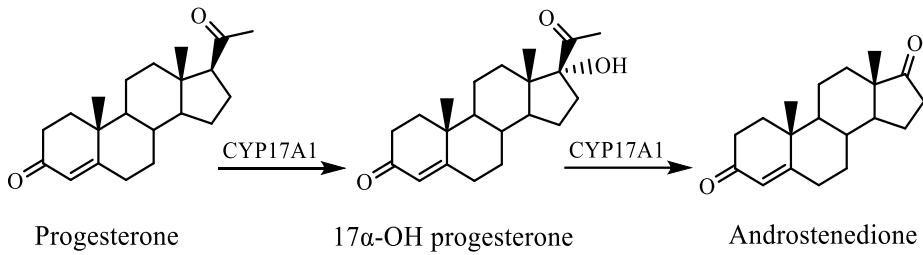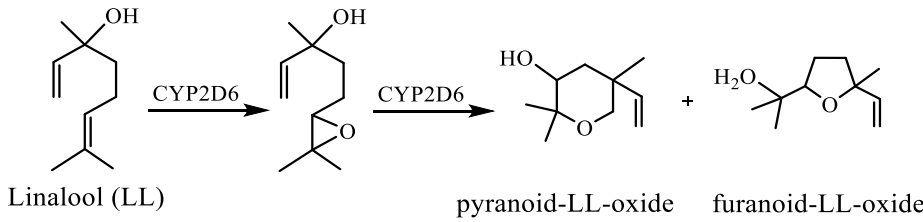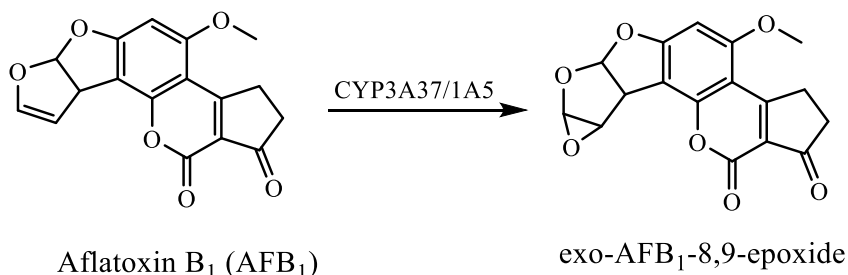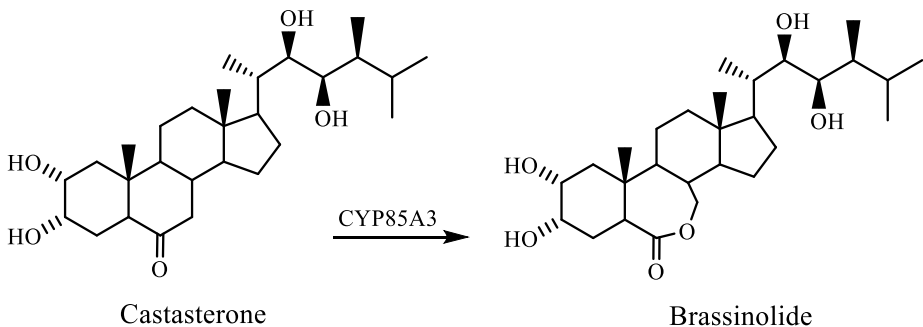
1.1.3. Reactions catalyzed by cytochromes P450
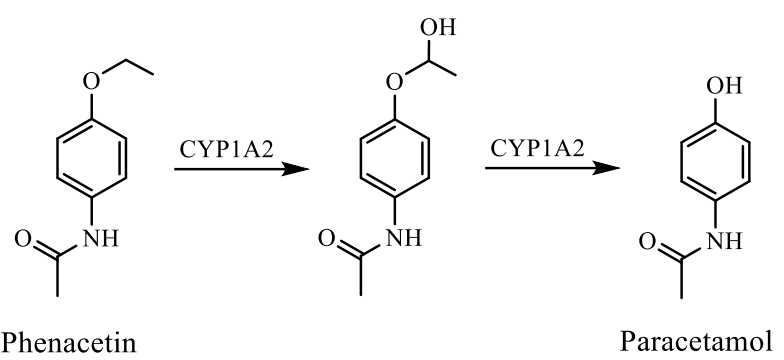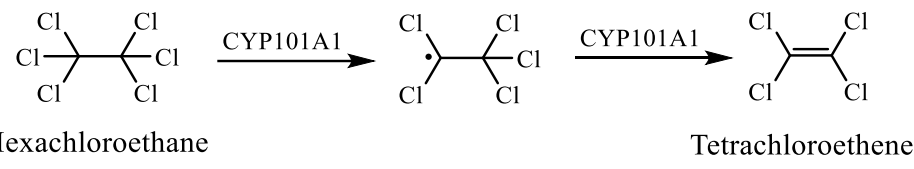
There are numerous reports of reactions catalyzed by cytochrome P450 monooxygenases, and as mentioned earlier, they are known for their special ability to oxygenate carbon-hydrogen bonds (Montellano, 2005). Table 1.1 below illustrates some common and uncommon reactions catalyzed by these wild-type enzymes to show their

broad substrate specificity. The focus of this study, however, lies on the O-dealkylation and reductive dehalogenation reactions.

Table 1.1.   Various reactions of cytochromes P450.

Type of reaction	Ref.
C-Hydroxylation	
Aliphatic	
Arachidonic acid (AA) → 18-OH AA (CYP102A1)	(Kim & Oh, 2013; Pikuleva, 2006)
Aromatic	
Cholesterol → 7α-hydroxycholesterol (CYP7A1)	
Dehydrogenation/Desaturation	
Valproic acid (VPA) → 4-ene-VPA (CYP2A6/2B6/2C6)	(Argikar & Remmel, 2009)
Oxidative Deamination	
Amphetamine → 2-phenylpropane (CYP2D6)	(Axelrod, 1955)

7

Type of reaction	Ref.

Oxidative C-C cleavage

Progesterone → (CYP17A1) → 17α-OH progesterone → (CYP17A1) → Androstenedione

(Guengerich & Yoshimoto, 2018)

Epoxidation

Alkene

Linalool (LL) → (CYP2D6) → (CYP2D6) → pyranoid-LL-oxide + furanoid-LL-oxide

(Meesters et al., 2007; Snyder et al., 1993)

Arene

Aflatoxin B$_1$ (AFB$_1$) → (CYP3A37/1A5) → exo-AFB$_1$-8,9-epoxide

Baeyer-Villiger Oxidation

Castasterone → (CYP85A3) → Brassinolide

(Nomura et al., 2005)

Type of reaction	Ref.

O-Dealkylation

Phenacetin   Paracetamol   (von Grafenstein et al., 2014)

Reductive dehalogenation

Hexachloroethane   Tetrachloroethene   (Walsh et al., 2000)

1.1.4. Topography of cytochromes P450

In 1985, CYP101A1 from *Pseudomonas putida* was the first P450 enzyme whose 3D crystal structure was successfully determined and served as a paradigm in elucidating other P450s (Poulos et al., 1985). In general, these enzymes consist of 400-500 amino acids and have a size of 44-47 kDa (Figure 1.3). Typically, they are built up of ~13 α-helices (A – L), and ~5 β-sheets or beta-domains (Figure 1.4). The protein itself has a triangular shape with heme as a prosthetic group in its center, placed in a parallel position to the triangle plane. The heme iron of the proximal side is bound to a cysteine residue, Cys357, while on the distal side of the heme is where the active site is located (Peterson & Graham, 1998). The most conserved features of P450s surround the heme and the active site. These include the α-helices D, L, I, E, residue Cys357, and of course the heme itself (Denisov et al., 2005). Despite cytochromes P450 having a fair amount of conserved features, there is still enough diversity in their structure for different substrates to bind.

```
10          20          30          40          50
MTTETIQSNA  NLAPLPPHVP  EHLVFDFDMY  NPSNLSAGVQ  EAWAVLQESN

60          70          80          90          100
VPDLVWTRCN  GGHWIATRGQ  LIREAYEDYR  HFSSECPFIP  REAGEAYDFI

110         120         130         140         150
PTSMDPPEQR  QFRALANQVV  GMPVVDKLEN  RIQELACSLI  ESLRPQGQCN

160         170         180         190         200
FTEDYAEPFP  IRIFMLLAGL  PEEDIPHLKY  LTDQMTRPDG  SMTFAEAKEA

210         220         230         240         250
LYDYLIPIIE  QRRQKPGTDA  ISIVANGQVN  GRPITSDEAK  RMCGLLLVGG

260         270         280         290         300
LDTVVNFLSF  SMEFLAKSPE  HRQELIERPE  RIPAACEELL  RRFSLVADGR

310         320         330         340         350
ILTSDYEFHG  VQLKKGDQIL  LPQMLSGLDE  RENACPMHVD  FSRQKVSHTT

360         370         380         390         400
FGHGSHLCLG  QHLARREIIV  TLKEWLTRIP  DFSIAPGAQI  QHKSGIVSGV

410         415
QALPLVWDPA  TTKAV
```

A helix | G helix
B helix | H helix
B' helix | I helix
C helix | J helix
D helix | K helix
E helix | K' helix
F helix | L helix

X : underlined are the β-sheets

Figure 1.3. **Cytochrome P450cam amino acid sequence starting from the N-terminus until the C-terminus (EC: 1.14.15.1). Each helix is highlighted while each β-sheet is underlined with a different color (UniProtKB - P00183).**
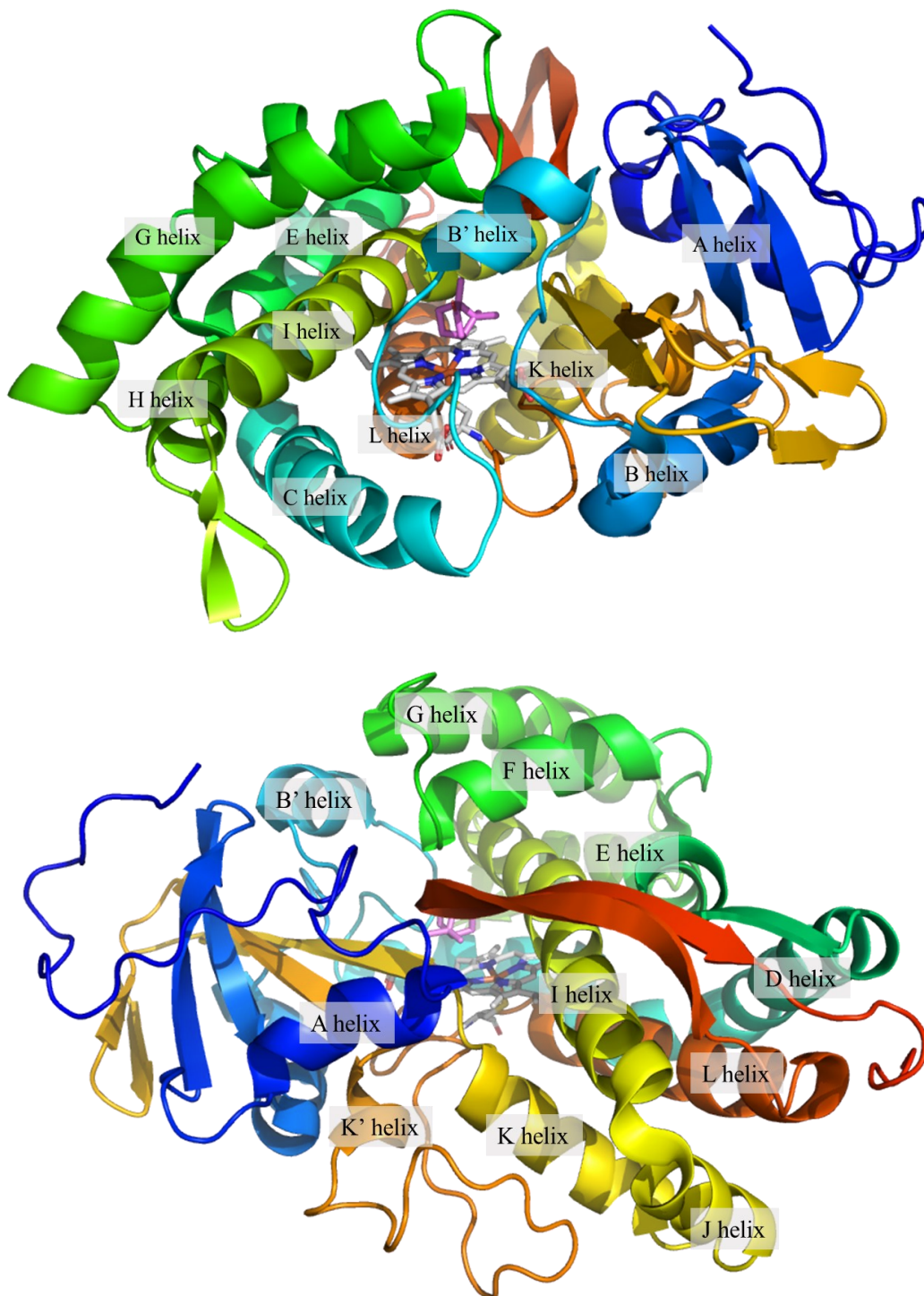
Figure 1.4. **Crystal structure of cytochrome P450cam. Both figures are views from the side to showcase the location of the different helices surrounding heme and camphor. They are colored from blue (Helix A) to red (Helix L) according to their sequence ID. The structures were generated from the RCSB PDB, entry 2CPP.**

The binding of the substrate, and therefore its recognition by the enzyme, happens at specific regions called substrate recognition sites (SRS), that were firstly mapped onto mammalian CYP2 proteins before being aligned to correspond to P450$_{cam}$ (Figure 1.5) (Gotoh, 1992). Six of them have been observed at a radius of 10 Å surrounding camphor: 1) SRS-1: the small B' helix in between the BC loop, 2) SRS-2: the C-terminus of F helix, 3) SRS-3: the N-terminus of G helix, 4) SRS-4: the central part of I helix, 5) SRS-5: the C-terminus of K helix and part of the beta-domain between K and K' helices, and 6) SRS-6: the central part of the β-sheet after L helix. These sequences are highly flexible and capable of altering their 3D arrangement, hence, increasing the substrate selectivity.
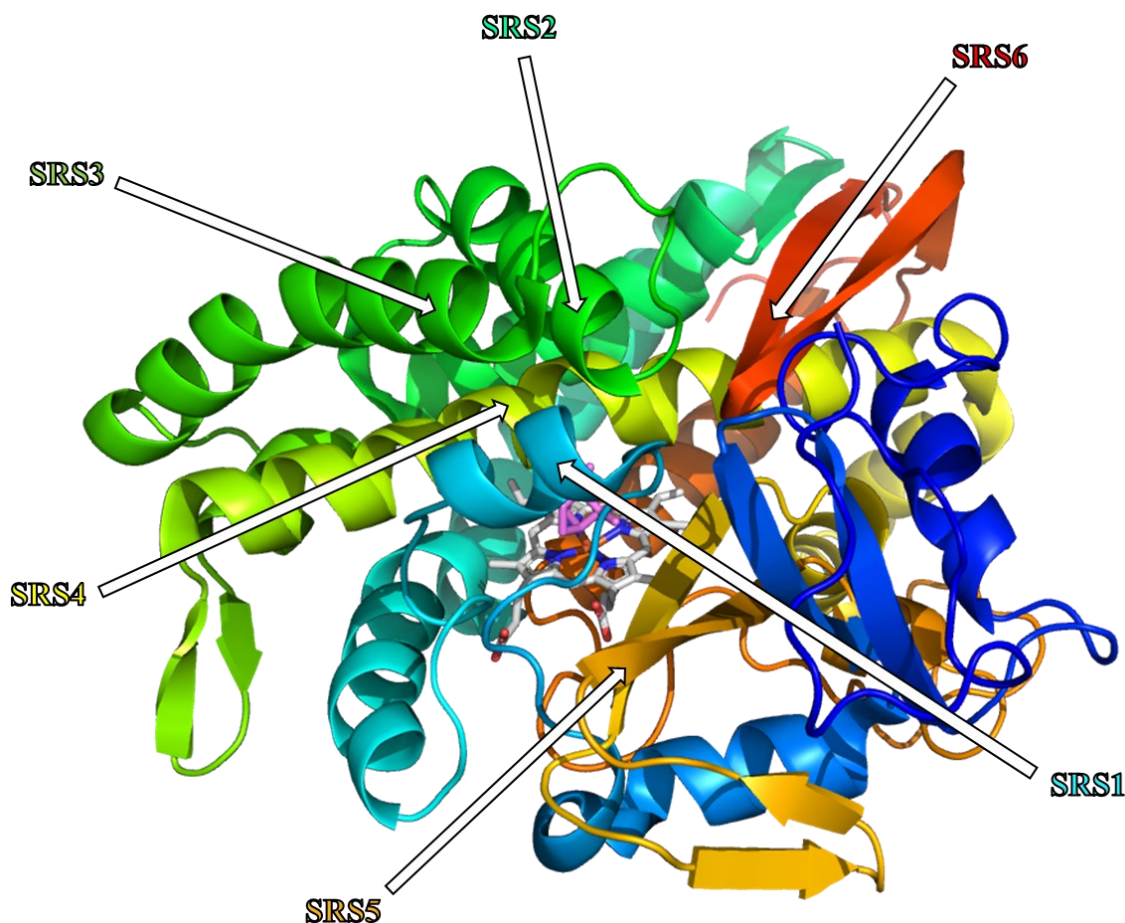
Figure 1.5. **The six substrate recognition sites (SRS) of cytochrome P450$_{cam}$. The structure was generated from the RCSB PDB, entry 2CPP.**

Over the heme, the residues at closer proximity in P450$_{cam}$ include: D297, G248, L244, T101, T252, and V295, followed by F87, F98, I395, V247, V396, and Y96, and finally T185 (Figure 1.6) (Poulos et al., 1985). Since the majority of the P450 substrates are lipophilic, they mostly bind to the hydrophobic active site, which is lined with non-polar residues. These hydrophobic residues are F87, F98, V247, V295, and V396, and modulate the substrate stability and specificity through Van der Waals interactions (Poulos et al., 1987). There are also some polar residues such as D251, T101, T185, T252, and Y96 which are responsible for the enzyme's functionality, with Y96 H-bonding with the substrate (Montellano, 2005) and D251 being essential for proton delivery (Schlichting, 2000). As the substrate is positioned to the binding pocket, important hydrophobic interactions take place within the heme's surface, between residue L244, the isopropyl chain of residue V295, and camphor's C-8 and C-9 methyl groups (Sono et al., 1996).
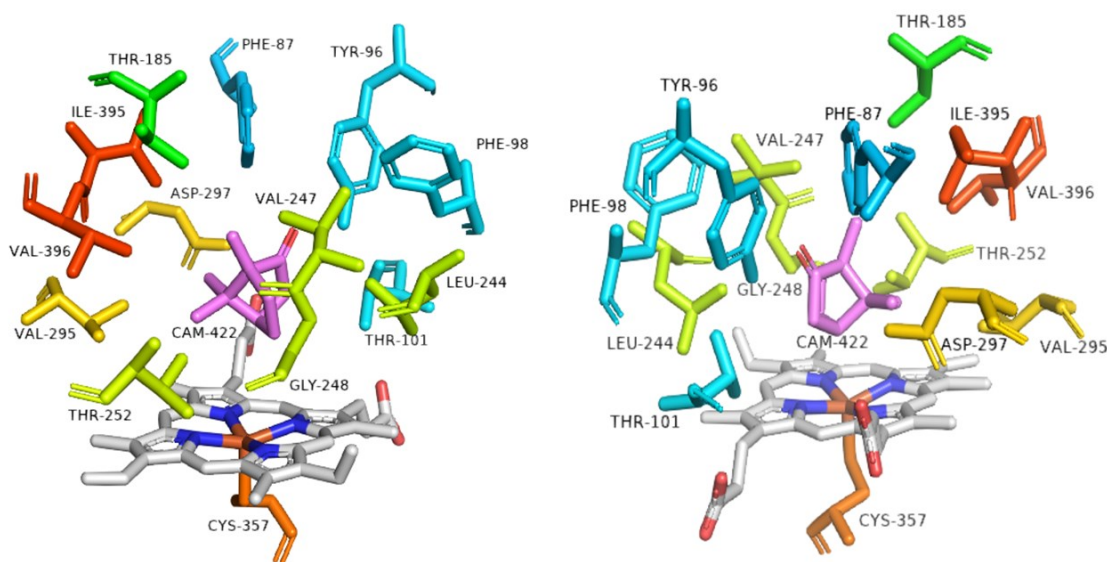
Figure 1.6.   Camphor-bound active site of cytochrome P450$_{cam}$. Both figures are views from the side to show the location of the different amino acid residues surrounding camphor at a distance of 5 Å. The residues are colored according to their sequence ID. The structures were generated from RCSB PDB, entry 2CPP.

It is generally believed that the proximal ligand of heme, Cys357, controls the reactivity of the enzyme. This ligand is surrounded by a H-bonding network called the "Cys pocket", and is lined with the residues G359, L358, and Q360 (Poulos et al., 1987). These residues are responsible for the stability of Cys357 by forming three H-bonds

between their amide groups (-NH) and the sulfur, and another one between Q360's side chain to the carbonyl group of Cys357 (Galinato et al., 2011). The observed characteristic 450 nm peak of P450s in the reduced ferrous-carbon monoxide complex results from the thiolate-cysteine ligand at the fifth position of heme-iron (Omura & Sato, 1964). This axial ligand is of great importance for the function of the enzyme as it pushes electron density through to bound dioxygen, assisting with the scission of O-O bond and leading to a pull from the ferryl oxygen, resulting in the activation of the monooxygenase reaction by C-H bond cleavage(Dawson & Sono, 1987; Groves, 2014).

The small B' helix opens and closes the entry channel of P450$_{cam}$, coordinating the orientation and binding of the substrate around the heme (OuYang et al., 2006). In this region, there are some significant active site residues such as Y96, located at the C-terminus (Atkins & Sligar, 1990; Y.-T. Lee et al., 2010). A unique feature of P450$_{cam}$ is that this residue H-bonds with tyrosine's hydroxyl group to the C-2 carbonyl group of camphor and coordinates a potassium ion, K$^+$, resulting in a strong binding of camphor (Primo et al., 1990). Studies have shown that around 50 mM of K$^+$ is necessary to convert the enzyme to its high spin state and stabilize it upon camphor binding (Hoa & Marden, 1982; Peterson, 1971). The binding between camphor and K$^+$ is maintained by the backbone carbonyl oxygens of G93, E94, and Y96 of B' helix, E84, and two water molecules (OuYang et al., 2006; Poulos et al., 1987). As the entry channel closes upon K$^+$ binding and substrate entry, B' helix remains oriented, but during P450$_{cam}$'s open form it has been revealed that the helix appears perturbed (OuYang et al., 2006; Tripathi et al., 2013).

The diversity in substrate specificity of cytochromes P450 is due to variations of its structure around the binding pocket which consists of the B' helix, BC loop, FG loop, F and G helices. Upon camphor binding, regions near B' helix slide over the heme and I helix, resulting in a closed conformation (Hays et al., 2004; Y.-T. Lee et al., 2011; Stoll et al., 2012). The entry channel surface of the enzyme includes the residues T192 and S190 of the FG loop which are 20 Å from the binding site. T192 is responsible for directing the substrate into the entry channel and consequently, to the active site, while S190 which is on the opposite side, does not have a major role in substrate recognition (Behera &

Mazumdar, 2008). Additional studies showed that the F and G helices and FG loop are retracted by 5-6 Å and 9 Å respectively from their position when camphor is absent, and in low concentration of monovalent cations, the B' helix and K^+ become disordered, resulting in an open conformation (Hays et al., 2004; Y.-T. Lee et al., 2010; Stoll et al., 2012).

Movements of F and G helices, C helix and B' helix of P450$_{cam}$ are associated with binding to the enzyme's ferredoxin, putidaredoxin (PdX) (S. S. Pochapsky et al., 2003; Rui et al., 2006; Sevrioukova & Poulos, 2011; Tripathi et al., 2013). Not only does PdX participate in electron delivery to P450$_{cam}$, but it is also considered to have an effector role during catalysis by enforcing the correct orientation of the substrate before the second electron transfer (Y.-T. Lee et al., 2010; OuYang et al., 2006). More recent studies have compared the open and closed forms of the enzyme, suggesting that there are some significant changes happening to the proximal region near the binding site of PdX (Y.-T. Lee et al., 2010). An NMR study focusing on the distal side groups of P450$_{cam}$ showed that T252 and the cysteine ligand are perturbed when PdX is present, indicating once again that when PdX binds, it results in changes to the environment of the binding pocket (Tosha et al., 2003). To illustrate the effector role of PdX, L358P substitution mimic models have been used for the P450$_{cam}$-PdX complex. PdX basically pushes the heme (proximal side), resulting in changes to the active site's structure that ultimately lead to the catalytic activation of dioxygen. In this scenario, residues D38 and W106, are the key to the PdX-induced perturbation, while the C-terminal W106 is critical for electron delivery to P450$_{cam}$ (Sevrioukova & Poulos, 2011; Sligar et al., 1974). Also, it is important to mention that modelling studies and spectroscopic methods indicate that PdX binds to the opposite site of the heme (proximal side of P450$_{cam}$), resulting in changes to the other side, where the binding pocket is located (S. S. Pochapsky et al., 2003; T. Pochapsky, 1996; Zhang et al., 2008).

The I helix has a central conserved region near the heme that is involved in dioxygen activation, and specifically, residues D251, G248 and T252 which are located near the dioxygen's binding site. In the ferrous state of the enzyme, D251 cannot H-bond as it is perpendicular to the helical axis, but the ferrous enzyme-dioxygen state allows the

peptide to rotate and create a helical H-bond. Upon oxygen binding to this enzyme-substrate complex, these movements of D251 cause the adjacent G248-T252 H-bond to weaken. G248 then positions itself closer to dioxygen which opens the I helix groove, so that catalytic waters can enter the active site and create a proton relay network with the distal oxygen atom which is necessary for the scission of the O-O bond (Nagano & Poulos, 2005; Schlichting, 2000). Moreover, residues D251 and T252 are known as the "alcohol-acid pair" in P450$_{cam}$ and are critical for the oxygen activation and proton transfer (Gerber & Sligar, 1994; Martinis et al., 1989). Other residues important for proton delivery and H-bonding interactions are T101, T185 and T252, as their alcoholic and methyl side chains can interact with the surrounding residues (Manna & Mazumdar, 2006).

1.2. Bacterial cytochrome P450 - CYP101A1

The large superfamily of cytochrome P450 monooxygenases has been investigated a lot, but this study focuses specifically on cytochrome P450$_{cam}$ (CYP101A1) from the soil bacterium *P. putida,* as this system is soluble and can be purified quickly in large quantities in *Escherichia coli* cells (Montellano, 2005). P450$_{cam}$ is known to catalyse the bicyclic monoterpene camphor **10** regio- and stereo-selectively to the hydroxylated products 5-exo-hydroxycamphor **11** and concomitantly to 5-ketocamphor **12** (Figure 1.7) (Auclair et al., 2001; Davydov et al., 2001).
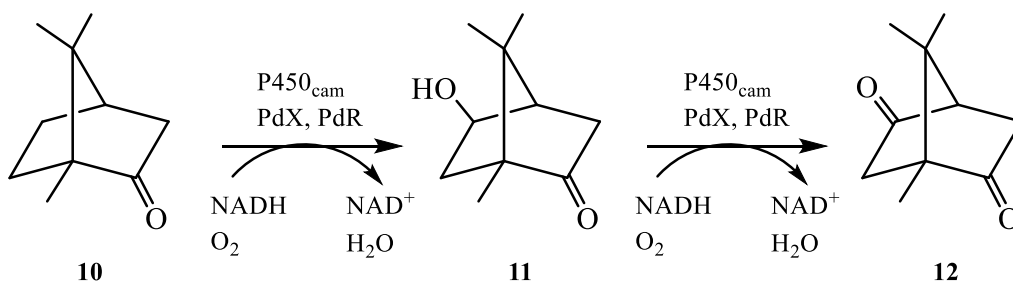
Figure 1.7. **Camphor hydroxylation to 5-exo-hydroxycamphor and 5-keto-camphor by cytochrome P450$_{cam}$.**

Cytochrome P450$_{cam}$ belongs to the Class I electron transport system which contains three elements as mentioned earlier (Figure 1.1, Ia). More specifically, 1) a FAD-containing reductase, putidaredoxin reductase (PdR) which transfers the electrons from
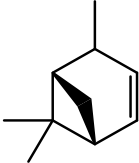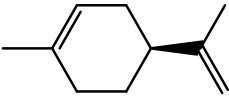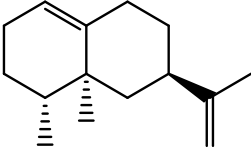
NADH to 2) an Fe_2S_2 ferredoxin, putidaredoxin (PdX), which in turn receives them and directly donates them to 3) the terminal oxidase, cytochrome $P450_{cam}$ (Sevrioukova & Poulos, 2011; Sibbesen et al., 1996).

1.2.1. Active site mutations of cytochrome $P450_{cam}$

The wild-type cytochrome $P450_{cam}$ has been engineered through mutagenesis studies around its active site and cysteine pocket to change the specificity from its natural substrate, camphor, and concomitantly increase the substrate acceptance.

Cytochrome $P450_{cam}$ catalyzes conversion of the bicyclic monoterpene (+)-camphor to 5-exo-hydroxycamphor, thus, mutations in its active site have been generated to accept other terpenes (Table 1.2). Since monoterpenes (+)-α-pinene and (S)-limonene are structurally similar to camphor, Bell *et al*. assumed that they could bind in a similar orientation to the active site (Bell, Chen, et al., 2003; Bell et al., 2001). To improve the enzyme-substrate fit and promote successful oxidation by $P450_{cam}$, they generated variants of residues F87, Y96, and V247. Initially, the triple mutant F87W/Y96F/V247L was the most selective for (+)-α-pinene, giving 85% (+)-*cis*-verbenol, but due to steric hindrance, it showed weak binding and low activity. Double mutant F87W/Y96F and triple mutant F87W/Y96F/V247L were the most selective for (S)-limonene, giving 82% (–)-*trans*-isopiperitenol, but again not very active, while (–)-perillyl alcohol (anti-cancer properties) was not reported (Bell et al., 2001). Later on, studies of the crystal structure revealed that the L244A mutation was beneficial, increasing the selectivity of pinene oxidation. Mutant F87W/Y96F/L244A gave 86% (+)-*cis*-verbenol, while Y96F/L244A/V247L gave 32% (+)-verbenone, showcasing that it is possible to create variants that directly oxidize (+)-α-pinene to (+)-verbenone (useful for applications in synthesis) (Bell, Chen, et al., 2003). The same variants were used along with the WT enzyme for the sesquiterpene (+)-valencene. Although the variants were not so active, the most selective were F87A/Y96F/L244A/V247L giving 86% (+)-*trans*-nootkatol, and F87V/Y96F/L244A giving 47% (+)-nootkatone as main monooxygenation products out of the 17 possible that can be formed from valencene (Sowden et al., 2005).

Table 1.2.   **P450cam mutants with terpenes as substrates.**
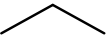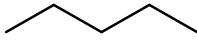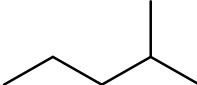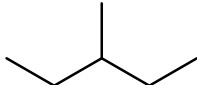
Substrate	Active mutants	Ref.
(+)-α-pinene	**Y96F/V247L**: most active giving 70% (+)-*cis*-verbenol and 91% NADH coupling efficiency in comparison to WT 23%. **F87W/Y96F/L244A**: most selective giving 86% (+)-*cis*-verbenol and 95% NADH coupling efficiency in comparison to WT 23%. **Y96F/L244A/V247L**: most selective giving 32% (+)-verbenone.	(Bell, Chen, et al., 2003; Bell et al., 2001)
(S)-limonene	**Y96F/V247L**: most active giving 70% (–)-*trans*-isopiperitenol and 62% NADH coupling efficiency in comparison to WT 5.1%. **F87W/Y96F** and **F87W/Y96F/V247L**: most selective giving 82% (–)-*trans*-isopiperitenol.	(Bell et al., 2001)
(+)-valencene	**F87V/Y96F/L244A**: most selective giving 47% nootkatone. **F87A/Y96F/L244A/V247L**: most selective giving 86% (+)-*trans*-nootkatol.	(Sowden et al., 2005)

The active site topology of P450cam has also been engineered to accept hydrocarbons, such as linear and branched alkanes, by adding more bulk (Table 1.3). The EB mutant (F87W/Y96F/T101L/L1244M/V247L) has been reported by Bell *et al*. for propane oxidation (Bell, Orton, et al., 2003), but additional mutations were introduced to further decrease the binding pocket to accept the smaller alkane, ethane (F. Xu et al., 2005). Mutant EB/L294M/T185M/L1358P/G248A oxidized ethane to ethanol (no ethanal) at a rate of 78.2 nmol (nmol P450cam)$^{-1}$(min)$^{-1}$ and NADH oxidation activity of 741 min^{-1} (F. Xu et al., 2005). Studies from the same group also targeted the gaseous alkanes propane and butane that successfully turned over to propan-2-ol and butan-2-ol respectively, by

being exclusively oxidized at the secondary CH bonds (Bell et al., 2002). At first, mutant F87W/Y96F/T101L/V247L had the highest activity, turning over propane at a rate of 110 min^{-1} in comparison to WT 0.08 min^{-1}, and butane, at a rate of 750 min^{-1} versus WT 0.4 min^{-1}. Then, residues such as F87, Y96, V247 and V396 we focused, which are farther away from the heme, while the resultant variant F87W/Y96F/V247L was used as a template for the addition of more mutations to increase the activity towards propane. The quintuple mutant F87W/Y96F/T101L/L244M/V247L oxidized propane at a rate of 176 min^{-1} and NADH oxidation rate of 266 min^{-1}, compared to WT with camphor. The quadruple mutant F87W/Y96F/T101L/V247L oxidized butane at a rate of 755 min^{-1} and NADH oxidation rate of 795 min^{-1}. Variant F87W/Y96F/V247L oxidized pentane to 2-pentanol and 3-pentanol (2:1) (no 1-pentanol or pentanal) at a rate of 237 min^{-1} and 46.5% coupling (Bell, Orton, et al., 2003).

So far, studies have shown that Y96A and Y96F variants oxidize linear alkanes up to 19 times more than the WT due to increased hydrophobicity of the active site (Stevenson et al., 1996). Mutations of residue V247 to accommodate branched alkanes have resulted in improved product rates. Examples of such compounds include 2-methylpentane, 3-methylpentane, 2-methylhexane, hexane and heptane, while the best mutants were found to be Y96F/V247L for hexane, Y96F for 2-methylpentane, and Y96A/V247A for 3-methylpentane (Stevenson et al., 1996, 1998).

Table 1.3. **P450$_{cam}$ mutants with alkanes as substrates.**

Substrate	Active mutants	Ref.
Ethane	**EB/L294M/T185M/L1358P/G248A**: reduces active site volume, oxidizing ethane to ethanol.	(F. Xu et al., 2005)
Propane	**F87W/Y96F/T101L/L244M/V247L**: most active for propane at a rate of 176 min^{-1} and 66% coupling.	(Bell et al., 2002; Bell, Orton, et al., 2003)
Butane	**F87W/Y96F/T101L/V247L**: most active for butane at a rate of 755 min^{-1} and 95% coupling.	
Pentane	**F87W/Y96F/V247L**: 46.5% coupling compared to WT 1.1%	
Hexane	**Y96F/V247L**: most active for hexane with product rate of 176.1 min^{-1} and 66.8% coupling.	(Stevenson et al., 1996, 1998)
2-methylpentane	**Y96F**: most active for 2-methylpentane with product rate of 97 min^{-1} and 43,7% coupling.	
3-methylpentane	**Y96A/V247A**: most active for 3-methylpentane with product rate of 199 min^{-1} and 63.6% coupling.	

Aromatic compounds can also be engineered to fit cytochrome's P450$_{cam}$ pocket (Table 1.4). In fact, Loida and Sligar were the first ones to try fitting a non-natural substrate by varying the active site volume, and for their experiments they used ethylbenzene (Loida & Sligar, 1993). To achieve tight coupling, it was found that the key factor was the substrate positioning to the heme. At first, variant T101M blocked ethylbenzene from accessing the heme, but additional bulk overcame that effect. The triple mutant T101M/T185F/V247M hydroxylated ethylbenzene to R:S 1-phenylethanol (87:13 ratio) and had 13% NADH coupling compared to WT 5%. Fowler *et al.* were the first to report a rational redesign of P450$_{cam}$ by mutating only Y96 to Y96A (Fowler et al., 1994). This
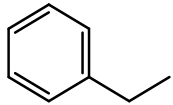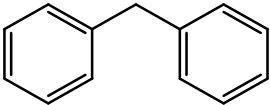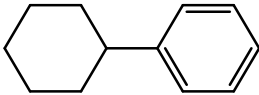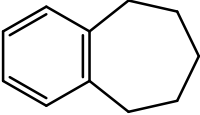
resulted in the tight binding of the bi-aryl compound diphenylmethane, which was oxidized to p-hydroxydiphenylmethane at a NADH turnover rate of 6 s^{-1}. Speight *et al.* generated a randomized library where only Y96 and F98 were mutated and screened for diphenylmethane hydroxylation too (Speight et al., 2004). In the case of Y96A, they achieved up to 92% conversion to the para-hydroxy product. Later on, Hoffmann *et al.* composed a library of ~300,000 variants and screened them for activity on diphenylmethane (Hoffmann et al., 2011). One of the best variants, 6h1h10 (F87I/Y96M/T101I/L244N/D297I/I395N), had 75% activity over WT towards camphor, thus, it was subjected to further mutagenesis and revealed that positions F87, Y96, and L244 were important for selectivity. Moreover, size reduction at 396 position with variants 5a6b3-I396A and -I396G (F87I/Y96M/L244N/D297T/I395M/V396I-), switched the main product to diphenylmethanol. England *et al.* showed that mutants Y96A and Y96F can hydroxylate another aromatic compound, phenylcyclohexane, at C3 and C4 positions (which are closest to the iron center), forming *cis*-3-phenylcyclohexanol, *cis*-4-phenylcyclohexanol and *trans*-4-phenylcyclohexanol. More specifically, mutant Y96F had the highest selectivity for *cis*-3-phenylcyclohexanol, giving 81%, while Y96A for *cis*-4-phenylcyclohexanol, giving 45% (England et al., 1996).
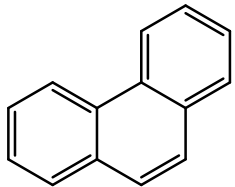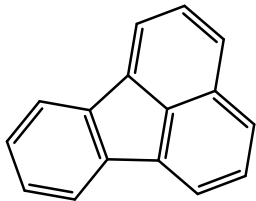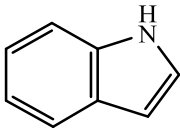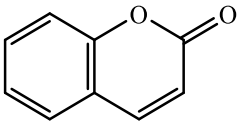
Studies by Mayhew *et al.* were conducted on four benzocycloarene compounds (benzocyclobutene, benzocyclopentene, benzocyclohexene, and benzocycloheptene) using mutant Y96F to understand how the product distribution and the catalytic rate are affected (Mayhew et al., 2002). All the products were hydroxylated at C1 of the alicyclic ring, except benzocyclohentene that gave hydroxylated products at both C1 and C3 positions. NADH coupling ranged from 35-70% with the highest being for benzocycloheptene, in comparison to WT 10-12%. This observation along with molecular dynamic calculations of the steric constraints showed that removing the hydroxyl group of Y96 results in better oxidation of these benzocycloarene compounds (Mayhew et al., 2002). For larger polycyclic compounds such as pyrene, benzo[α]pyrene, phenanthrene and fluoranthene, the oxidation was enhanced over WT by mutating F87 and Y96. Mutant F87A/Y96F had the highest NADH oxidation rate for phenanthrene at 374 min^{-1} (31% of WT rate), followed by F87L/Y96F with a NADH oxidation rate of 144 min^{-1} for fluoranthene. In regard to the

coupling efficiency, pyrene had the highest at 23%, however, the turnover rate of NADH was slow (Harford-Cross et al., 2000).

Heterocyclic compounds have also been engineered for their ability to get oxidized by cytochrome P450$_{cam}$ mutants. Çelik *et al*. used high-throughput screening to create a library using residues F98 and Y96, which were randomized and screened in a 96-well microplate for indole hydroxylation (Çelik et al., 2005). Good activity was noticed when F98 was maintained while Y96 was mutated to A/C/Q/G/M/S/T, with an activity order of M > A > C > T = Q = S > G. Manna and Mazumdar mutated residues F87, Y96, T101 and L244 to change the substrate specificity of P450$_{cam}$ (Manna & Mazumdar, 2010). As a result, single mutant Y96F was found to be best for catalyzing indole to indigo with a 5-fold NADH consumption rate than WT. However, variant Y96F/L244A had a 6-fold NADH consumption rate than WT and a higher yield of indigo (but less indirubin) which was enhanced by the presence of H$_2$O$_2$. This group also tested the same mutants for their ability to catalyze coumarin, finding out that the double mutant hydroxylated the compound at positions C3, C4, C6, C7 to hydroxycoumarin, with a NADH consumption rate of 35 min^{-1} compared to WT 3 min^{-1} (Manna & Mazumdar, 2010).

Table 1.4. **P450_{cam} mutants with aromatic systems as substrates.**

Substrate	Active mutants	Ref.
Ethylbenzene	**T101M/T185F/V247M**: most effective resulting to R:S 1-phenylethanol (87:13 ratio) and 13% NADH coupling compared to WT 5%.	(Loida & Sligar, 1993)
Diphenylmethane	**Y96A**: most active achieving 92% conversion to p-hydroxydiphenylmethane. **F87I/Y96M/T101I/L244N/D297I/I395N**: 75% activity over WT towards camphor. **F87I/Y96M/L244N/D297T/I395M/V396I -I396G** and **-I396A**: switched main product to diphenylmethanol.	(Fowler et al., 1994; Hoffmann et al., 2011; Speight et al., 2004)
Phenylcyclohexane	**Y96F:** highest selectivity for *cis*-3-phenylcyclohexanol, giving 81%. **Y96A**: highest selectivity for *cis*-4-phenylcyclohexanol, giving 45%.	(England et al., 1996)
Benzocycloheptene *Benzocycloarenes*	**Y96F**: 35-70% NADH coupling compared to WT 10-12%, with the highest being for benzocycloheptene.	(Mayhew et al., 2002)

Substrate	Active mutants	Ref.
Phenanthrene Fluoranthene *Polycyclics*	**F87A/Y96F**: highest NADH oxidation rate for phenanthrene at 374 min^{-1} (31% of WT rate). **F87L/Y96F**: NADH oxidation rate of 144 min^{-1} for fluoranthene.	(Harford-Cross et al., 2000)
Indole	**Y96M**: best activity. **Y96F/L244A**: 6-fold NADH consumption rate than WT and a higher indigo yield.	(Çelik et al., 2005; Manna & Mazumdar, 2010)
Coumarin	**Y96F/L244A**: NADH consumption rate of 35 min^{-1} compared to WT 3 min^{-1} and 5/8-hydroxycoumarin were favored.	(Manna & Mazumdar, 2010)
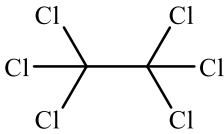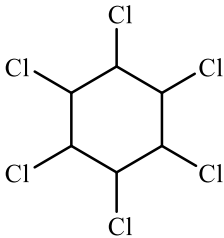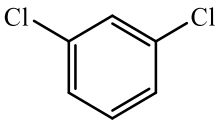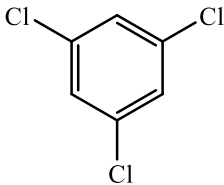
Another type of compound that is of great importance is polychlorinated pollutants. They are persistent and difficult to degrade due to their lipophilic nature and bioaccumulate in the environment causing adverse health effects on humans. Oxidation of low molecular weight chloroalkanes dates back to the 1980s. In 1994, Lefever and Wackett did a study on multiple compounds including 1,2-dichloropropane, 1,1,1-trichloroethane, 1,1,2-trichloroethane, 1,1,1,2-tetrachloroethane, 1,1,2,2-tetrachloroethane, pentachloroethane and hexachloroethane (Table 1.5) (Lefever & Wackett, 1994). These were all oxidized poorly by P450$_{cam}$, but they believed that random or site-directed mutagenesis protocols could improve their rates and coupling efficiencies. Cytochrome P450$_{cam}$ can turn over the
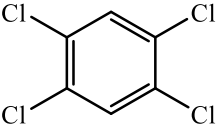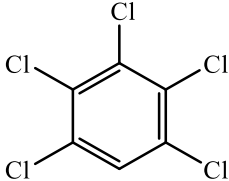
chlorinated compounds hexachloroethane and pentachloroethane through reductive dehalogenation, thus, this activity was investigated through active-site mutagenesis studies. Walsh *et al.* found that mutants Y96A and Y96F increased the active-site hydrophobicity and enhanced the binding of hexachloroethane, but the reaction rate was weakened (Walsh et al., 2000). Mutant F87Y did not affect the rate of dehalogenation but it decreased the substrate binding. Mutant Y96H increased the reaction rate by 40% at pH 6.5 but again, it decreased the binding of hexachloroethane. Bulkier mutations on residues F87, T101, V247 increased the rate but affected again the binding. At pH 7.4, variant F87W/V247L was found to be the best for reducing hexachloroethane to tetrachloroethene with 2.5 times the activity of the WT. Sen *et al.* compared camphor with hexachlorocyclohexane, which led them to engineer site-specific mutations of P450$_{cam}$ that increased the binding affinity (Sen et al., 2011). T101V was found to increase hydrophobicity while F87W reduced the active-site space. High affinity was noticed with mutants Y96F/T101V ($K_d = 0.7\ \mu M^{-1}$) and Y96F/L244A ($K_d = 0.8\ \mu M^{-1}$). However, single mutant Y96F showed the best affinity ($K_d = 0.5\ \mu M^{-1}$) and coupling efficiency (15%).

Polychlorinated aromatic compounds have also been studied. Jones *et al.* discovered that for most of these substrates, the point mutation F87W increases the activity up to 10-fold because it reduces the volume on top of the binding site, bringing the substrate closer to the heme (Jones et al., 2000). Introducing F98W decreased the NADH turnover but increased the coupling efficiency for less chlorinated compounds. Triple mutant F87W/Y96F/F98W resulted in a 92% coupling for 1,3-dichlorobenzene and 97% for 1,3,5-trichlorobenzene. Single mutant Y96F caused a 100-fold increase in activity for heavily chlorinated compounds such as pentachlorobenzene and hexachlorobenzene. Introducing V247L increased the NADH turnover and more specifically, variant F87W/Y96F/V247L resulted in a NADH turnover of 107 min^{-1} for 1,2,4,5-tetrachlorobenzene and 229 min^{-1} for pentachlorobenzene. The same group reported that variant F87W/Y96F/L244A/V247L could oxidize pentachlorobenzene to pentachlorophenol (Jones et al., 2000). Then, through crystal structure studies they were able to further understand the structure-activity correlations in pentachlorobenzene oxidation. They noticed that a chlorine atom could position itself in a cavity created by L244A, allowing bulkier chlorinated compounds to bind. Moreover, L244A broke the hydrogen bond between the OH of T252 and the

carbonyl oxygen of G248, forming an open oxygen-binding groove that allowed the mutant to deviate from its conformation without causing a loss in activity. Binding interaction analysis introduced T101A, a mutation that reorients the substrate while preserving other van der Waals contacts and resulting in more efficient oxidation. The quintuple variant F87W/Y96F/T101A/ L244A/V247L was 3-fold more active than the quadruple one, with a NADH rate of 481.2 min^{-1}, product rate of 214.4 min^{-1}, and coupling of 45.9%.

Table 1.5.   P450$_{cam}$ mutants with halogenated systems as substrates.

Substrate	Active mutants	Ref.
 Hexachloroethane	**F87W/V247L**: most active with reaction rate of 80 min^{-1} compared to WT 32 min^{-1}.	(Walsh et al., 2000)
 Hexacyclochlorohexane	**Y96F**: highest affinity (K$_d$ = 0.5 μM^{-1}) and best coupling efficiency (15%). **Y96F/T101V** and **Y96F/L244A**: good affinity (K$_d$ = 0.7 and 0.8 μM^{-1}, respectively).	(Sen et al., 2011)
 1,3-dichlorobenzene 1,3,5-trichlorobenzene	**F98W**: decreased the NADH turnover but increased the coupling efficiency. **F87W/Y96F/F98W**: 92% coupling for 1,3-dichlorobenzene. **F87W/Y96F/F98W**: 97% coupling for 1,3,5-trichlorobenzene.	(Jones et al., 2000)

Substrate	Active mutants	Ref.
1,2,4,5-tetrachlorobenzene	**F87W/Y96F/V247L:** NADH turnover of 107 min^{-1} for 1,2,4,5-tetrachlorobenzene.	(Jones et al., 2000)
Pentachlorobenzene	**Y96F**: 100-fold increase in activity. **F87W/Y96F/V247L**: NADH turnover of 229 min^{-1} for pentachlorobenzene. **F87W/Y96F/T101A/L244A/V247L**: NADH rate of 481.2 min^{-1}, pentachlorophenol rate of 214.4 min^{-1} and coupling of 45.9%.	(Jones et al., 2000; F. Xu et al., 2007)

1.3. Honey bees: exposure to Varroa and pesticides

The western honey bee species, *Apis mellifera L.*, are frequent floral visitors and vital pollinators for a variety of agricultural crops (Calderone, 2012). They pollinate 90% of the most prevalent food crops (vegetables, fruits, legumes, etc.), which are essential for a balanced human diet that would impoverish if they were to disappear (Klein et al., 2007). Over the years, *A. mellifera* have been domesticated and transported to every continent except Antarctica, making them the most frequent single species pollinator worldwide (E. Weber, 2012).

In recent years, the honey bee population has been going through perturbations that result from several factors including climatic conditions (temperature, humidity, latitude), different species, pathogens (viruses, microorganisms, mites), food resources, etc. The most significant reason for its decline is *Varroa destructor,* an ectoparasitic mite that is causing problems such as colony collapse disorder, acute bee paralysis, and deformed wings (Bowen-Walker et al., 1999; Bowen-Walker & Gunn, 2001). Varroa mites parasitize nurse bees as they are responsible for feeding and caring for the larvae, having a negative influence on the bee's reproductive success. Hence, they depend entirely on their host for

survival, while their life cycle is constituted by two phases: the non-reproductive and the reproductive phase. During the first stage, they parasitize the bodies of the nurse bees and feed on their fat body. Afterward, the mites move into brood cells before they are capped over. Then, they enter the second stage where they feed on the late-stage larva or developing pupa, lay eggs and reproduce. As the adult bees emerge out of the brood cell, the mites ride on them, and a new cycle begins (Mondet et al., 2018; Ramsey et al., 2019). Varroa infestation on the bees is also causing varroosis, a disease that impairs the colony and leads to brood damage. Infested colonies usually collapse within 1-2 years if they do not get any treatment. Studies have found that the loss of fat body during the development of the larvae reduces the adult bee's size and weight, causing decreased flight performance and sperm production (Genersch, 2010; Ramsey et al., 2019). Parasitized bees have a reduced orientation and homing ability, resulting in difficulties returning to the colony or getting lost during the flight. Their immune system also gets weaker, making them susceptible to other secondary pathogens. Soon after the mite's adverse effect on the bees, most of them are born with atrophied/deformed wings and have a smaller size (Bowen-Walker & Gunn, 2001).
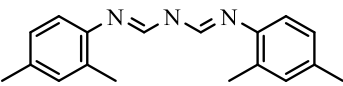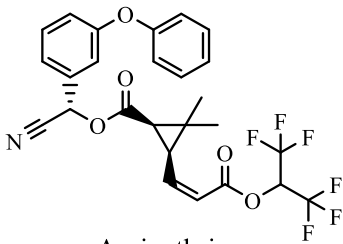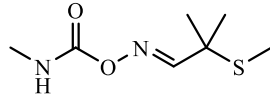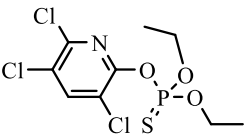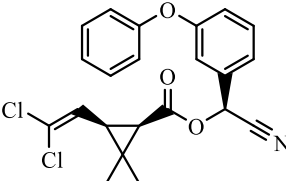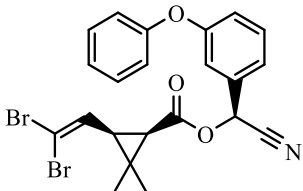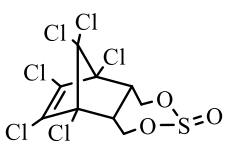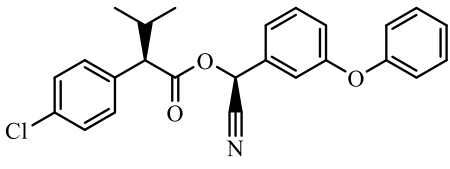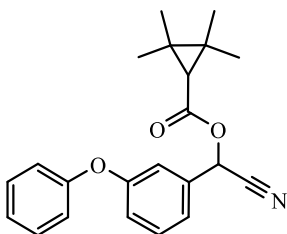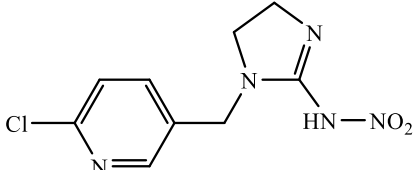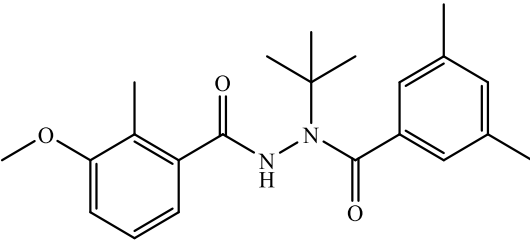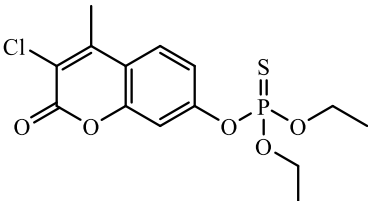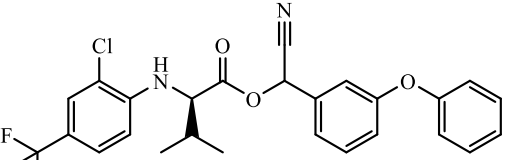
Besides varroa, another factor that impacts the bees' wellbeing, are pesticides applied to agricultural and horticultural landscapes to treat the mite and other pests that affect the plants (Table 1.6). Residues have been found in beehive matrices such as beeswax, bee bread, bee brood, honey, propolis, pollen, and on honey bees per se (Al Naggar et al., 2015; Bogdanov, 2015; Morales et al., 2020; Mullin et al., 2010; Orantes-Bermejo et al., 2010). A large-scale study conducted by Mullin *et al.* in North America, discovered 121 different insecticides, acaricides, herbicides, fungicides, and their metabolites within 887 samples of different hive matrices (Mullin et al., 2010). Out of 259 wax and 350 pollen samples, one systemic pesticide was detected in at least 60% of them, while half the samples had always chlorothalonil (fungicide), coumaphos, and fluvalinate (acaricides used in the hives to treat against varroa). The most encountered pesticides in wax were coumaphos (98.1%), fluvalinate (98.1%), and coumaphos oxon (coumaphos metabolite, 89.9%). In pollen, the most detected were fluvalinate (88.3%), coumaphos (75.1%), and chlorothalonil (52.9%). Out of 140 bee samples, there were much fewer detections, with the highest being for fluvalinate (83.6%) and coumaphos (60%). On the

comb wax, they also found near ppm levels of chlorpyrifos, aldicarb, deltamethrin (insecticides), iprodione (fungicide and nematicide), and methoxyfenozide (insecticide). The most frequently encountered pesticides besides the aforementioned were amitraz (acaricide, used widely to treat bees against varroa), pendimethalin (herbicide), endosulfan (insecticide and acaricide), fenpropathrin (insecticide), esfenvalerate (insecticide), and atrazine (herbicide) (Mullin et al., 2010).

A more recent study has evaluated the migration and persistence of environmental contaminants, such as plant protection chemicals and veterinary products, towards the hive (Morales et al., 2020). Amitraz was used on 2 beehive groups, and samples of bee bread, bee brood, and beeswax were tested for 5 months. This resulted in 31 residues of different pesticides, with the highest being in beeswax. As expected, amitraz had the highest concentration of 16.9 mg/kg, followed by coumaphos at 7.1 mg/kg and fluvalinate at 1.8 mg/kg. Veterinary treatment chemicals were found to have migrated from the wax to the bee brood and bread, while plant products were found mostly in the bee bread. In the bee brood, the highest concentration was of amitraz, followed by coumaphos, fluvalinate, acrinathrin (insecticide and acaricide), and cypermethrin (insecticide). Although no pesticide was applied on the hive except amitraz, this proves that the bee brood can be affected from contaminated beeswax and bee bread. These positive findings correspond with previous studies, suggesting that such chemicals have been accumulating from recycled wax of previous seasons (Lozano et al., 2019; Morales et al., 2020).

Pesticides can also get transferred into the hive through contaminated pollen and nectar by bees or beekeepers. Tomé *et al.* used *in vitro* rearing to characterize the effect of 7 frequently encountered pesticides in developing honey bees (Tomé et al., 2020). These included amitraz, coumaphos, fluvalinate, chlorpyrifos, imidacloprid (insecticide), chlorothalonil, and glyphosate (herbicide). The pesticides were fed to larvae for 6 days, and their impact on the development, morphology, and physiology of the newly emerged adult bees was assessed. Even though this scenario is not representative of the real world, their findings suggested that the bee survival and health are affected from pesticide exposure, emphasizing the importance of proper hive management for contamination control (Tomé et al., 2020).

Table 1.6.   Structure of various pesticides

Insecticides

Amitraz

Acrinathrin

Aldicarb

Chlorpyrifos

Cypermethrin

Deltamethrin

Endosulfan

Esfenvalerate

Fenpropathrin

Imidacloprid

Methoxyfenozide

| Acrinathrin | Amitraz | Endosulfan |

Acaricides

Coumaphos

τ-fluvalinate

30

Herbicides

Atrazine

Glyphosate

Pendimethalin

Fungicides

Chlorothalonil

Iprodione
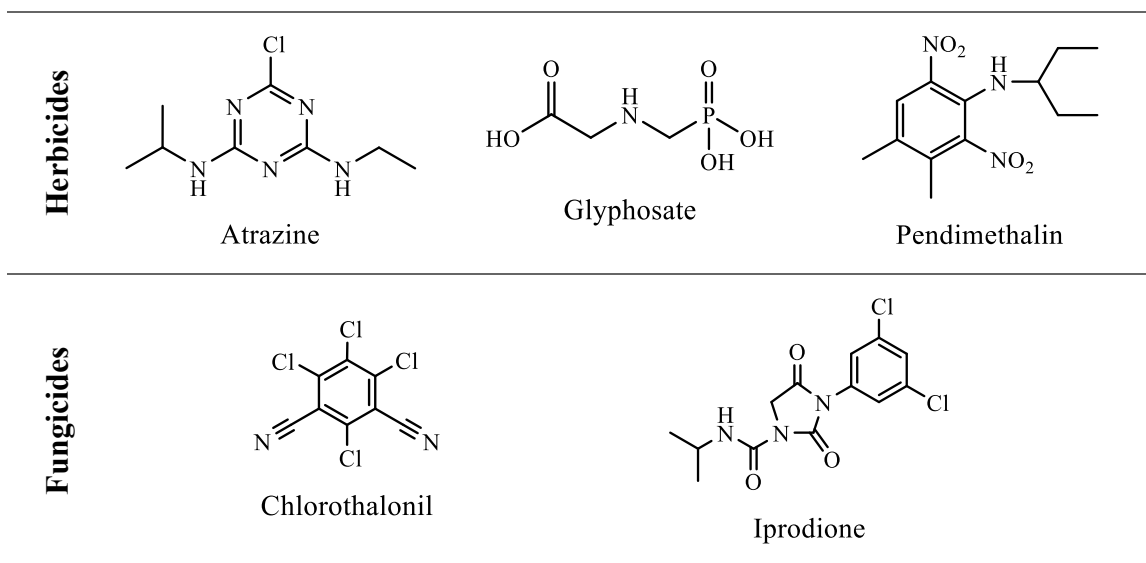
1.3.1. Honey bee detoxification systems

The *A. mellifera* complete genome was obtained in 2006, and it contains 236 Mb and 10157 predicted genes. Compared to *Drosophila melanogaster* (fruit fly), it has more protein-coding genes for pollen and nectar utilization as well as for odorant receptors, and a paucity of genes responsible for gustatory receptors, innate immunity, and detoxification enzymes (Weinstock et al., 2006). The honey bee's detoxification mechanisms have been investigated through toxicity assays, transcript gene expression, protein expression towards xenobiotics, and functional characterization. These types of mechanisms involve several genes and pathways, with cytochrome P450 being the key enzyme for xenobiotic resistance (Gong & Diao, 2017). In general, detoxification of natural and synthetic xenobiotics involves the conversion of lipid to water-soluble substances such as pesticides, natural products, chemical carcinogens and mutagens, plant toxins, drugs, etc. Insects have a deficit of detoxification genes belonging to the 3 main pathways of metabolic resistance: Phase I (functionalization), Phase II (conjugation), and Phase III (excretion) (Figure 1.8) (Berenbaum & Johnson, 2015; Gilbert, 2012).

PHASE I **PHASE II** **PHASE III**
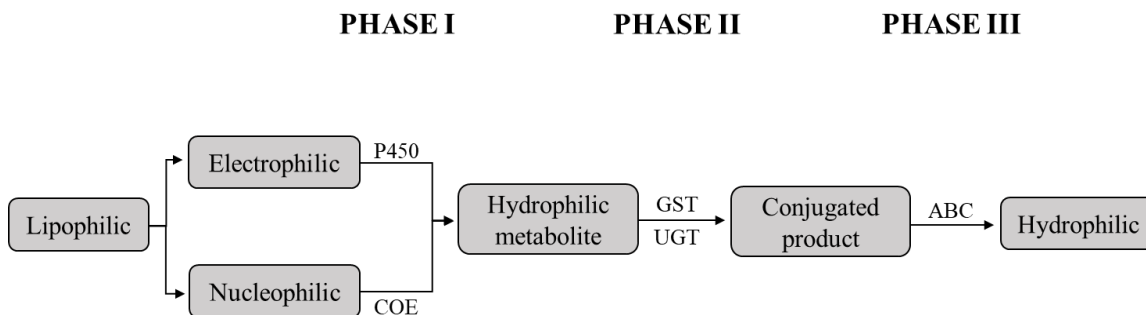
Figure 1.8. **Pathways of metabolic resistance. COE is carboxylesterases, GST is glutathione-S-transferases, UGT is uridine 5′-diphospho-glucuronosyltransferases and ABC: ATP-binding cassette transporters.**

In Phase I, the structure of xenobiotics is altered enzymatically mainly by cytochrome P450s and carboxylesterases (COE), and even through flavin-dependent monooxygenases and cyclooxygenases, making them less potent for interaction with target lipophilic sites (Sehlmeyer et al., 2010; J. Xu et al., 2013). *A. mellifera* utilizes 48 P450 genes for detoxification of honey and pollen flavonoids, pesticides, and mycotoxins (Claudianos et al., 2006; Iwasa et al., 2004; Mao et al., 2009). Specifically, CYP4, CYP6, CYP9, CYP301, CYP302, CYP303, CYP305, CYP306, CYP307, CYP314, CYP315, and CYP343 families are the most potent for the metabolism of xenobiotics.

CYP4AA1 and CYP4G11 have been sequenced independently by polymerase chain reaction (PCR), however, there is not much information about them as they were not on contiguous pieces of assembled DNA, thus, they are an educated guess (Claudianos et al., 2006). Genes of the CYP6 family are known to be overexpressed the most in honey bees, contributing considerably to insecticide resistance. CYP6BC1 is also an informed guess through PCR (Claudianos et al., 2006), while CYP6BD1, CYP6AS2, and CYP6AS5 are upregulated in worker bees by p-coumaric acid (main pollen cell wall constituent) and CYP6AR1 by imidacloprid (insecticide) (Derecka et al., 2013; Mao et al., 2013). Honey bees have also been treated with a sublethal dose of thiacloprid (neonicotinoid insecticide) and undergone transcriptome profiling, as a result, CYP6BE1 and CYP6AS5 were confirmed to be upregulated by quantitative PCR (qPCR) (Alptekin et al., 2016). Genes CYP6AS1, CYP6AS3, CYP6AS4, and CYP6AS10 are upregulated in pollen, honey, and propolis and can metabolize quercetin, a flavonoid that is abundant in the bee diet and is

32

known for upregulating detoxification genes (Ardalani et al., 2021; Johnson et al., 2012; Mao et al., 2009). CYP6S14 is upregulated by thymol, a monoterpene that is used as an acaricide against Varroa (Boncristiani et al., 2012). Another P450 family that contributes to the detoxification of xenobiotics is CYP9. The impact of coumaphos and fluvalinate (insecticides) has been explored through genome-wide expression patterns of worker bees, as they are the most frequently encountered pesticides in the beehive. Despite the different modes of action of these pesticides, it was discovered that CYP9S1 and CYP9Q3 are induced by a pollen-based diet, contributing to the reduced sensitivity of the bees towards the pesticide chlorpyrifos (Schmehl et al., 2014). The midgut P450s of *A. mellifera* have been expressed and it was demonstrated that CYP9Q1, CYP9Q2, and CYP9Q3 can metabolize fluvalinate to a metabolite suitable for cleavage by COEs. Also, real-time PCR assays have shown that CYP9Q1 and CYP9Q2 transcripts were enhanced by bifenthrin (insecticide), while CYP9Q3 were repressed (Mao et al., 2011).

A number of genes encoding the detoxification enzymes CYP301A1, CYP305D1, and CYP315A1 have also been identified and overexpressed against thiacloprid (Alptekin et al., 2016). Honey bee exposure to coumaphos led to an increase in the expression of CYP305D1 (Schmehl et al., 2014). Additionally, several honey bee sequences have close similarities and even precise orthologs with *D. melanogaster* enzymes, and is likely that their roles are similar in *A. mellifera.* Genes that are believed to be involved in ecdysone (steroidal pheromone) regulation during the adult cuticle formation are CYP18A1, CYP301A1, CYP302A1, CYP306A1, CYP307A1, CYP314A1, and CYP315A1. More educated guesses of other detoxification enzymes include CYP303A1 and CYP343A1, while there are mentions about CYP15A1, CYP18A1, CYP334, CYP336, and CYP342 families since they have similar orthologs with *D. melanogaster* (Claudianos et al., 2006).

Phase I has also COEs that participate in exogenous and endogenous functions and detoxify xenobiotics. In *A. mellifera,* the COE activity is induced by different classes of pesticides (Carvalho et al., 2013). The honey bee genome has 24 functional genes belonging to 10 out of 14 COE clades named from A to N, but only 8 of these genes belong to the intracellular catalytic class that is involved in xenobiotic detoxification (Yu et al., 2009).

In Phase II, there are reactions for solubilization and transport of conjugation products from the previous phase. The core enzymes are glutathione-S-transferases (GST), while other enzymes include aminotransferases, phosphotransferases, sulfotransferases, glycosyltransferases, and glycosidases (J. Xu et al., 2013). GSTs detoxify electrophilic xenobiotics through conjugation with glutathione (plant antioxidant) and consist of 6 subclasses: delta, epsilon, theta, zeta, omega, and sigma. Specifically, delta and epsilon are responsible for detoxification in insects, and out of these classes, *A. mellifera* has 10 functional genes discovered so far. The honey bee genome also has 12 Uridine 5'-diphospho- glucuronosyltransferases (UGT) that are responsible for rendering nucleophilic substrates hydrophilic, however, there are no known UGT natural substrates for herbivorous insects such as bees (Ahn et al., 2012).

In Phase III, conjugates of Phase II are transported out of the cells for excretion, whereas the principal proteins are ATP-binding cassette (ABC) transporters (transmembrane proteins) which are known for their multidrug resistance (Dermauw & Van Leeuwen, 2014). These proteins hydrolyze ATP and transfer conjugated or polar products across the lipid membranes to the extracellular space and excrete them. There are approximately 8 subfamilies of ABC proteins in insects from ABCA to ABCH, but additional ones exist in other taxa (Gott et al., 2017). There are not many of them known in insects, and *A. mellifera* has a small inventory of 41, with 15 of them belonging to the ABCG subfamily. The ABC subfamilies that are implicated in xenobiotic metabolism are ABCB FT (full transporter) composed of P-glycoproteins (multidrug resistance), followed by ABCC and ACBGs that consist of other drug resistance proteins (Dermauw & Van Leeuwen, 2014). ABC transporters are associated with the transport and/or resistance of 27 different pesticides from various classes, including organophosphates, pyrethroids, carbamates, neonicotinoids, macrocyclic lactones, cyclodienes, benzoylureas, phenylpyrazoles, and dichlorodiphenyltrichloroethane (DDT) (Buss & Callaghan, 2008; Dermauw & Van Leeuwen, 2014).

1.4. Thesis overview and objectives

The focus of my thesis was to study the degradation of pesticides by cytochromes P450. To address this objective, my research involves two projects: the dehalogenation of polychlorinated compounds by mutants of cytochrome P450$_{cam}$ (CYP101A1) from the soil bacterium *P. putida*, and the dealkylation of dialkoxybenzene compounds by honey bee (*A. mellifera*) cytochromes P450.

Cytochrome P450$_{cam}$'s substrate is camphor, thus, my objective was to degrade the similarly structured polychlorinated pollutants namely endosulfan (ES), ES diol, ES lactone, ES ether, ES sulfate and heptachlor, using the P450$_{cam}$ mutants ES6 and ES7. Unlike the wild-type enzyme, the mutants can accommodate and turnover these larger compounds. In an attempt to confirm that the mutants can dehalogenate the desired substrates, colorimetric assays utilizing 4-aminoantipyrine, hydrogen peroxide and horseradish peroxidase were carried and monitored through UV-Vis spectroscopy. These assays were successful since there was color forming, which is indicative of the production of phenols and/or o-quinones. Steady-state kinetic studies were also conducted to determine the rate of product formation (V_{max}), the binding affinity (K_M) of the substrate, and subsequently, the turnover number (k_{cat}) and catalytic efficiency (k_{cat}/K_M). The rate of the product formation at low substrate concentrations was then compared to determine which of the two mutants is more active and towards which substrate, in comparison to the wild-type enzyme. Finally, molecular docking studies were performed *in silico* on the MOE software to visualize the orientation of each substrate to the active site of the mutants and the wild-type.

Cytochromes P450 can be found in different body parts of honey bees (e.g. head, thorax, abdomen), and different tissues (e.g. hypopharyngeal gland, fat body, midgut, malpighian tubules) that are responsible for the metabolism and detoxification of pesticides. My objective here was to investigate whether the honey bee P450's can degrade the dialkoxybenzene compounds namely 1-allyloxy-4-propoxybenzene, 1,4-dipropoxybenzene and 1,4-diallyloxybenzene, which have been tested against *Varroa destructor*, a parasite that infests the bees. In order to verify the dealkylation of these

compounds, **3c**{*3,6*} treated and untreated honey bees were tested in colorimetric assays using again the same method with 4-AAP, but this time including a NADPH regeneration system containing NADPH, glucose-6-phosphate (G6P) and glucose-6-phosphate dehydrogenase (G6PDH). The assays were successful since there was color forming, which is indicative of the production of phenols. Steady-state kinetic studies were also conducted to determine the rate of product formation (V_{max}) and calculate the specific activity (nmol/min/µg) of the enzymes. Finally, the formation of the single and/or double dealkylated products of the dialkoxybenzenes was determined and quantified through GC-MS analysis.

Chapter 2.

Bacterial cytochromes P450 in degradation of polychlorinated pesticides

2.1. Past mutagenesis studies

Mutagenesis is a process that alters the DNA sequence to induce mutations and produce desired modified organisms and biomolecules, including mutated proteins. Since $P450_{cam}$'s substrate is camphor, it was first mutated in order to expand its substrate acceptance. To create variants of this enzyme, two approaches have been used by our group: Sequence Saturation Mutagenesis (SeSaM) and Site-Directed Mutagenesis.

SeSaM was performed by a previous PhD, Dr. Brinda Prasad (Prasad, 2013). This is a method developed by Schwaneberg *et al.* in 2004 that results in random mutations which aim for the directed evolution of enzymes. It can generate a mutant library in 4 steps: 1) generation of DNA fragments with random length, 2) addition of universal bases at the 3' termini of these fragments, 3) elongation to the full-length genes with PCR, and 4) replacement of the universal bases using the standard nucleotides (Wong et al., 2004). A SeSaM-mutated library of $P450_{cam}$ was selected against endosulfan (ES) as a substrate with m-CPBA as a shunt, and seven mutants (ES1-ES7) survived that were able to metabolise the compound (Table 2.1) (Prasad, 2013).

Table 2.1. **SeSaM P450cam mutants.**

Clone	Mutation
ES1	T56A/N116H/D297N
ES2	F292S/A296V/K314E/P321T
ES3	Q108R/R290Q/I138N
ES4	S221R/I281N
ES5	A296P
ES6	G120S
ES7	V247F/D297N/K314E

To facilitate the production of the P450cam mutants, site-directed mutagenesis was performed by a current PhD, Dr. Abdul Rehman (Rehman, 2021). This method was patented by Stratagene in 1998 and it can introduce desired mutations into a genome in a controlled way. It helps with studying the impact that an amino acid has to the protein's function, structure and interactions with other proteins. It consists of 3 steps: 1) Synthesis of the mutant strand, which includes the performance of thermal cycling to denature the DNA template, anneal of mutagenic primers and extension with a DNA polymerase template, 2) digestion of the parental methylated DNA with the restriction enzyme Dpn I, and 3) transformation of the mutated molecule into competent cells for nick repair (Agilent Technologies, 2015). To facilitate the expression and purification of the P450cam mutants, the WT P450cam plasmid was placed in a ligation-independent cloning (LIC) vector with a purification His-tag (6 residues) at the N-terminus which can be cleaved by Factor Xa protease. Finally, the isolated plasmid was transformed into BL21 (DE3) competent *E. coli* cells (Rehman, 2021). Moreover, a bicistronic recombinant expression vector was used, containing both the electron transfer partners of P450cam, putidaredoxin (PdX) and putidaredoxin reductase (PdR) that was constructed by a current PhD student, Priyadarshini Balaraman. Both genes in this vector also have a His-tag for easier purification. This construct was finally transformed into BL21 (DE3) competent *E. coli* cells for expression (Kammoonah et al., 2018).

2.2. Polychlorinated substrates

Endosulfan is an organic hexachlorinated pesticide that was used against insects and mites, resulting in its spread across a variety of food crops (Campbell et al., 1991; Grout & Richards, 1992; Hough-Goldstein & Keil, 1991; Weiss et al., 1991). The Stockholm Convention has classified endosulfan as a Persistent Organic Pollutant (POP), and in 2011, it was banned by most European countries, Brazil and Australia (Hogue, 2011; Stockholm Convention, 2001). In 2016, its use was phased out in the US (US EPA, 2010) and banned in Canada (PMRA, 2011).

Endosulfan exists as a set of two diastereomers: α and β endosulfan, while technical grade endosulfan is usually a ratio of 7:3 (α:β) (Schmidt et al., 1997; Scippo et al., 2004). It is very persistent in the environment as it has a long half-life in soil (35-37 days for α ES and 104-265 days for β ES) (Jiménez Torres et al., 2016) and can accumulate in marine environments due to its hydrophobicity (log $K_{owα}$ 4.74 and log $K_{owβ}$ 4.78) (Shen et al., 2005; Shen & Wania, 2005), causing toxicity to the sea life (Teklu et al., 2016; Wessel et al., 2007). Endosulfan is also neurotoxic towards adult humans (Enhui et al., 2016), and can cause adverse effects to human fetuses and newborns (Cappiello et al., 2014; Cerrillo et al., 2005). Moreover, it can be transported atmospherically over large distances, reaching remote regions such as Antarctica (Kelly & Gobas, 2003; Luek et al., 2017; Pozo et al., 2006; J. Weber et al., 2006).

Endosulfan **13** is degraded through oxidation of its sulfite ester to a sulfate moiety **14**. It can then be mono hydrolyzed to endosulfan diol monosulfate or doubly hydrolyzed to endosulfan diol **15** under alkaline conditions (Kullman & Matsumura, 1996). Endosulfan sulfate and diol are the major metabolites, while other metabolites include endosulfan ether **16**, hydroxyether and lactone **17** (Figure 2.1) (Lehotay et al., 1998; Wan et al., 2006). Biodegradation of endosulfan and its metabolites has been studied with fungal strains such as *Chaetosartorya stromatoides, Aspergillus terricola,* (Hussain, Arshad, Saleem, & Zahir, 2007), *Mortierella sp*. (Kataoka et al., 2010), *Cladosporium oxysporum* and *Aspergillus terreus* (Mukherjee & Mittal, 2005), and with bacterial strains such as *Mycobacterium sp.*

(Sutherland et al., 2002), *Pseudomonas aeruginosa, Pseudomonas spinosa* and *Burkholderia cepacian* (Hussain, Arshad, Saleem, & Khalid, 2007).
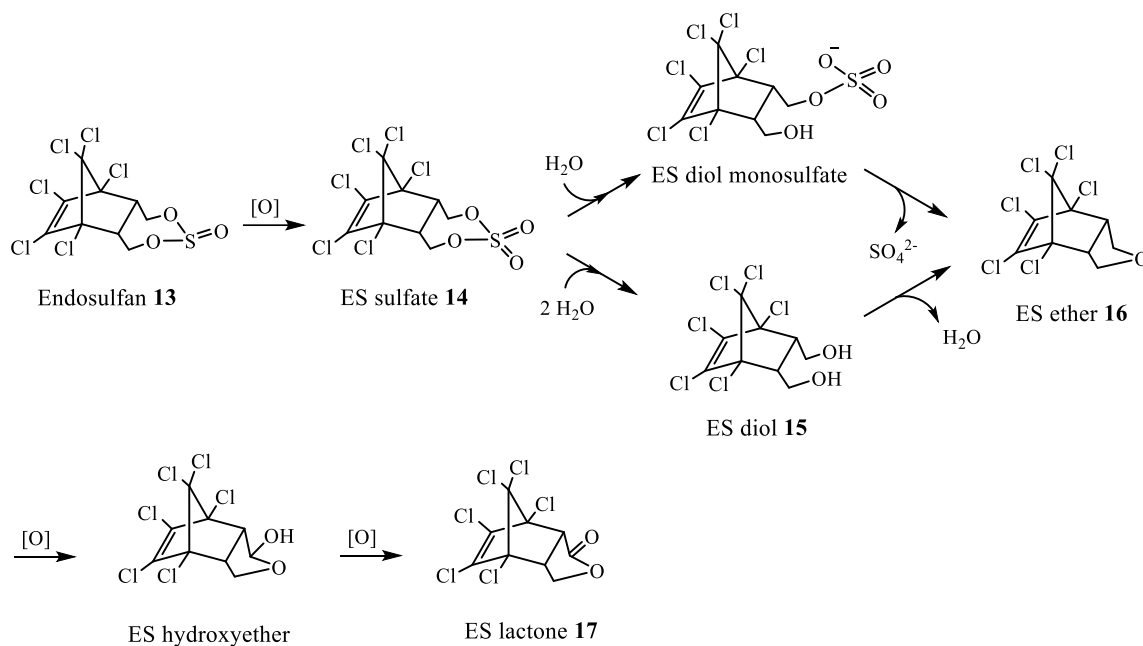
Figure 2.1. **Endosulfan and its known metabolites.**

Heptachlor is a chlorinated dicyclopentadiene compound that was isolated in 1946 from technical chlordane and was mostly used during the 1960s and 1970s by farmers and exterminators against termites (ASTDR, 1989). Most of its applications were banned during the 1980s in many countries and its use was restricted by the Stockholm treaty in 2001 (Stockholm Convention, 2001).

Heptachlor (technical grade) contains ~72% heptachlor with the rest being other related compounds such as trans-chlordane (~20%) and trans-nonachlor (~8%) (NCI, 1977). Due to its hydrophobicity (log K_{ow} 3.87-5.44) it has a long half-life in soil (up to 2 years under certain conditions), so it accumulates in the food chain and is persistent to the environment (ATSDR, 2007; WHO, 2004). It is toxic towards aquatic life (ECETOC, 2003; USEPA, 1980) and causes neurotoxicological effects to rats (Moser, 2001). In humans, it accumulates in adipose tissues increasing the likelihood of breast cancer (Høyer et al., 1998; Ward et al., 2000; Zheng et al., 2000), while it has also been found in breast milk (Alawi, 2002; Stuetz et al., 2001).

Heptachlor **18** can be transformed by abiotic processes and may undergo significant photolysis, oxidation and volatilization (Mabey et al., 1982; Mill et al., 1982). It can get dechlorinated to chlordene and then hydroxylated to 1-hydroxychlordene. Its chloro-cyclopentene moiety can also be epoxidized to heptachlor epoxide (major metabolite), which is more persistent and toxic than heptachlor (Huber, 1993; Wauchope et al., 1992). In aquatic environments, hydrolysis of the epoxide moiety results in heptachlor diol (Figure 2.2). Heptachlor degradation includes conversion to heptachlor epoxide in animals (Harris et al., 1956), plants (Gannon & Decker, 1958), and soil (Gannon & Bigger, 1958; Lichtenstein & Schulz, 1960). Heptachlor and heptachlor epoxide can be degraded by white rot fungi such as *Pleurotus ostreatus* (Purnomo et al., 2014) and several from the genus *Phlebia* (Xiao et al., 2011), as well as by soil bacteria such as *Bacillus subtilis, Bacillus cereus, Pseudomonas putida* (Pokethitiyook & Poolpak, 2012), *Pseudomonas fluorescens, Micrococcus flavus, Bacillus polymyxa* and *Flavobacterium sp.* (Doolotkeldieva et al., 2021).
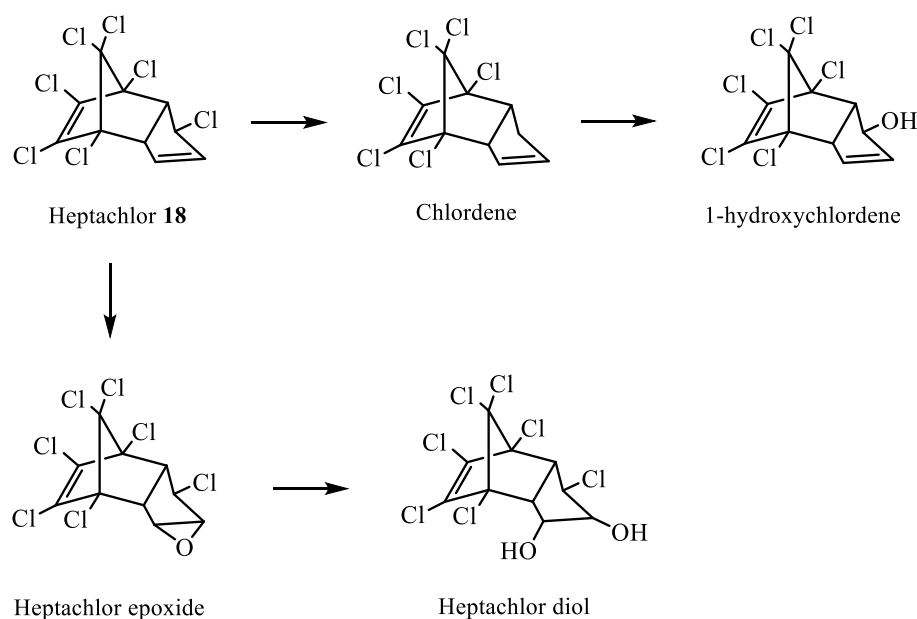
Figure 2.2.   Heptachlor and its known metabolites.

2.3. Introduction

Cytochrome P450$_{cam}$ (CYP101A1) was isolated from the soil bacterium *P. putida* and shows promise in degrading polychlorinated organic pollutants similarly structured to its natural substrate, camphor. This enzyme was used as a template to create a series of mutants through SeSaM and site-directed mutagenesis, named ES1-ES7. The activity of these mutants has been previously tested by a current PhD, Dr. Abdul Rehman, using ES diol **15** as a substrate. It was found that ES2 and ES7 are the most active ones, while ES5 and ES6, even though they have only one mutation, show significant activity. ES1 and ES3 are less active and less stable so are hard to purify. Thus, my objective was to use the two most active mutants, ES6 (G120S) and ES7 (V247F, D287N, K314E), and find out whether the mutations of the WT enzyme have changed the activity of the protein to accept the desired substrates: ES α:β **13**, ES sulfate **14**, ES diol **15**, ES ether **16**, ES lactone **17**, and heptachlor **18**. Their activity was monitored through a colorimetric phenol detection assay as they are expected to produce phenols or o-quinones which can be easily detected via UV-Vis spectroscopy. Finally, kinetic studies followed by molecular docking simulations were performed to assess the effect the different mutations have on the activity towards various substrates in comparison to the WT enzyme.

2.4. Materials, equipment, and methods

All the chemicals used were of analytical grade and were purchased from Sigma-Aldrich (Oakville - Canada), Fisher Scientific (Ottawa - Canada) or Roche Diagnostics (Mannheim - Germany). Ultrapure water was used that was purified by a Synergy® UV Water Purification System from Millipore (Oakville - Canada). All the chemical structures were created with the latest version of the software ChemDraw Pro by PerkinElmer.

Bio-tryptone, Yeast extract, Sodium chloride (NaCl), Potassium chloride (KCl), Magnesium chloride (MgCl$_2$), Glucose, Kanamycin, Ampicillin, Isopropyl β- d-1-thiogalactopyranoside (IPTG), Ferrous chloride (FeCl$_2$), δ-Aminolevulinic acid (δ-ALA), Vitamin B$_1$ (thiamine), Riboflavin, Dipotassium hydrogen phosphate (K$_2$HPO$_4$), Potassium dihydrogen phosphate (KH$_2$PO$_4$), camphor, Ethylenediaminetetraacetic acid

(EDTA), Magnesium sulfate (MgSO$_4$), Phenylmethanesulfonyl fluoride (PMSF), DNase, RNase, Lysozyme, 4-(2-aminoethyl)benzenesulfonyl fluoride (AEBSF), Potassium hydroxide (KOH), Sodium hydroxide (NaOH), Hydrogen chloride (HCl), Tris hydrochloride (Tris HCl), Calcium chloride (CaCl$_2$), Sodium dithionite (Na$_2$S$_2$O$_4$), Imidazole (C$_3$N$_2$H$_4$), 4-Aminoantipyrine (4-AAP), Horseradish Peroxidase (Type VI, HRP), Hydrogen peroxide (H$_2$O$_2$), Nicotinamide adenine dinucleotide, reduced (NADH), Endosulfan (α:β, 7:3), ES sulfate, ES ether, ES diol, ES lactone and heptachlor.

All the buffers used had a pH of 7.4, which was recorded by an Orion 410A pH meter by ThermoFisher Scientific. Centrifugations were done on an Avanti J-26 XPI centrifuge by Beckman Coulter Inc. (Mississauga - Canada), equipped with either a JA-25.50 or a JLA-8.1000 rotor. Sonications were carried out at a 50% duty cycle using the Sonifier 450 by Branson Ultrasonics Corp. (Danbury - USA). The absorbance was monitored by Ultraviolet Visible spectroscopy using a UV-6300PC Double Beam Spectrophotometer by VWR® (Radnor - USA), with a photometric accuracy of ± 0,002 A at 1 A and ≤ 0,3% T.

Electrophoresis was performed using polyacrylamide gels (10%, 12%, 16%) with 10% sodium dodecyl sulfate (SDS-PAGE). The gels were made using a 29:1 ratio of acrylamide and N, N'-Methylenebisacrylamide, sodium dodecyl sulfate (SDS), ammonium persulfate (APS), N,N,N′,N′-Tetramethylethylenediamine (TEMED), resolving buffer was 18% Tris(hydroxymethyl)aminomethane (Tris(OH)), pH 8.8, and stacking buffer was 6.06% Tris(OH), pH 6.8. The running buffer contained Tris(OH), glycine and SDS. The loading buffer was made using 50% sucrose, Tris(OH), bromophenol blue, EDTA and the pH was adjusted at 8. The marker used was BLUelf Prestained Protein Ladder by FroggaBio. The gels were run on a Bio-Rad Mini-PROTEAN® Tetra System for vertical electrophoresis, powered by a Bio-Rad PowerPac 1000 at 120V. The gels were dried on a GD2A Gel Dryer by Labnet International.

Protein purification was done using a glass Bio-Rad Econo-Column® 0.7 × 50 cm for low-pressure, gravity chromatography that had a porous polymer bed support at its bottom to retain fine particles and filled with reusable His•Bind® Resin by Novagen. This

resin is used on proteins with a His-tag, resulting to a quick one-step purification by metal chelation chromatography, and can purify up to 20 mg of target protein on a single 2.5 mL column.

The His-tag was removed using Restriction Grade Factor Xa isolated from Bovine Plasma by MilliporeSigma™. This protease cleaves the protein at the C-terminal side of the recognition sequence Ile-Glu-Gly-Arg (after arginine), while the leftover tag is moved using Amicon® Ultra-15 Centrifugal Filter Units of 30k NMWL by MilliporeSigma™.

Kinetics studies were carried out using the latest version of Graphpad Prism. PyMOL by Schrödinger Inc. (New York - USA) is a visualization system that was used to verify the WT enzyme's structure taken from RCSB PDB (entry 2L8M) and generate the mutants ES6 and ES7. The enzyme-substrate complexes were simulated using Molecular Operating Environment (MOE) by Chemical Computing Group (Montreal - Canada).

2.4.1. Expression, lysis and dialysis of His-tagged proteins

Competent *E. coli* BL21 (DE3) cell strain containing the appropriate plasmid (WT $P450_{cam}$, PdX/PdR, PdX, ES6 and ES7) was inoculated into 50 mL of kanamycin-rich (30 mg/L) Super Optimal broth with glucose (SOC) (3.6 g/L) and incubated overnight at 37 °C, 200 rpm. The resulting culture was subsequently inoculated into 1L of kanamycin-rich (30 mg/L) Luria-Bertani (LB) broth and incubated at 37 °C, 200 rpm, until the optical density (OD) at 600 nm was around 1. Then, IPTG (20 mM) and the trace additives $FeCl_2$ (0.1 μM), δ-ALA (1 mM) and Vitamin B_1 (10 μM) were added, including Riboflavin (1 μM) for PdX/PdR only, and the culture was grown overnight at 27 °C, 200 rpm. The cells were harvested by centrifugation at 4 °C, 6000 rpm for 30 mins and the collected cell pellets were suspended into 50 mL of lysis buffer (50 mM phosphate buffer, 200 mM KCl, pH 7.4). Lysis took place on ice (4 °C), and at that point, EDTA (0.1 mM) was added and stirred for 15 mins while the pH was adjusted to 7.4 using concentrated KOH. Then, a protease inhibitor cocktail of PMSF (100 μL of 40 mg/mL stock in EtOH), AEBSF (100 μL of 1 mg/mL stock) and lysozyme (100 μL of 100 mg/mL stock), including camphor (50 μL of 152 mg/mL stock in EtOH) for the WT only, was added and stirring continued for 40 min. Sonication was carried out at a 50% duty cycle for 10 mins, following that, $MgSO_4$

44

(10 mM) was added and the pH was readjusted to 7.4. DNase (100 µL of 100 mg/mL stock) and RNase (100 µL of 10 mg/mL stock) were added and stirring was carried on for 30 mins, followed by another sonication for 5 mins. The lysate was homogenized using a Tissue Grinder Potter-Elvehjem chamber and pestle, and harvested by centrifugation at 4 ºC, 6000 rpm for 30 min. The supernatant was collected and dialyzed using a Fisherbrand dialysis tube of 6-8k MWCO in lysis buffer (50 mM phosphate buffer, 200 mM KCl, pH 7.4) overnight.

2.4.2. Nickel (Ni^{2+}) affinity chromatography and His-tag cleavage

All the enzymes (WT P450$_{cam}$, ES6, ES7, PdX/PdR, PdX) were purified but only the WT and the mutants had their His-tag cleaved. The dialysate was purified through His•Bind® Resin, where the His-tag sequence of the protein binds to Ni^{2+} cations that are immobilized on the resin using nickel sulfate ($NiSO_4$) as a charge buffer, allowing rapid purification under native conditions. The unbound proteins were washed away while the target protein was recovered by elution with increasing imidazole concentrations (3 mM, 10 mM, 60 mM and 250 mM) in phosphate buffer (50 mM potassium phosphate, 200 mM KCl, pH 7.4). The collected fractions were analyzed by UV-Vis spectroscopy (275-279 nm PdX, 280 nm total protein, 418 nm WT and mutants, 454 nm PdR) and SDS-PAGE. The pure protein fractions were then dialyzed against Tris buffer (20 mM Tris HCl, 50 mM KCl, 1 mM $CaCl_2$, pH 7.4) to remove the imidazole present as it can interfere with the protein's activity prior to conducting an assay, and were concentrated through ultracentrifugation using a millipore filter of 30k NMWL. The absorbance was checked again through UV-Vis spectroscopy and the His-tag was cleaved using Factor Xa protease by adding 10 µL per 2 mg of protein and incubating at room temperature for 36-48 hours. The successful cleavage of the protein was confirmed through SDS-PAGE, while the remaining Factor Xa enzyme and the leftover Hig-tag was removed using Ni^{2+} affinity chromatography with the His•Bind® Resin. The final purified protein was confirmed through UV-Vis spectroscopy and SDS-PAGE and concentrated through ultracentrifugation.

2.4.3. Silver staining of SDS-polyacrylamide gels

Silver staining is a sensitive protein visualization method that uses silver in the form of silver nitrate ($AgNO_3$) to stain the gel by interacting with certain protein functional groups, revealing the location of the protein bands. The gel was processed on a Rocker II 260350 (Boekel Scientific). It was first fixed in a fixing solution (10% MeOH, 5% AcOH) for 30 min and then washed with 95% EtOH for approximately 30 min until it shrank. It was subsequently treated with fresh formaldehyde solution (40% MeOH, 0.5 µL/mL 37% CH_2O) for 15-30 min until it swelled and was rinsed thrice with water. It was sensitized with 0.02% $Na_2S_2O_3$ and rinsed again thrice with water. A solution of 0.2% of $AgNO_3$ was used for 10 min to deposit the metallic silver on the gel and then rinsed thrice with water. The development of the bands was done using fresh developing solution (30 mg/mL sodium carbonate, 2 µL/mL 37% CH_2O, 0.4 µL/mL 1% $Na_2S_2O_3$) and quenched quickly with quenching solution (50% MeOH, 12% AcOH) to avoid overstaining. It was finally washed with 50% MeOH for 30 min to prevent bleaching over time and was then dried for 3 hours at 40 °C (Figures A.1 and A.2, Appendix A).

2.4.4. Carbon monoxide spectrum for WT P450$_{cam}$ and mutants

The absorbance of the oxidized protein (low spin, resting state) in phosphate buffer (50 mM potassium phosphate, 200 mM KCl, pH 7.4) was determined through UV-Vis spectroscopy (250-500 nm). A sample was taken and a small amount of camphor was added and equilibrated for 30 min to ensure a trough at < 400 nm (high spin, type I spectra). CO gas was then bubbled for a few seconds, followed by the addition of anaerobic Tris(OH) buffer that was saturated with $Na_2S_2O_3$ in order to reduce the P450 iron heme. This was repeated a few times and the absorbance was recorded each time to achieve the characteristic Fe^{II}-CO peak (reduced form) at 450 nm and determine the active protein concentration (Figures A.3, Appendix A).

2.4.5. *In vitro* colorimetric phenol detection assay with 4-AAP, HRP and H_2O_2

To investigate the products of the substrate oxidation and HCl elimination, a colorimetric system involving 4-AAP in the presence of HRP and H_2O_2, was used to detect phenols and/or o-quinones through UV-Vis spectroscopy at approximately 500 nm (Figure 2.3) (Varadaraju et al., 2018). 4-AAP is a metabolite of antipyrine that has been broadly used as an analytical reagent for estimating phenols and it was firstly used by Emerson in 1943 (Emerson, 1943). HRP is a heme-containing enzyme, and as the name suggests, it is found in the roots of horseradish. It utilizes H_2O_2 to oxidize a variety of phenols and aromatic amines (substrate/oxygen donor), resulting in color products that are quantifiable spectrophotometrically (Klibanov et al., 1980). During catalysis, an enzyme-intermediate is formed by a single two-electron transfer and is then reduced by two single-electron transfers from the substrate (Morawski et al., 2001; Morishima et al., 1986). 4-AAP acts as a hydrogen donor increasing the absorbance, which results from the decomposition of H_2O_2 from HRP. As a result, the quantitative speed can be measured and then compared to the oxidation of the substrate, allowing faster and easier detection of phenols and quinones and determination of reaction rates.

This method was previously optimized by a current PhD, Dr. Abdul Rehman, using crude lysate of ES7 to obtain the right conditions, and was tested against ES and ES diol at 100 mM and 200 mM. The absorbance was maximum at 506 nm, while three controls were run to exclude random activity and these were: 1) no substrate, 2) no ES7 and 3) no HRP. The results revealed that the formation of a colored 4-AAP adduct requires both the substrate and the P450 enzyme to be present, but not HRP. HRP is generally added to create ortho or para quinones which react with 4-AAP to form an adduct, but since colored products were formed despite omitting HRP, this suggested that the mutant formed a quinone (Rehman, 2021). However, HRP was kept in the assay to ensure that the product was a result of the action between the mutant and the substrate, and not caused by other reagents in the mixture.
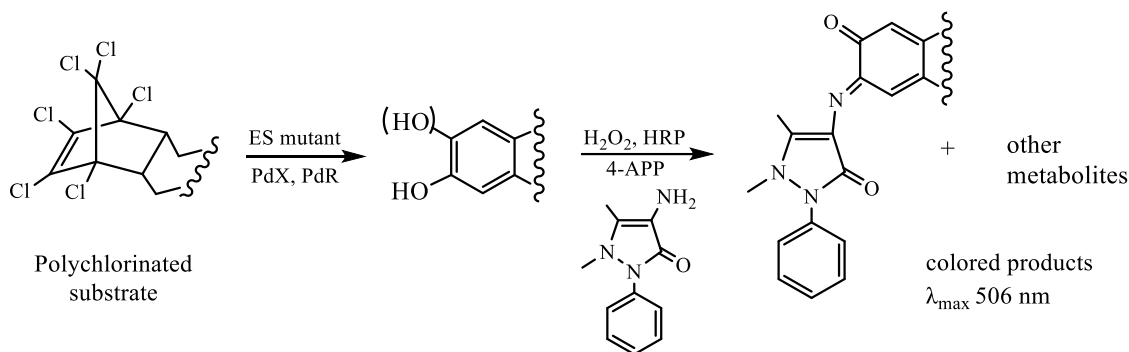
Figure 2.3.   Expected dehalogenation products of the colorimetric assay.

2.4.6. Kinetics and statistical analysis

The colorimetric phenol detection assay produces orange-colored products which are analyzed through UV-Vis spectroscopy. The more intense the color is, the higher the observed absorbance is, reflecting the concentration of the product that was formed. This colorimetric reaction was calibrated using one of the major expected products, 5,6-dihydroxy-2-benzofuran-1(3H)-one. The standard curve that was generated was then used to convert the absorbance to product concentration, and subsequently get the rate of the product formation.
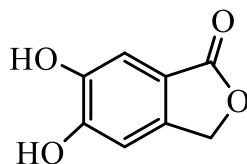
5,6-dihydroxy-2-benzofuran-1(3H)-one

Kinetic studies were carried and plotted on GraphPad Prism, and the data were expressed using the allosteric sigmoidal model. The kinetic parameters V_{max}, K_M, k_{cat} and k_{cat}/K_M were subsequently calculated. V_{max} is the maximum velocity of the reaction at saturating substrate concentrations. K_M (Michaelis-Menten constant) is related to K_{half} (for allosteric sigmoidal kinetics) and represents the binding affinity of the substrate towards the enzyme and the lower it is, the more efficient the enzyme is. The k_{cat} is known as the turnover number, which reflects the number of substrate molecules that are being transformed to product per enzyme molecule (active site) per unit of time, the higher it is,

the more active the enzyme is. Finally, k_{cat}/K_M is used to measure and compare the catalytic efficiency of different enzymes, the higher it is, the better the enzymatic efficiency/reaction is (Price & Stevens, 1999).

Dixon's Q test was carried out to test whether there was any value that differed from the majority of the population and if there were any outliers that needed to be rejected (Dean & Dixon, 1951). This test had the following steps: 1) all the values were arranged in ascending order, 2) the experimental Q-value (Q_{exp}) was calculated (population size, N=3) (Dixon, 1953), 3) the Q_{exp} was compared to the critical Q-value (Q_{crit}) which corresponds to different confidence levels (CL) (Table A.1, Appendix A) (Rorabacher, 1991), and 4) the Q_{exp} and Q_{crit} were compared, where if $Q_{exp} > Q_{crit}$, the value in question can be characterized as an outlier and rejected (CL was set at 99%).

Unpaired student t-test was applied for pairwise comparison between the different enzymes of the same substrate and concentration to check for significant difference between the different means (Student, 1908). Kruskal-Wallis test, followed by original false discovery (FDR) method of Benjamini and Hochberg, was carried out on GraphPad Prism to determine whether there was a significant difference across the different substrates withing the same enzyme and concentration. Kruskal-Wallis test, also known as one-way ANOVA on ranks, is a non-parametric method (does not assume a normal distribution) that is used on three or more groups to assess the differences against the average ranks and test if the samples originate from the same population (Kruskal & Wallis, 1952). The Benjamini and Hochberg method with FDR, is a multiple-comparison correction used to test the multiple hypotheses and avoid Type I and Type II errors (wrongful rejection or false positive) (Benjamini & Hochberg, 1995).

2.4.7. Molecular docking simulations

The amino acid sequence and crystal structure information of the P450$_{cam}$ (CYP101A1) were obtained from the RCSB Protein Data Bank (PDB) database. The reduced CO-bond protein in the presence of camphor with PDB code 2L8M was used as a template for the docking studies (Asciutto et al., 2011). The .pdb file was loaded into PyMOL and the natural substrate was removed along with the CO moiety. The enzyme

was then mutated to obtain ES6 (G120S) and ES7 (V247F/D297N/K314E). This was done by clicking Display → Sequence, to view the amino acid sequence. By going to Wizard → Mutagenesis → Protein, the respective residue can be selected. "No mutation" option was then changed to the desired residue (mutation). The rotamer picked was the one with the highest mutation chance (%). Prior to docking, the polychlorinated substrates were constructed in MOE using "Builder" by clicking Edit → Build → Molecule. The 2D structure was first copied from ChemDraw, pasted into the Builder and converted into 3D through energy minimization (Compute → Energy minimize). The file of the substrates was then converted to .mdb so that it could get imported into the MOE database and used for docking.

The .pdb file of the protein was imported into MOE. Each residue was protonated at pH 7.4, temperature of 300 K and salt concentration (KCl) of 0.2 M, while the charge was assigned using the default settings through Compute → Prepare → Protonate 3D (Labute, 2009), followed by energy minimization of the structure using the "Amber10:EHT" forcefield (RHS → Minimize). The potential docking sites were identified through Compute → Site Finder, which is an algorithm that ranks the binding sites according to their size (Volkamer et al., 2010). "Site 1" was selected (highest-ranked site, protein + heme) and all the "Atoms" were isolated by a selection of "Dummies" that act as placeholders in this program.

The ligands were docked by choosing all the atoms of the P450 polypeptide and the porphyrin moiety as the receptor. A placement methodology named "Triangle matcher" was used to generate poses through systematic alignment of ligand triplets of atoms on triplets of receptor site points (alpha spheres). These poses were then scored by the London dG function which can estimate the free energy of the binding of the ligand for a given pose. The final energy was scored by the GBVI/WSA dG (Generalized Born Volume Integral/ Weighted surface area) function (Labute, 2008), resulting in up to 30 poses. The distribution of poses was obtained from the docking results table on "Database viewer" that ranked them according to each structure's conformational energy (E_{conf}) in kcal/mol (Cornell et al., 1995). The pose with the lowest E_{conf} was selected (Table A.5, Appendix A).

2.5. Results and conclusions

2.5.1. Steady-state kinetic assays of WT P450$_{cam}$, ES6 and ES7 with ES diol, ES lactone, ES ether, ES sulfate, ES α:β and heptachlor using 4-AAP coupled with H$_2$O$_2$ and HRP

The reaction mixture was a freshly prepared solution of phosphate buffer (50 mM potassium phosphate, 200 mM KCl, pH 7.4) containing 1 mM H$_2$O$_2$ and 2 mM 4-AAP, along with 2.2 µg HRP (1 U/ml stock), 1.68 mM NADH, 1 µM of purified P450$_{cam}$ enzyme, 2 µM PdX/PdR, 8 µM PdX, and the desired substrate (in EtOH) diluted in final concentrations of 50/100/200/300/400//500 µM. The total volume of the assay was 500 µL and the absorbance was monitored by UV-Vis spectroscopy at 506 nm for 3 minutes until a stable value was reached. The assay was performed by mixing all the materials together excluding the substrate, blanking the spectrophotometer, and then adding the substrate to record the absorbance. Three controls were run: 1) without the substrate, 2) without the enzyme, or 3) without NADH, to ensure there were not any other reactions resulting in colored products. All assays were done in triplicate (Figures 2.4, 2.5, 2.6).
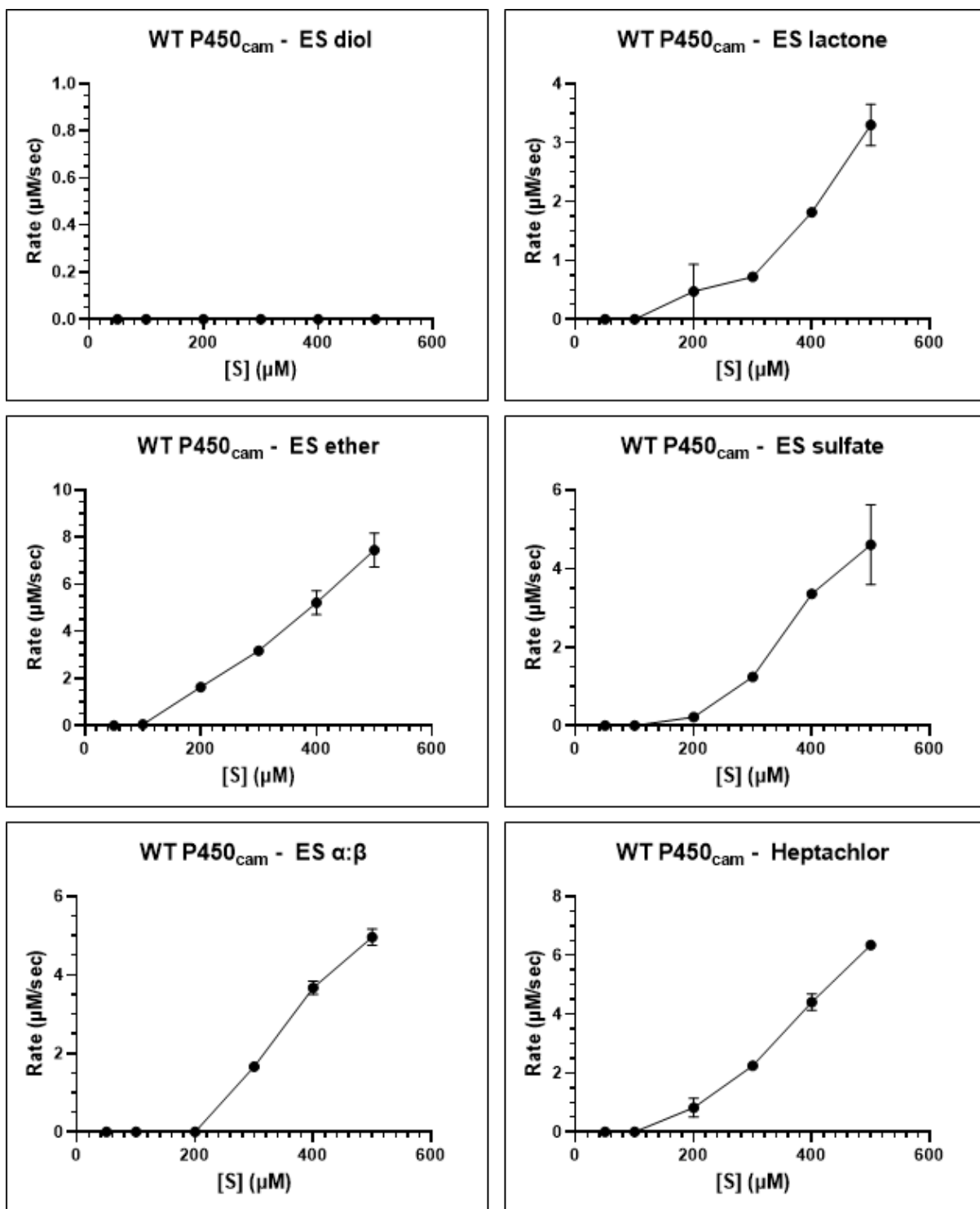
Figure 2.4. **Steady-state kinetic assay plots for WT P450$_{cam}$ and all the polychlorinated substrates. Rate refers to the rate of product formation. The bars represent means ± S. E (3 replicates).**
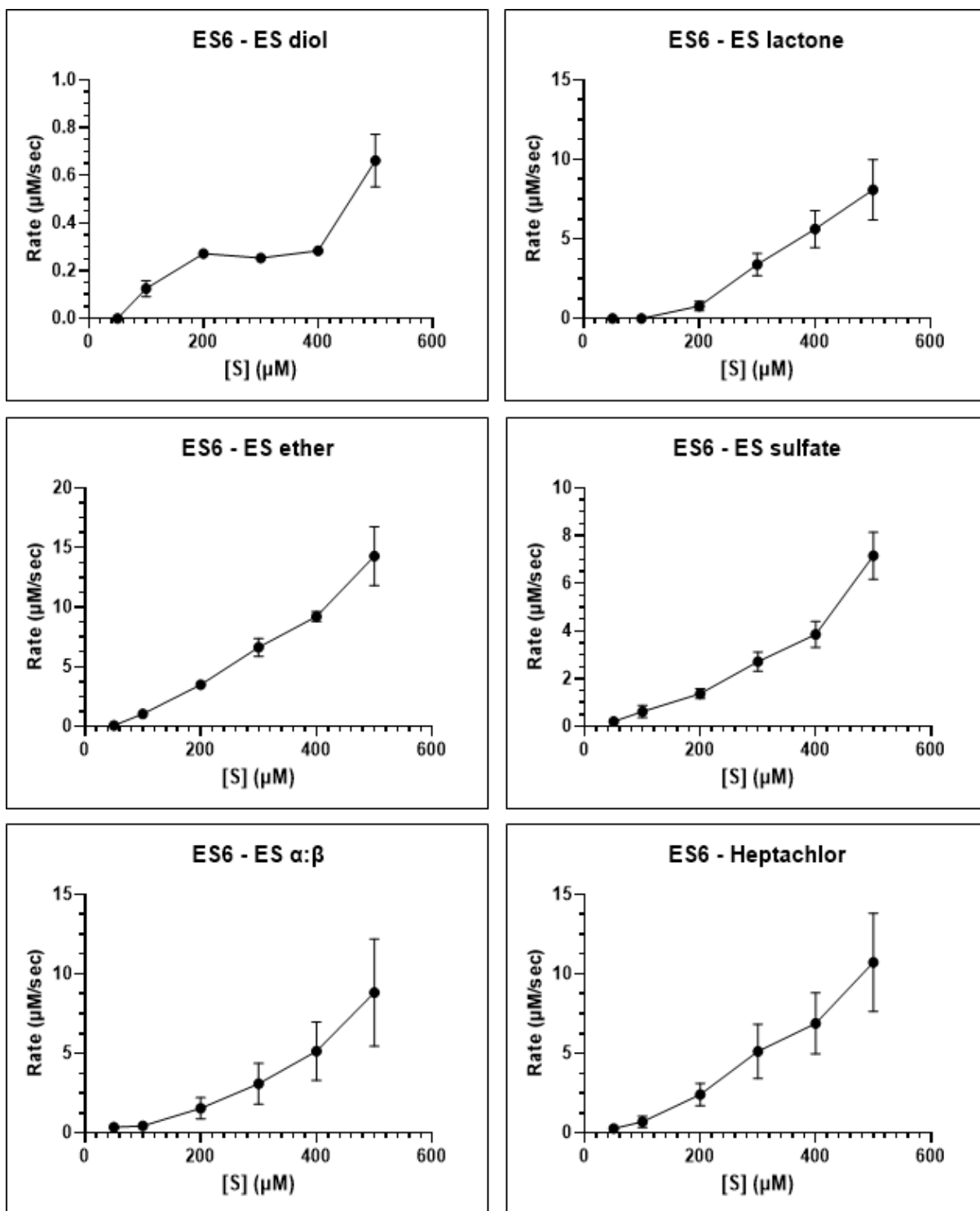
Figure 2.5. Steady-state kinetic assay plots for mutant ES6 and all the polychlorinated substrates. Rate refers to the rate of product formation. The bars represent means ± S. E (3 replicates).
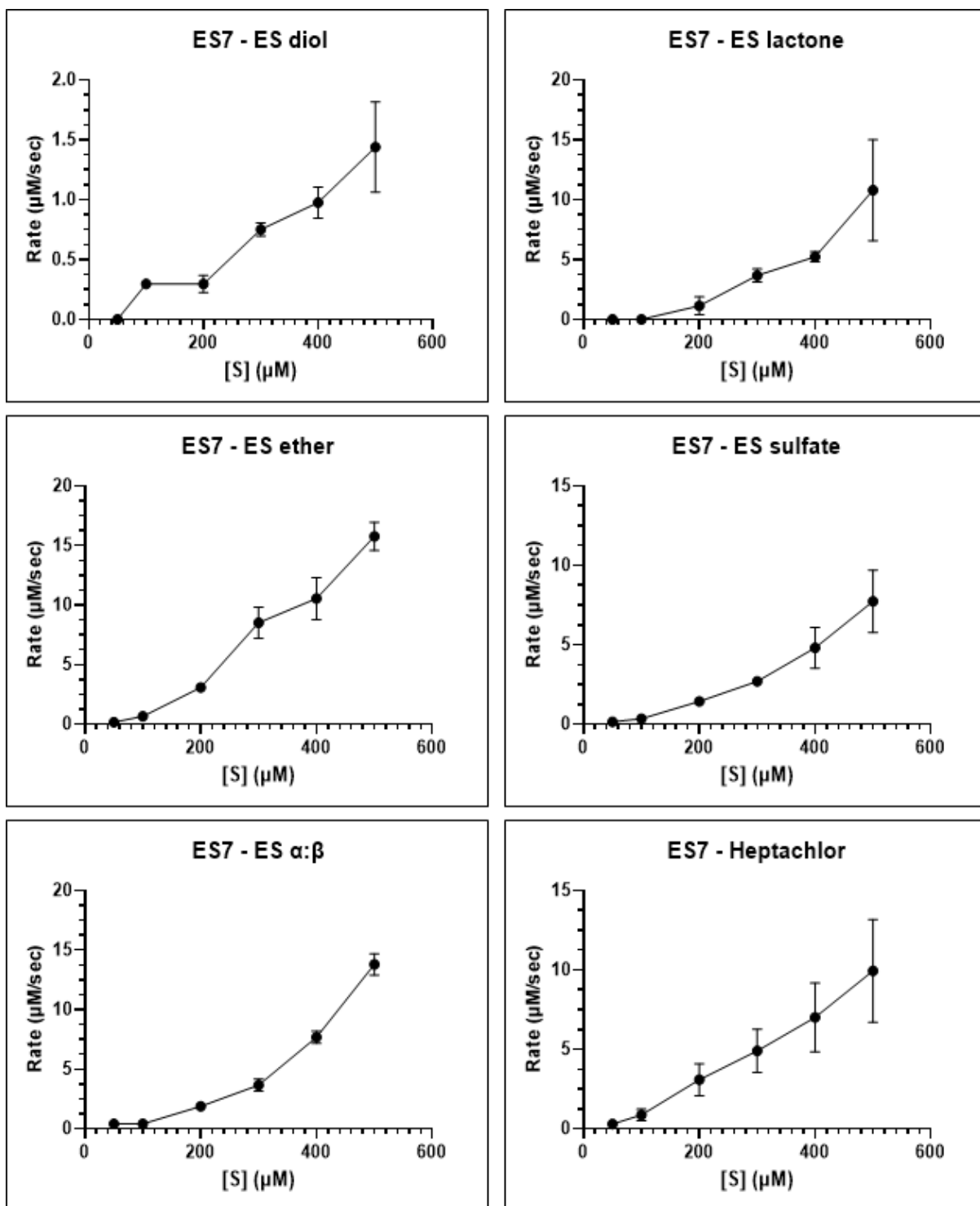
Figure 2.6. Steady-state kinetic assay plots for mutant ES7 and all the polychlorinated substrates. Rate refers to the rate of product formation. The bars represent means ± S. E (3 replicates).

No outliers were found using Dixon's Q test (Tables A.2, A.3 and A.4, Appendix A). From the steady-state kinetic results, the enzymes display a sigmoidal curve on the plot of the rate of the product formation towards the substrate concentration instead of the hyperbola predicted using the typical Michaelis-Menten kinetics model. This could be due to various reasons such as the fact that the catalytic activity of the mutants affects the turnover of the enzyme during the formation of the colored product and that in general, not all substrate-enzyme complexes are very productive. Another reason could be that maybe there could be more than one active site, however, due to the hydrophobicity of these polychlorinated substrates, there are limitations when it comes to increasing the substrate concentration to test this hypothesis. In order for the substrate to be turned over, it needs to bind to the enzyme, something that is evident through the color formation of the assay. Moreover, the sigmoidal curve does not reach saturation, but if the substrate concentration were to be increased, this would result in its precipitation which would subsequently provide inaccurate readings. For that reason, the maximal velocity (V_{max}) and hence the concentration needed to reach $V_{max}/2$ (K_M), is difficult to estimate, same for the dependent k_{cat} and k_{cat}/K_M values.

The rough estimates of the steady-state kinetic parameters (V_{max}, K_M, k_{cat}, k_{cat}/K_M) from the dehalogenation of the polychlorinated substrates are shown in Tables 2.2, 2.3 and 2.4.

Table 2.2. **Steady-state kinetic parameters for the dehalogenation of ES diol, ES lactone, ES ether, ES sulfate, ES α:β and heptachlor by WT P450$_{cam}$. N/D: not detected.**

	WT P450$_{cam}$			
Substrate	V_{max} (μM/s)	K_M (μM)	k_{cat} * (s^{-1})	k_{cat}/K_M (μM$^{-1} \cdot$ s^{-1})
ES diol	0E+00	N/D	0E+00	N/D
ES lactone	2E+03	5E+03	2E+03	4E-01
ES ether	2E+01	6E+02	2E+01	3E-02
ES sulfate	5E+00	4E+02	5E+00	1E-02
ES α:β	6E+00	4E+02	6E+00	2E-02
Heptachlor	1E+01	5E+02	1E+01	2E-02

*k_{cat}=V_{max}/[E] and since [E]=1 μM then k_{cat}=V_{max} in this case.

Table 2.3. **Steady-state kinetic parameters for the dehalogenation of ES diol, ES lactone, ES ether, ES sulfate, ES α:β and heptachlor by mutant ES6.**

	ES6 (G120S)			
Substrate	V_{max} (μM/s)	K_M (μM)	k_{cat} * (s^{-1})	k_{cat}/K_M (μM$^{-1} \cdot$ s^{-1})
ES diol	2E+03	2E+10	2E+03	1E-07
ES lactone	1E+01	4E+02	1E+01	3E-02
ES ether	6E+03	2E+04	6E+03	3E-01
ES sulfate	2E+10	3E+04	2E+10	7E+05
ES α:β	5E+03	1E+04	5E+03	5E-01
Heptachlor	2E+03	1E+04	2E+03	2E-01

*k_{cat}=V_{max}/[E] and since [E]=1 μM then k_{cat}=V_{max} in this case.

Table 2.4. **Steady-state kinetic parameters for the dehalogenation of ES diol, ES lactone, ES ether, ES sulfate, ES α:β and heptachlor by mutant ES7.**

ES7 (V247F/D297N/K314E)				
Substrate	**V_{max} (µM/s)**	**K_M (µM)**	**k_{cat} * (s^{-1})**	**k_{cat}/K_M ($µM^{-1} \cdot s^{-1}$)**
ES diol	9E+02	3E+08	9E+02	3E-06
ES lactone	2E+03	4E+03	2E+03	5E-01
ES ether	3E+01	5E+02	3E+01	6E-02
ES sulfate	4E+03	1E+04	4E+03	4E-01
ES α:β	2E+10	1E+04	2E+10	2E+06
Heptachlor	1E+03	2E+04	1E+03	5E-02

*$k_{cat}=V_{max}/[E]$ and since $[E]=1$ µM then $k_{cat}=V_{max}$ in this case.

From these K_M values it is difficult to say whether the mutants exhibit more efficient binding than the WT enzyme, as in almost every case, the K_M is bigger than the maximum substrate concentration. Both ES6 and ES7 have a higher K_M than the WT, except ES6 with ES lactone **17**, and ES7 with ES lactone **17** and ES ether **16**. V_{max} values are also quite inconsistent, with most of the times being much higher than the highest rate. Even though the activity of the mutants (k_{cat}) and their catalytic efficiency (k_{cat}/K_M) is better than the WT, once again, both of these parameters depend on V_{max} and K_M respectively. Those inaccuracies are likely due to the fact that saturation is never reached. However, it was not possible to reach higher substrate levels, as they would precipitate. For these reasons, it was more appropriate to compare the enzymatic activities across the different enzymes.

2.5.2. Comparison of enzymatic activities of WT P450$_{cam}$, ES6 and ES7 with substrates ES diol, ES lactone, ES ether, ES sulfate, ES α:β and heptachlor

To compare the catalytic activity between mutants ES6 and ES7 versus the WT-P450$_{cam}$, kinetic assays were performed using ES α:β **13,** ES sulfate **14**, ES diol **15,** ES ether **16**, ES lactone **17** and heptachlor **18**. Since these substrates exist in nature at low

concentrations, it was important to investigate the effect the various mutations have in limited substrate concentrations.

The reaction mixture was once again prepared in the same way as described earlier in the chapter. The generated bar graphs depict the rates of the product formation for each enzyme at the different substrate concentrations (Figure 2.7).
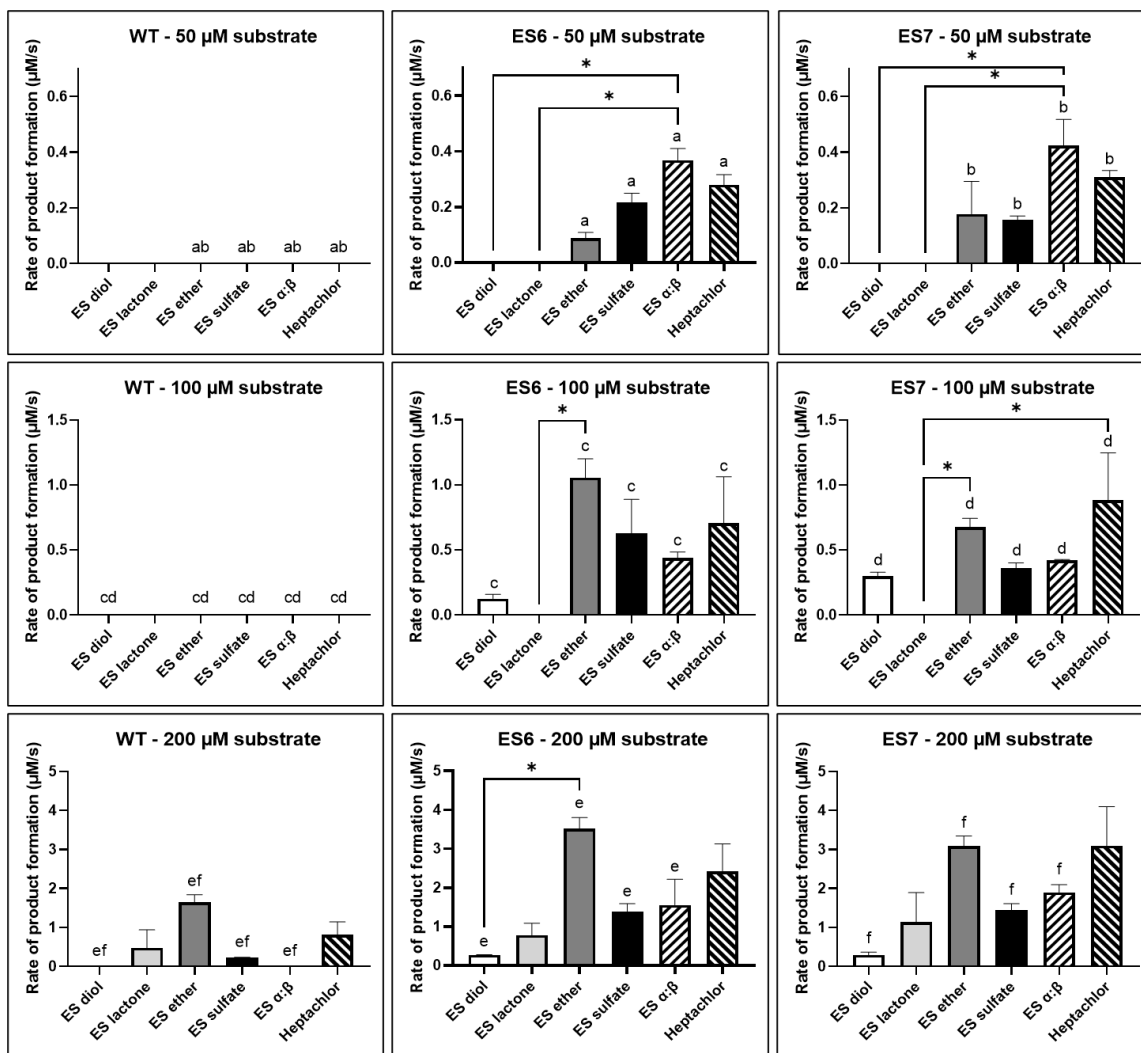
Figure 2.7. **Kinetic comparison of WT P450$_{cam}$ and mutants ES6 and ES7 with ES diol, ES lactone, ES ether, ES sulfate, ES α:β and heptachlor at concentrations of 50 µM, 100 µM, 200 µM. The bars represent means ± S. E (3 replicates). The same letter indicates significant difference between the different enzymes for each substrate at different substrate concentration. These pairwise comparisons were done using student's t-test (p<0.05). The asterisk indicates significant difference between all substrates within the same enzyme and substrate concentration. These multiple comparisons were done using Kruskal-Wallis test, followed by Benjamini and Hochberg FDR adjustment (p<0.05).**

Student's t-test was carried for a pairwise comparison between the different enzymes for each substrate across the different substrate concentrations. Kruskal-Wallis test, followed by Benjamini and Hochberg FDR adjustment were also done for a multiple comparison between the different substrates across the different substrate concentrations and different enzymes.

The t-test showed no significant difference between ES6 and ES7 for any substrate at any concentration. There is however significant difference ($p < 0.05$) between the WT compared to both ES6 and ES7 at 50 μM substrate concentration for ES ether **16**, ES sulfate **14**, ES α:β **13** and heptachlor **18**. Likewise for 100 μM substrate concentration, this time including ES diol **15**. For 200 μM substrate concentration, there is significant difference ($p < 0.05$) between WT and both mutants for ES diol **15**, ES ether **16**, ES sulfate **14** and ES α:β **13.**

Kruskal-Wallis, followed by the FDR Benjamini-Hochberg method showed no significant difference in the WT enzyme across the different substrates. For ES6, at 50 μM substrate concentration, there is significant difference ($p < 0.05$) between ES diol **15** - ES α:β **13** and ES lactone – ES α:β **13**. At 100 μM, there is significant difference ($p < 0.05$) between ES lactone **17** – ES ether **16**, and at 200 μM, between ES diol **15** – ES ether **16**. For ES7, at 50 μM substrate concentration, there is significant difference ($p < 0.05$) between ES diol **15** - ES α:β **13** and ES lactone – ES α:β **13**, and at 100 μM, between ES lactone **17** – ES ether **16** and ES lactone **17** – Heptachlor **18**. No significant difference for the 200 μM substrate concentration.

WT P450$_{cam}$ was conspicuously less active than ES6 and ES7. More specifically, at 50 μM substrate concentration the WT enzyme was inactive, whereas the mutants showed activity with the highest being for ES α:β **13** and heptachlor **18**. ES diol **15** and ES lactone were **17** undetectable with both of them. Once more, the WT was inactive at 100 μM substrate concentration. On the other hand, ES6 and ES7 were more active with ES ether **16** and heptachlor **18**. The least activity was noticed with ES diol **15**, while once again, no activity was detected with ES lactone **17**. Lastly, at 200 μM substrate concentration some activity was evident for the WT, with the highest being with ES ether

16. The mutants were more active with ES ether **16**, followed by heptachlor **18**. The least activity was noticed with ES diol **15**. This time, there was some activity with ES lactone **17** that was interestingly higher than with ES diol **15**.

Overall, the WT P450$_{cam}$ was only active at 200 µM, but still approximately three times less active than ES6 and ES7. ES α:β **13** was the substrate best turned over by both mutants at the lowest concentration, and substrates ES ether **16** and heptachlor **18** at the highest concentrations. Intermediate activity was noticed against ES sulfate **14**, while the least (if not at all) activity was with ES diol **15** and ES lactone **17**.

2.5.3. *In silico* molecular docking simulations of WT P450$_{cam}$ and mutants with the polychlorinated substrate

Molecular docking simulations were necessary in order to understand the way these polychlorinated substrates position themselves into the active site of the enzymes (Figures 2.8, 2.9 and 2.10). The ligand interactions can be seen in Figures A.5, A.6 and A.7, Appendix A. One of the challenges when it comes to engineering the active site of cytochrome P450$_{cam}$, is that unnatural substrates tend to have poor affinity and binding for the enzyme, as they cannot properly position themselves above the porphyrin and get turned over efficiently. This is because they are either too small, resulting in gaps in the active site cavity, or too large, making them unable to fit in the right position (Jones et al., 2000).
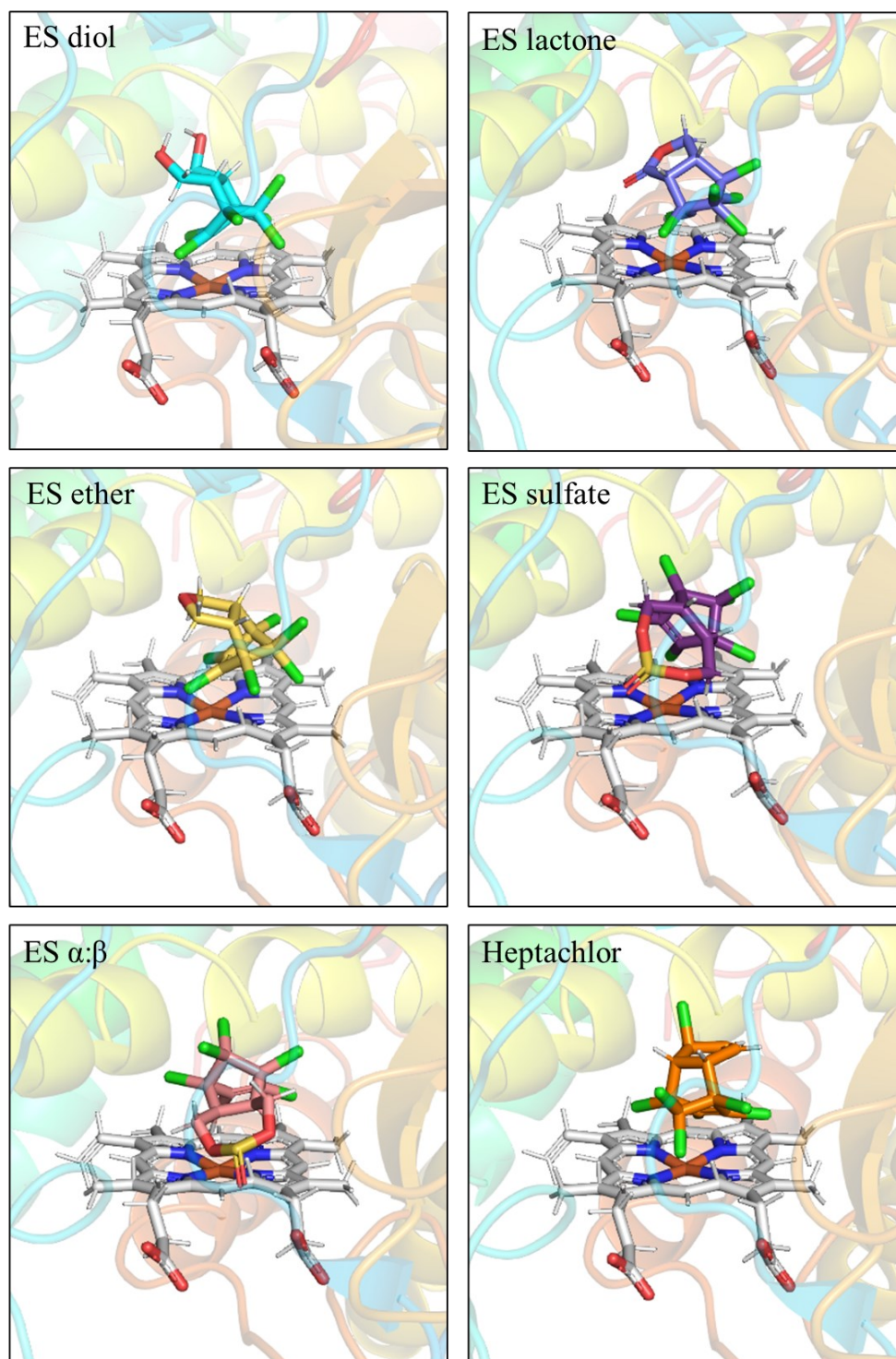
Figure 2.8. Results from docking all the substrates into WT P450cam, which was obtained from modifying PDB 2L8M. The iron-heme is grey, the oxygen atoms red, the nitrogen atoms ultramarine and the chloride atoms green. The carbon chain for each substrate has a different color, cyan for ES diol, faded blue for ES lactone, yellow for ES ether, purple for ES sulfate, salmon pink for ES α:β and orange for heptachlor.
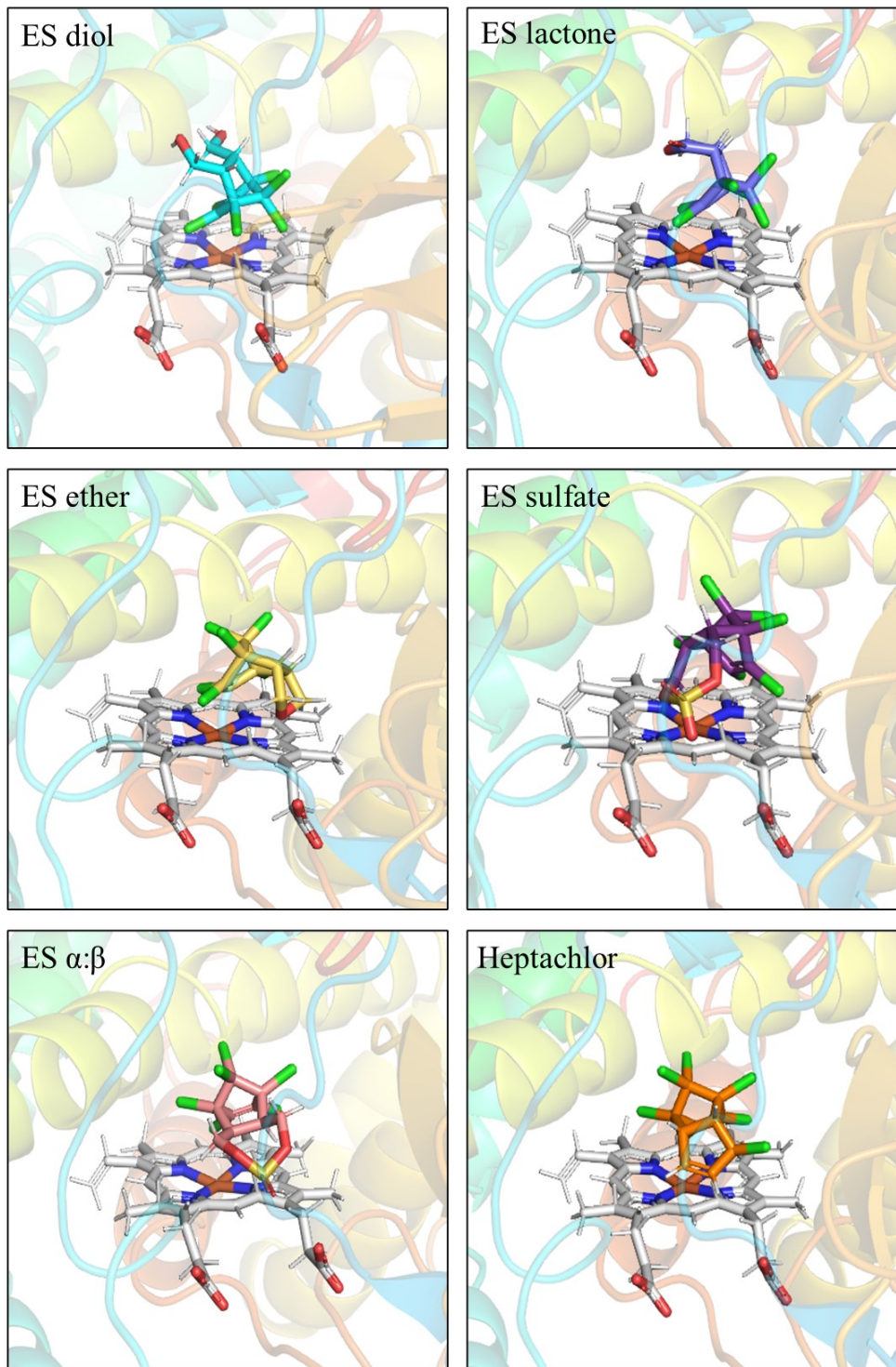
Figure 2.9. **Results from docking all the substrates into ES6, which was obtained from modifying PDB 2L8M. The iron-heme is grey, the oxygen atoms red, the nitrogen atoms ultramarine and the chloride atoms green. The carbon chain for each substrate has a different color, cyan for ES diol, faded blue for ES lactone, yellow for ES ether, purple for ES sulfate, salmon pink for ES α:β and orange for heptachlor.**
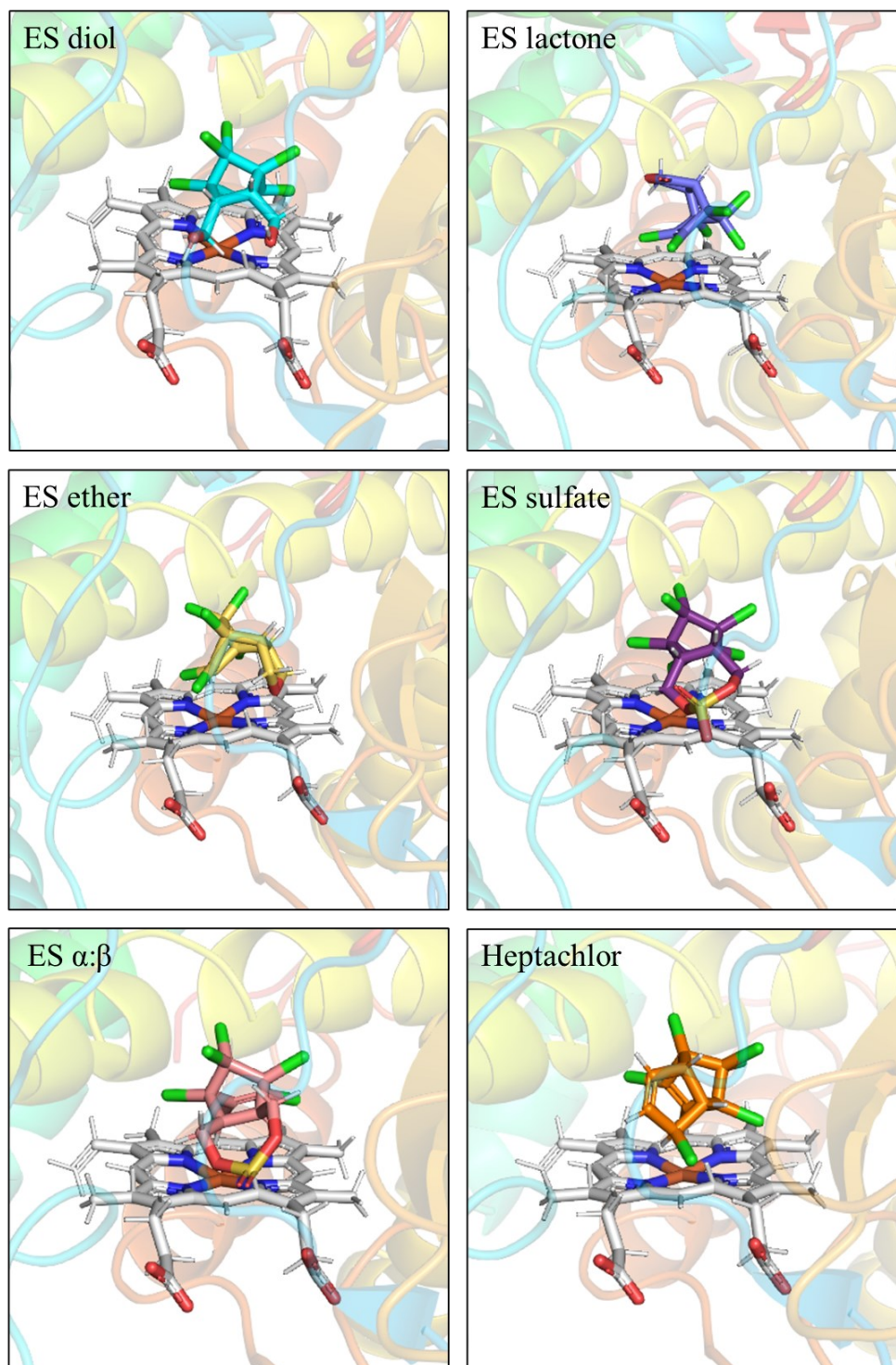
Figure 2.10. **Results from docking all the substrates into ES7, which was obtained from modifying PDB 2L8M. The iron-heme is grey, the oxygen atoms red, the nitrogen atoms ultramarine and the chloride atoms green. The carbon chain for each substrate has a different color, cyan for ES diol, faded blue for ES lactone, yellow for ES ether, purple for ES sulfate, salmon pink for ES α:β and orange for heptachlor.**

The single mutant ES6 (G120S), has glycine replaced with serine, which is bulkier and has an uncharged polar side chain. Residue Gly120 is a component of the CD loop of the WT enzyme, which is located near the heme. There are no reported mutations of this residue in the literature, however, Colthart *et al.* did some NMR studies to investigate the conformational changes upon the binding and removal of the substrate (Colthart et al., 2016). They discovered that chemical shift changes occurred by mutating L244A, which is on I helix that is located on top of the CD loop, causing subsequent perturbations on the loop and especially on Gly120.

The triple mutant ES7 (V247F/D297N/K314E) has valine replaced with phenylalanine which also has a hydrophobic side chain but it is bulkier, aspartic acid (negatively charged side chain) replaced with the uncharged polar asparagine, and lysine (positively charged side chain) replaced with the negatively charged glutamic acid. Residue Val247 has been well studied since it modulates the substrate specificity and stability (Poulos et al., 1987). It is located on the upper part of the active site and specifically on I helix (Poulos et al., 1985). Mutation to V247F has been shown to play a part in the oxyfunctionalization of several monoterpenes (Hernandez-Ortega et al., 2018). Furthermore, this mutation was also identified in a study of the biodegradation of 3-chloroindole by previous students of this group (Kammoonah et al., 2018; Prasad, 2013). However, another study showed that this mutation reduced the total turnover number and regioselectivity of α-isophorone oxidation (Tavanti et al., 2017). Studies on other mutations on this residue involve V247A and V247L, which participate in the oxidation of some alkanes (Bell et al., 2002; Bell, Orton, et al., 2003; Stevenson et al., 1996, 1998), while the second is also responsible for the oxidation of a few terpenes (Bell, Chen, et al., 2003; Bell et al., 2001; Sowden et al., 2005) and some chlorinated compounds (Jones et al., 2000; Walsh et al., 2000; F. Xu et al., 2007). Furthermore, mutation V247M has shown to be involved in the hydroxylation of ethylbenzene (Loida & Sligar, 1993). Residue Asp297 is at a closer proximity to the heme, specifically on the β-sheet between K and K' helices, thus, closer to camphor. The amide side chain of this highly polar residue participates in H-bonding with the heme-7-propionate (Poulos et al., 1985, 1987). This creates a tetrad network that includes the heme-7-propionate, Asp297, Arg299 and Gln322, which is essential for blocking bulk water entrance to the active site (Hayashi et al., 2009). Mutation

to D297N has shown that this tetrad is still being formed (Sakurai, 2009). Moreover, D297N is a recurring mutation in the SeSaM library generated by the previous PhD student Dr. Prasad, and was shown to help by increasing the catalytic efficiency and rate of formation at low concentrations of 3-chloroindole (Prasad, 2013). Other mutations of this residue include D297I and D297T, which have been found to oxidize diphenylmethane (Fowler et al., 1994; Hoffmann et al., 2011; Speight et al., 2004), while D297M was shown to reduce the oxidation activity with propane and butane (Bell, Orton, et al., 2003). Finally, Lys314 is located on the same β-sheet, near Asp297, but it is positioned away from the active site cavity. Mutant K314E was surprisingly recurring in the SeSaM library, however, it has never been reported before.

2.5.4. Proposed mechanism of dehalogenation

Under oxidizing conditions and NADH as the electron donor, the $P450_{cam}$ mutants along with their redox partners PdX and PdR, initiate the degradation by epoxidation of the double bond of the hexachlorinated part of the substrates **13-18** to generate **19**, which quickly gets protonated to **20**. A nucleophilic attack of a water molecule to the carbon cation forms **21**, which immediately releases 2HCl molecules, giving the strained species **22**. This species is unstable, thus it rearranges to **23** and is further hydrolyzed to **24**, which releases 2HCl molecules, resulting in **25**. Decarboxylation occurs to give **26**, that releases the fifth HCl molecule and forms the quinone hydroxyl species **27**. This tautomerizes to the di-keto species **28**, and the last HCl molecule is also released to give **29**. Finally, reduction of this ketone (quinone) to alcohol with NADH results in **30**, which is the most likely final product of this dehalogenation reaction, along with quinone **29** itself (Prasad, 2013).
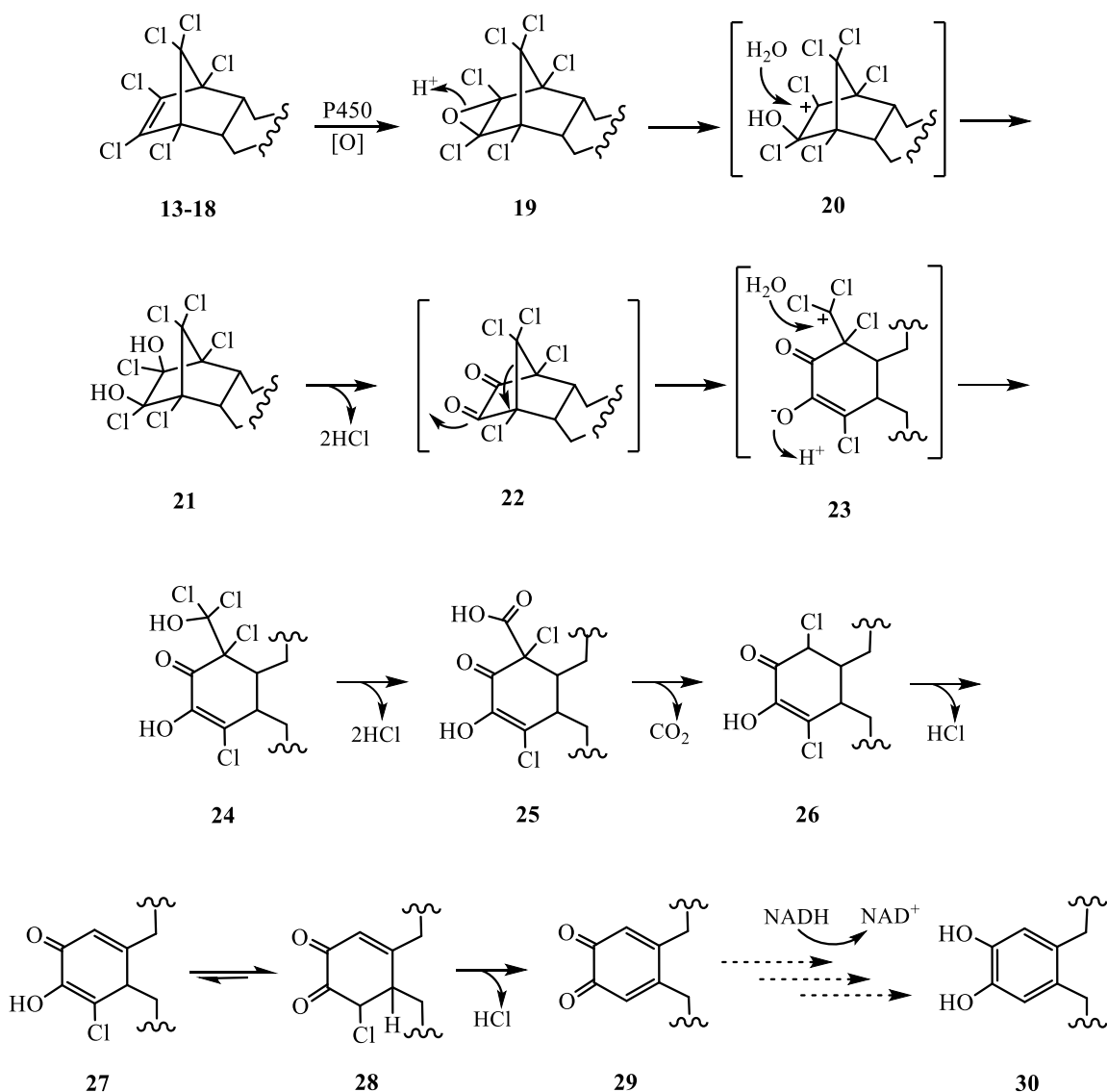
Figure 2.11.   Proposed dehalogenation mechanism of polychlorinated substrates.

2.6.   Conclusions

4-AAP colorimetric assays were carried out followed by steady state kinetic assays using WT P450$_{cam}$, ES6 and ES7 with ES α:β **13,** ES sulfate **14**, ES diol **15,** ES ether **16**, ES lactone **17** and heptachlor **18,** at concentrations of 50/100/200//300/400/500 μM. The rate of product formation at low substrate concentrations was compared between the WT and the mutants in order to determine the effect the mutations have on the activity of the enzyme. There was no significant difference between the mutants, but there was significant difference between them and the WT enzyme. There was also significant difference across

some of the substrates. Mutant ES6 showed the highest rate of product formation with substrates ES α:β **13** at 50 μM and ES ether **16** at 100/200 μM, while the lowest detected rate was with ES ether **16** at 50 μM and ES diol **15** at 100/200 μM. Mutant ES7 showed the highest rate of product formation with substrates ES α:β **13** at 50 μM and heptachlor **18** at 100/200 μM, while the lowest detected rate was with ES sulfate **14** at 50 μM and ES diol **15** at 100/200 μM. Overall, both mutants resulted in a 3-fold increase of the rate of product formation compared to the WT.

Moreover, molecular docking studies were carried out in order to visualize the way the substrates are binding to the enzymes and determine how the different variants affect the size of the catalytic pocket and subsequently the turnover success. Both mutants had similar rates of product formation despite ES6 having only one mutation, while ES7 having three. It is evident that these substitutions caused changes in the WT P450$_{cam}$, resulting in the increased activity and giving the enzyme the ability to accept unnatural substrates.

Chapter 3.

Insect cytochromes P450 in degradation of dialkoxybenzene pesticides

3.1.   Past studies and production of dialkoxybenzene minilibraries

Chemical signals (e.g., tastes, odors) from insects towards plants, parasites and vice versa, are important guides for the detection and selection of hosts for feeding, recognition of predators and discovery of mates (De Moraes et al., 1998; Isman, 2002). Antifeedants are compounds that are known to have insecticidal effects since they negatively influence the feeding habits of insects. These substances are found in plant secondary metabolites such as terpenoids, alkaloids and phenolics (Ahmed & Brattsten, 1986). Phenolics specifically, are essential as they participate in the plant defense, growth, reproduction etc. (Bhattacharya et al., 2010), and several of these are being used against fungi and bacteria (Bennett & Wallsgrove, 1994).

We have been interested in creating analogues that mimic known odorants and can either enhance or inhibit behavioural traits of insects. Since chemical cues play an important role in multiple functions of insects, and especially their sense of smell, my group has worked on the development of low-molecular weight phenolic odorants that can be easily produced using common chemicals such as hydroquinone (Akhtar et al., 2007; Paduraru et al., 2008). Arthropods the group has been working on include the cabbage looper, *Trichoplusia ni*, and the honey bee parasite, *Varroa destructor*. Varroa is becoming resistant towards commercially available acaricides, so finding new compounds to treat beehives against this mite is essential to the beekeeping industry. The most active feeding deterrent against *T. ni* is also the most active acaricide against varroa mites, 1-allyloxky-4-propoxybenzene, coded as compound **3c**{*3,6*} in the original system (Figure 3.1). The first libraries of dialkoxybenzene compounds were prepared by Paduraru *et al*. and were tested against *T. ni.* (Akhtar et al., 2007; Paduraru et al., 2008). Later studies, described in Eliash *et al*., focused on the host choice of varroa mites (Eliash et al., 2014). From the various dialkoxybenzenes that were tested against varroa, compound **3c**{*3,6*} was found to

paralyze and kill the mites. Structure-activity studies done by another MSc in the group, Soniya Dawdani, showed that 1,4-dipropoxybenzene (**3c**{*3,3*}) and 1,4-diallyloxybenzene (**3c**{*6,6*}) were both active, but less than **3c**{*3,6*} (Figure 3.1) (Dawdani, 2021). Field trials with compound **3c**{*3,6*}, done jointly between our lab and Dr. S. Pernal (Agriculture and AgriFood Canada) demonstrated that this compound is active and of potential use in the management of the varroa mite infestation of bee colonies (unpublished). Tests in cages with bees fed **3c**{*3,6*} showed that the compound is not toxic to them (Singh et al., 2020), which raises the question whether bees can metabolize this compound.

| 1-allyloxy-4-propoxy benzene | 1,4-dipropoxy benzene | 1,4-diallyloxy benzene |
| **3c {3,6}** | **3c {3,3}** | **3c {6,6}** |
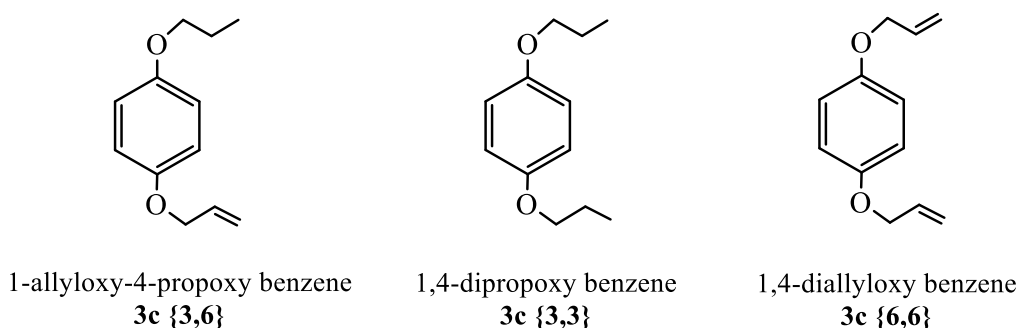
Figure 3.1.   Dialkoxybenzene compounds.

3.1.1. Feeding, olfaction, oviposition deterrence and physicochemical properties of the dialkoxybenzene compounds

It has been previously found through studies of my group, that some of these dialkoxybenzene compounds possess feeding and oviposition deterrence towards the invasive pests, *T. ni* (Akhtar et al., 2007, 2010)*,* and gypsy moth larvae, *Lymantria dispar* (Plettner & Gries, 2010). Laboratory leaf disc choice bioassays revealed that the para-substitured dialkoxybenzenes were the most active, with 65% of them having an antifeeding effect in a range of 53-100% at concentrations of 50 µg/cm^2. The overall best antifeeding and antioviposition effects were from compounds with medium-sized groups such as propyl, allyl etc., with the highest being for **3c**{*3,6*} (Akhtar et al., 2007, 2010). Moreover, this compound also showed low toxicity towards cabbage looper larvae (Akhtar et al., 2010; Ebrahimi & Plettner, 2014), while it was more effective than the insect repellent N,N-Diethyl-3-methylbenzamide (DEET) (Akhtar et al., 2010). Other studies investigated the bacterial degradation of **3c**{*3,6*} from cytochrome P450. *In vitro* assays

showed that the stains ATCC 17453 and ATCC 17484 from the soil bacterium *P. putida*, were responsible for the dealkylation of the compound. In comparison to the control, the concentration of **3c**{*3,6*} was decreased (either metabolized or evaporated) by ~75% with ATCC 17453 and ~40% with ATCC 17484 (Ebrahimi & Plettner, 2014). Recently, electrophysiological and behavioral assays were conducted to assess the olfactory effects of **3c**{*3,6*} towards varroa mites and honey bees. The results of the study were similar to a previous study (Singh et al., 2015), and demonstrated that the compound inhibits the mite's ability to respond to the honey bee odor, in respect of host choice communication. Additionally, the response towards **3c**{*3,6*} was a bit stronger than DEET, while further observations revealed that varroa becomes paralyzed (Dawdani, 2021; Singh et al., 2020), and around half the mites die during the assay (Singh et al., 2020). Paralytic activity, detachment from the bee abdomen and eventually death, was also caused by **3c**{*6,6*} (Dawdani, 2021).

These dialkoxybenzene compounds show potential as insect management agents, however, if they are meant to be used for pest control, it is important to know their physicochemical properties (i.e., water solubility, hydrophobicity/lipophilicity, volatility, interaction with soil) in order to predict their fate in the environment. Water solubility represents the capability of a compound to dissolve in water, however, it is not enough to determine the leaching out of soil since these pesticides tend to distribute in other phases too such as air, solids, and hydrophobic mediums. Hydrophobicity/lipophilicity is crucial for the sorption, partition, and uptake of pollutants, and can be determined using the octanol-water partition coefficient (K_{ow}) (Leo et al., 1971). During partitioning, a compound is being distributed between two immiscible phases (1-octanol and water) until it reaches equilibrium. This system is used as the basis for this interaction between the aqueous and biological phase (Jaworska et al., 1995) thanks to the amphiphilic nature of 1-octanol which makes it a great candidate for modeling the distribution of chemicals (Amellal et al., 2001). The larger the K_{ow} is, the more hydrophobic the compound is, thus the less it will leach out of soil and organic matter (Streit, 1992). Previous studies by my group have calculated the K_{ow} values of the dialkoxybenzene compounds through GC-MS and determined that they have acceptable physicochemical properties (Ebrahimi, 2012; Ebrahimi et al., 2013; Kammoonah, 2016). More specifically, the most hydrophobic one

was **3c**{*6,6*} with a K$_{ow}$ of 3.5, followed by **3c**{*3,6*} at 2.4 and then **3c**{*3,3*} at 1.46 (Ebrahimi, 2012). It was also determined that these compounds partition less in water and air and adsorb more onto soil and solid (Ebrahimi et al., 2013). Volatility is another important parameter used to determine the transport of chemicals through air (Dörfler et al., 1991), and their efficiency is linked to the evaporation process (Samsonov et al., 1998). This was measured using the liquid-gas partition coefficient (K$_{l/g}$) through GC-MS, and the larger it is, the less volatile the compound is. The least volatile was **3c**{*6,6*} with a K$_{l/g}$ of 9.25, followed by **3c**{*3,6*} at 4.33 and then **3c**{*3,3*} at 3.22 (Ebrahimi et al., 2013). Finally, soil is another important factor in the fate and persistence of chemicals (Bollag et al., 1992; Walker et al., 1992). It mainly consists of inorganic matter and a small amount of organic material (Dube et al., 2001). The sorption of pollutants can either result in the accumulation to the solid components (inorganic) for more hydrophilic, polar molecules, or adsorption by organic matter of less polar molecules due to hydrophobic interactions (Delle Site, 2001; Wauchope et al., 2002).

3.2. Introduction

A library of dialkoxybenzene compounds was previously synthesized by our group (Paduraru et al., 2008), with some of them having acaricidal activity against *Varroa destructor* (Dawdani, 2021). Specifically, 1-allyloxy-4-propoxybenzene (**3c**{*3,6*}) was the most potent one, showing promise as a new control agent against the mites. The ability of three of these dialkoxybenzene compounds, namely 1-allyloxy-4-propoxy benzene (**3c**{*3,6*}), 1,4-dipropoxy benzene (**3c**{*3,3*}) and 1,4-diallyloxy benzene (**3c**{*6,6*}) to get metabolized by the honey bees was tested. Since varroa mites feed on the fat body, an organ encompassing the abdomen with multiple functions including pesticide detoxification, we suspected that the part of the degradation process occurs there. Thus, my objective was to use the abdomen of treated (1 mM **3c**{*3,6*}) and untreated bees, to detect whether these compounds are being metabolized by cytochromes P450, and subsequently identify their dealkylation products. The formation of products was firstly confirmed through a colorimetric phenol detection assay as they are expected to produce phenols which can be easily detected via UV-Vis spectroscopy. Finally, GC-MS quantitative assays were performed to identify these products and support the initial hypothesis.

3.3. Materials, equipment, and methods

All the chemicals used were of analytical grade and were purchased from Sigma-Aldrich (Oakville - Canada), Fisher Scientific (Ottawa - Canada) or Roche Diagnostics (Mannheim - Germany). Ultrapure water was used that was purified by a Synergy® UV Water Purification System from Millipore (Oakville - Canada). Honey bees were collected from an apiary in Langley, BC (Canada) and placed in a bee-collection jar before being freshly frozen at -79 °C. The buffer used had a pH of 7.4, which was recorded by an Orion 410A pH meter by ThermoFisher Scientific. All the chemical structures were created with the latest version of the software ChemDraw Pro by PerkinElmer, whilst the kinetics studies were carried out using the latest version of Graphpad Prism.

Monosodium phosphate (NaH_2PO_4), Potassium chloride (KCl), Sodium hydroxide (NaOH), Styrene maleic acid (SMA), acidified Coomassie Brilliant Blue G-250 (Bradford reagent), Bovine serum albumin (BSA), 4-Aminoantipyrine (4-AAP), Horseradish Peroxidase (Type VI, HRP), Hydrogen peroxide (H_2O_2), Glucose-6-phosphate (G6P), Glucose-6-phosphate dehydrogenase (G6PDH), Nicotinamide adenine dinucleotide phosphate (NADPH), Methanol (MeOH), Hexane (Hex), Ethyl acetate (EtOAc), 1-allyloxy-4-propoxy benzene (**3c**{*3,6*}), 1,4-dipropoxy benzene (**3c**{*3,3*}), 1,4-diallyloxy benzene (**3c**{*6,6*}), 1,4-dimethoxy benzene (**3c**{*1,1*}), 1-hydroxy-4-propoxy benzene (**2c**{*3*}), 1-hydroxy-4-allyloxy benzene (**2c**{*6*}), hydroquinone (HQ).

Centrifugations were done on an IEC Micromax RF Refrigerated Microcentrifuge by Thermo Scientific. The absorbance was monitored by Ultraviolet Visible spectroscopy using a UV-6300PC Double Beam Spectrophotometer by VWR® (Radnor - USA), with a photometric accuracy of ± 0,002 A at 1 A and ≤ 0,3% T. The assay samples were analyzed by Gas Chromatography Mass Spectrometry (GC-MS) on a Varian Saturn 2000 MS that had a 30 m length Supelco SPB-5 Capillary GC Column of 0.25 mm inner diameter and 0.25 μm film thickness. The method used was programmed as follows: 80 °C (5 min hold), 10 °C per min until 250 °C (1 min hold), total run time of 23 min. The volume of the injected sample was always 1 μL. Calibration curves were obtained for 1-allyloxy-4-propoxy benzene (**3c**{*3,6*}), 1,4-dipropoxy benzene (**3c**{*3,3*}), 1,4-diallyloxy benzene

(**3c**{*6,6*}), 1-hydroxy-4-propoxy benzene (**2c**{*3*}), 1-hydroxy-4-allyloxy benzene (**2c**{*6*}) and hydroquinone (HQ), at concentrations of 10/15/20/50/100/150 μg/μL.

3.3.1. Bee protein extraction using SMA copolymer

The styrene maleic acid (SMA) copolymer used was synthesized by a group member, Dr. Govardhana Pinnelli, with styrene and maleic anhydride, following a standard protocol (S. C. Lee et al., 2016). SMA is an amphiphilic molecule that allows membrane proteins to be extracted from the cells without the need of a detergent by creating water-soluble nanodiscs which conserve a part of the protein's native membrane (Dörr et al., 2016; S. C. Lee et al., 2016; Smirnova et al., 2018). Honey bee abdomens were dissected, weighted and rinsed with phosphate buffer (100 mM NaH_2PO_4, 50 mM KCl, pH: 7.4 using concentrated NaOH). The membranes were extracted using 2.5% SMA in phosphate buffer (1g SMA per 10g of wet membrane) at room temperature through homogenization with a Tissue Grinder Potter-Elvehjem (PTFE) chamber and pestle. The extracted wet membranes were then separated from the bee's exoskeleton and an equal amount of phosphate buffer was added to collect any leftover membranes, resulting in a 1.25% SMA extract. The membranes were firstly centrifuged at 10.000 ×g for 5 min and the supernatant was collected and kept in the fridge at 4 °C. Into the debris, 1:1 of 2.5% SMA buffer to phosphate buffer was added, mixed and centrifuged again at 10.000 ×g for 5 min to collect any protein trapped in there. The supernatant was once again collected and combined with the previous one before being centrifuged again at 10.000 ×g for 20 min. Finally, the extracted protein was filtered using a 0.45 μm syringe filter to remove particulate impurities and then stored at 4 °C.

3.3.2. Bradford assay

Bradford assay is a quantitation method that utilizes Coomassie Brilliant Blue G-250 dye to bind to proteins and was developed by Bradford in 1976 for the determination of a solution's protein concentration (Bradford, 1976). This dye shifts between 3 species: a red/brown-colored cationic with A_{max} at 470 nm, a green-colored neutral with A_{max} at 650 nm, and a blue-colored anionic with A_{max} at 595 nm (Compton & Jones, 1985). It is more

commonly known as Bradford reagent, where the dye is acidified with phosphoric acid and exists in its red/brown form. Upon binding to the protein, it shifts to the blue form and can be detected spectrophotometrically at 595 nm (Sedmak & Grossberg, 1977). However, there can be interferences in the dye's action such as detergents, basic buffers or basic and aromatic amino acids (Compton & Jones, 1985). Since SMA is an aromatic copolymer, it also binds to the dye, hence, SMA controls were used to remove the background from the bee samples. Bovine serum albumin (BSA) was used to create a calibration curve. A stock of 0.1 mg/mL BSA was diluted in water to final concentrations of 0/1/2.5/5/10/50 μg per 1 mL assay volume, which also included 300 μL Bradford reagent. The color formation is rapid and the absorbance was recorded by UV-Vis spectroscopy at 595 nm. Through the standard BSA curve, the unknown samples were interpolated using the linear-regression model of Graphpad Prism, and the honey bee protein extract concentration was determined. This assay is quite sensitive and detects concentrations as low as 0.5 μg/mL (Ernst & Zor, 2010; Spector, 1978).

3.3.3. NADPH regeneration system

Insect cytochrome P450s belong to Class II microsomal P450s (Munro et al., 2007), making them dependent on NADPH, a cofactor that is quite expensive, thus a recycling system was required for such a stoichiometric analysis. The system is based on the oxidative pentose phosphate pathway, which acts as a shunt for the catabolism of glucose, leading to the production of NADPH. It is an alternative pathway to glycolysis that utilizes the enzymes glucose-6-phosphate dehydrogenase (G6PDH), gluconolactonase and 6-phosphogluconate dehydrogenase, for the conversion of glucose-6-phosphate (G6P) to ribulose-5-phosphate, a precursor of major biomolecules that are also a source of NADPH (Figure 3.2) (Spaans et al., 2015). The regeneration system involves G6P, G6PDH and NADPH, and was optimized according to Millipore Sigma's Enzymatic Assay of Glucose-6-Phosphate Dehydrogenase (EC 1.1.1.49) which was based on Noltmann's method (Noltmann et al., 1961).
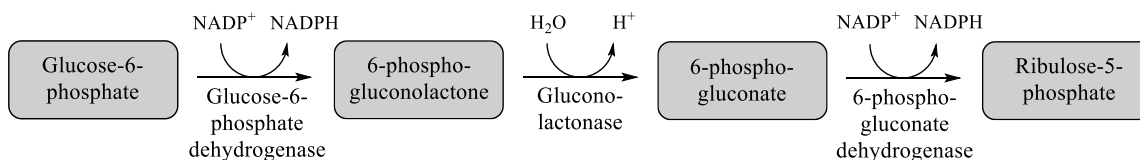
Figure 3.2.   Oxidative pentose phosphate pathway.

3.3.4. *In vitro* colorimetric phenol detection assay with 4-AAP, HRP and H$_2$O$_2$

To investigate the products of the substrate dealkylation, a colorimetric system involving 4-AAP in the presence of HRP and H$_2$O$_2$ was used to detect phenols through UV-Vis spectroscopy at approximately 500 nm as described in Chapter 2 (Figure 3.3).

This method was optimized by taking into account the conditions previously used in Chapter 2, the nature of SMA and the NADPH regeneration system that was used. The absorbance was measured at 506 nm, while in order to exclude random activity and confirm that the degradation is due to the presence of cytochrome P450s, three main controls were run: 1) no substrate, 2) no enzyme and 3) no NADPH.
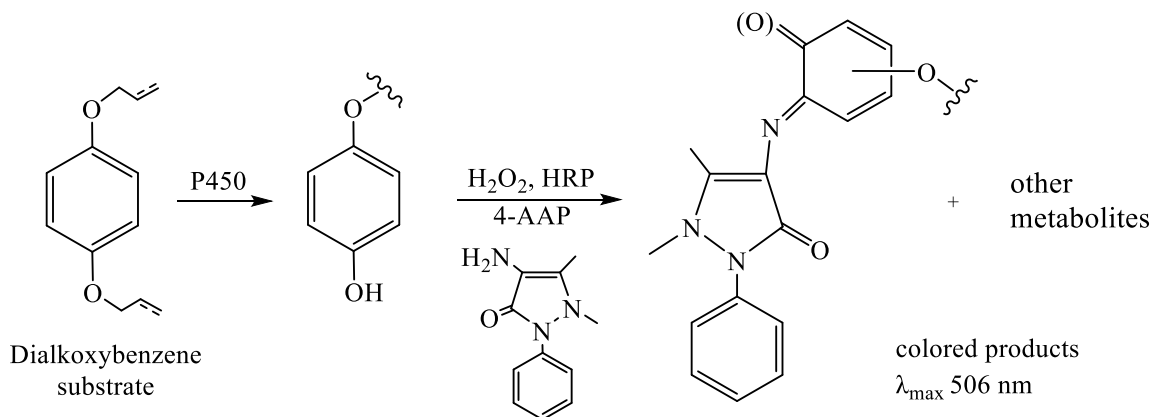
Figure 3.3.   Expected dealkylation and oxidation products of the colorimetric assay.

3.3.5. Extraction of GC-MS assay products

The assay mixture was prepared without adding 4-AAP, HRP and H$_2$O$_2$ and equilibrated on ice for 45 min. The products were separated from the aqueous solution through liquid-liquid extraction using a mixture of Hex:EtOAc (4:1) that contained 40

μg/μL 1,4-dimethoxy benzene (**3c**{*1,1*}) (internal standard). The extract (organic phase) was then dried for 20 mins using Na_2SO_4 and the samples were collected in a GC-MS vial and stored at 4 °C before being analyzed.

3.3.6. Kinetics and statistical analysis

The colorimetric phenol detection assay produces orange-colored products which are analyzed through UV-Vis spectroscopy. This colorimetric reaction was calibrated using the expected dealkylation products hydroquinone (HQ), 1-hydroxy-4-propoxybenzene (**2c**{*3*}) and 1-hydroxy-4-allyloxybenzene (**2c**{*6*}) (Figure B.2, Appendix B). The standard curve that was generated was then used to convert the absorbance to product concentration, and subsequently get the rate of the product formation. Kinetic studies were carried out and plotted on GraphPad Prism, and the data were expressed using the typical Michaelis-Menten model. The kinetic parameter V_{max} and the specific activity (nmol/min/μg) of the enzyme was also compared between the treated and untreated bees.

Hydroquinone	1-hydroxy-4-propoxybenzene	1-hydroxy-4-allyloxybenzene
HQ	**2c{3}**	**2c{6}**
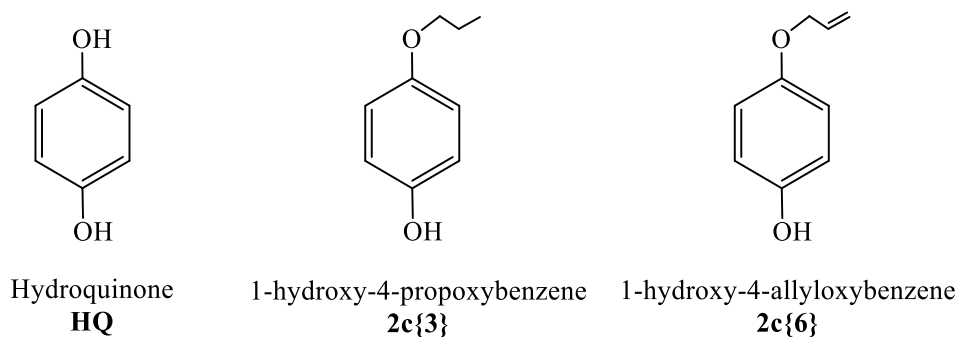
Unpaired student t-test was applied for pairwise comparison between the treated and untreated bees and the different compounds to check for significant difference between their means (Student, 1908), followed by the non-parametric Mann-Whitney test that checks whether two groups originate from different populations (Mann & Whitney, 1947).

3.4. Results and conclusions

3.4.1. Steady-state kinetic assays of honey bee protein extract with 3c{3,6}, 3c{3,3} and 3c{6,6} using 4-AAP coupled with H_2O_2 and HRP

The reaction mixture was a freshly prepared solution of phosphate buffer (100 mM NaH_2PO_4, 50 mM KCl, pH 7.4) containing 1 mM H_2O_2 and 2 mM 4-AAP, along with 2.2 µg HRP (1 U/mL stock), 1.2 mM G6P, 0.003 U/mL G6PDH, 0.1 mM NADPH, 40 µg/mL bee protein extract in 1.25% SMA buffer, and the desired substrate (in MeOH) diluted in final concentrations of 10/15/20/50/100/150 µM. The total volume of the assay was 1 mL and the absorbance was monitored by UV-Vis spectroscopy at 506 nm for 2 minutes until a stable value was reached. The assay was performed by mixing all the materials together excluding the substrate, blanking the spectrophotometer, and then adding the substrate to record the absorbance. Three controls were run: 1) without the substrate, 2) without the enzyme, and 3) without NADPH, to ensure there were no other reactions resulting in colored products. All assays were done in triplicate (Figure 3.4).
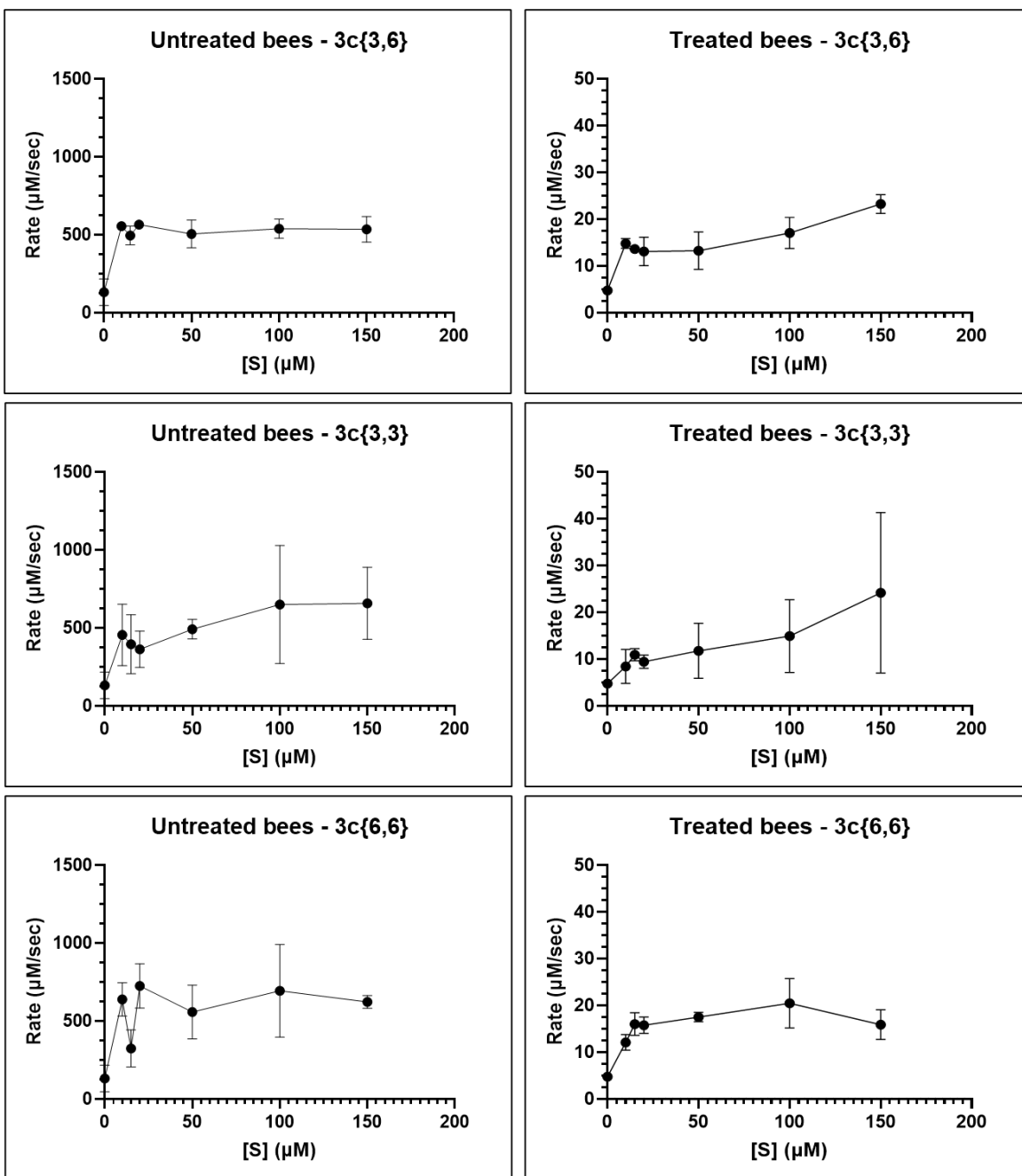
Figure 3.4. Steady-state kinetic assay plots for the untreated and treated honey bee extracts with the dialkoxybenzene compounds. Rate refers to the rate of product formation. The bars represent means ± S. E (3 replicates).

Student's t-test followed by Mann-Whitney's test were carried out for a pairwise comparison between the untreated and treated bee extracts and between the three substrates. It was found that there was a significant difference ($p<0.05$) between the two extracts for every substrate, however, there was no significant difference between the different substrates across the same bee extract.

The generated graphs seem to partially follow a Michaelis-Menten trend. For **3c**{*3,3*}, there is a noticeable variability for both the untreated and treated bees, with **3c**{*6,6*} also showing some variability for the untreated group. It is suspected that these values are more spread out due to some bee extracts originating from different bee batches and bee types (foragers, nurses, or both). Moreover, both the untreated and treated extracts appear to have already reached maximal activity, and not much increase was noticed with additional substrate concentration. The rate of product formation was similar between the different substrates but different for the untreated and treated group, with the first one having significantly higher rates. From the controls that were run for both groups, it was evident that there is activity without the addition of substrate (Figure B.1, Appendix B). Thus, it is suspected that there are probably endogenous phenols within the honey bees that reacted with 4-AAP. Since there is a lot of background activity in the extracts giving color in the coupled assay, the dealkylation of the substrates was later on investigated through GC-MS assays.

The maximum velocity (V_{max}) from the dealkylation of the dialkoxybenzene compounds was calculated as the average rate from all substrate concentrations (excluding 0 µM), since saturation is already reached and the rate does not increase upon the addition of more substrate (Table 3.1). Also, the net (corrected for background) specific activity (nmol/min/µg) of the enzyme was calculated for the dealkylation of the dialkoxybenzene compounds using the V_{max} (Table 3.1).

Table 3.1. **Maximum velocity (V$_{max}$) and specific activity (nmol/min/µg) for the dealkylation of 3c{3,6}, 3c{3,3} and 3c{6,6} by the untreated and treated bees.**

Substrate	Untreated		Treated	
	Vmax (µM/sec)	Specific activity (nmol/min/µg)	Vmax (µM/sec)	Specific activity (nmol/min/µg)
3c{3,6}	531.3	796.9	15.8	23.7
3c{3,3}	501.4	752.1	13.2	19.8
3c{6,6}	592.9	889.3	16.3	24.4

The specific activity represents the amount of substrate that is being turned over in a specific amount of time (minutes) over the amount of total protein (µg) used in the assay. However, the total amount of enzyme is unknown because the bee extracts were not purified, thus, the specific activity here can be used to confirm the consistency between the different bee extract batches, considering the normal experimental margin of error. Since I suspect the presence of endogenous phenols within both groups, and the rates for the untreated bees are much higher than those of the treated ones, the specific activity is analogous to the rate.

3.4.2. GC-MS quantitative assays

The reaction mixture was 0.5 mL and contained concentrated untreated bee extract of 200 µg/mL in 1.25% SMA buffer (100 mM NaH_2PO_4, 50 mM KCl, pH 7.4), 1.2 mM G6P, 0.003 U/mL G6PDH, 0.1 mM NADPH, and the desired substrate (in MeOH) diluted in final concentrations of 10/15/20//50/100/150 µM. The assay mixture was equilibrated on ice for 45 min and then the products were extracted. Three main controls were run: 1) without the substrate, 2) without the enzyme, and 3) without NADPH. Moreover, a cytochrome P450 inhibitor, 1-phenylimidazole, was also tested to verify that the dealkylation is indeed due to the action of P450s. The reaction was calibrated using 1-allyloxy-4-propoxy benzene (**3c**{*3,6*}), 1,4-dipropoxy benzene (**3c**{*3,3*}), 1,4-diallyloxy benzene (**3c**{*6,6*}), 1-hydroxy-4-propoxy benzene (**2c**{*3*}), 1-hydroxy-4-allyloxy benzene

(**2c**{*6*}) and hydroquinone (HQ) (Figure B.3., Appendix B). The total run time was 23 min, and the respective retention times, molecular weight and chromatographs can be seen on Table B.1, Figure B.4 and B.5, Appendix B.

The amount of substrate and products formed was calculated by measuring their peak area which was then converted to concentration in ng/µL (Tables B.2, B.3, and B.4, Appendix B) using the standard calibration curves, and subsequently to nmol. To visualize better the dealkylation rate, the estimated percentage of the total found dealkylated products, while accounting for the lost substrate was calculated, along with the estimated total dealkylation yield (Tables 3.2, 3.3 and 3.4).

Table 3.2.   GC-MS quantitation of 3c{3,6} and its products.

Assay concentration (µM)	3c{3,6} added (nmol)	3c{3,6} recovered (nmol)	2c{3} (nmol)	2c{6} (nmol)	HQ (nmol)	3c{3,6} lost + total dealkylated / added (%)	Total dealkylation yield (%)
10	5	0.9	1.2E-2	2.3E-2	2.5E-1	87	6
15	7.5	1.7	1.4E-2	1.8E-2	3.7E-1	82	5
20	10	3.6	6.0E-3	8.0E-3	3.0E-1	67	3
50	25	3.8	4.0E-3	6.0E-3	N/D	85	< 0.1
100	50	12.3	6.0E-3	1.1E-2	N/D	76	< 0.1
150	75	21	8.0E-3	1.2E-2	N/D	72	< 0.1

Table 3.3.   GC-MS quantitation of 3c{3,3} and its products.

Assay concentration (μM)	3c{3,3} added (nmol)	3c{3,3} recovered (nmol)	2c{3} (nmol)	3c{3,3} lost + total dealkylated / added (%)	Total dealkylation yield (%)
10	5	0.6	5.0E-3	89	0.1
15	7.5	1.3	2.0E-3	83	< 0.1
20	10	0.9	3.0E-3	91	< 0.1
50	25	5.2	2.0E-3	79	< 0.1
100	50	10.7	4.0E-3	79	< 0.1
150	75	22.6	2.0E-3	70	< 0.1

Table 3.4.   GC-MS quantitation of 3c{6,6} and its products.

Assay concentration (μM)	3c{6,6} added (nmol)	3c{6,6} recovered (nmol)	2c{6} (nmol)	3c{6,6} lost + total dealkylated / added (%)	Total dealkylation yield (%)
10	5	0.1	4.9E-2	99	1
15	7.5	0.1	2.3E-2	99	0.3
20	10	0.5	1.7E-2	96	0.2
50	25	1.8	3.4E-2	93	0.1
100	50	5.0	1.2E-2	90	< 0.1
150	75	5.2	3.0E-3	93	< 0.1

Regardless of the substrate being used, when it is more than 50 μM, the yield of the product forming drops significantly, with the lower assay concentrations having a much better turnover. Interestingly, the lowest concentration gave the best yield across every compound, which can be attributed to the fact that the concentration of the dialkoxybenzene compounds used in those assays is much higher than the one being used in a beehive setting. This lines up with the fact that the 4-AAP assays showed that the P450 enzymes are already saturated with substrate even at the lowest concentration. Compound

3c{*3,6*} gave both the single and double dealkylation products, while HQ was not detected for substrate concentrations of 50 μM and higher. Compound **3c**{*3,3*} gave only **2c**{*3*} and compound **3c**{*6,6*} gave **2c**{*6*}.

Due to the significant amount of lost substrate which accounted for more than 70%, and possibly lost product, controls were run using **2c**{*3*}, **2c**{*6*} and HQ as substrates. It was found that there were significant losses due to the possible desorption of these compounds, with HQ having the least recovery yield (Table B.5, Appendix B). Since this molecule is quite polar, it probably gets oxidized easily to a quinone, which could be a reason as to why it was so hard to detect. Moreover, another reason for losses besides the volatility of these compounds, is the possibility of the substrate and products being trapped in an emulsion formed and discarded during extraction, which is attributed to the amphiphilic nature of the SMA copolymer.

3.4.3. Proposed mechanism of dealkylation

Under oxidizing conditions and NADPH as the electron donor, cytochrome P450 along with a FAD-reductase, initiates the dealkylation of the **3c compounds** through hydroxylation near C1 or C4, generating a hemiacetal intermediate. This species is unstable, thus it releases the propio- or acryl-aldehyde part and simultaneously gets protonated resulting in **2c{3}** or **2c{6}**. Finally, the mono-alkoxybenzene compound is oxidized again through cytochrome P450 following the same mechanism, and ultimately forms **HQ** (Ebrahimi & Plettner, 2014).
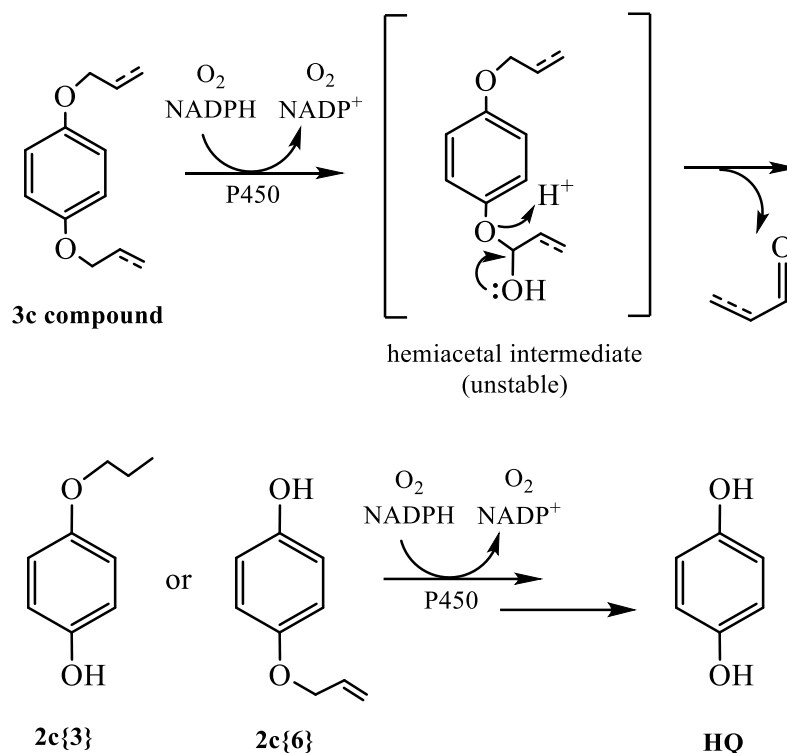
Figure 3.5.   Proposed dealkylation mechanism of dialkoxybenzene compounds.

3.5.   Conclusions

4-AAP colorimetric assays were carried out followed by steady state kinetic assays using treated (1mM **3c**{*3,6*}) and untreated honey bee extract with compounds **3c**{*3,6*}, **3c**{*3,3*} and **3c**{*6,6*} at concentrations of 10/15/20/50/100/150 μM. The rate of product formation did not increase upon altering the substrate concentration and was similar across the different compounds. However, the untreated bees had a significantly higher rate compared to the treated ones. GC-MS assays were carried out using concentrated untreated bee extract to quantitate the dealkylation products of the dialkoxybenzene compounds. All the formed products showed the highest dealkylation yields at the lowest substrate concentrations. Compound **3c**{*3,6*} gave all of the three expected products, while compounds **3c**{*3,3*} and **3c**{*6,6*} gave only **2c**{*3*} and **2c**{*6*}, respectively. From these results, it is evident that these dialkoxybenzene compounds can be indeed metabolized by the honey bee cytochromes P450.

Chapter 4.

Discussion and future studies

4.1. Polychlorinated compounds

In this project, I used two cytochrome P450$_{cam}$ mutants, ES6 and ES7, and tested them for their ability to degrade ES α:β **13**, ES sulfate **14**, ES diol **15**, ES ether **16**, ES lactone **17**, and heptachlor **18**. I monitored the formation of the dehalogenated products through 4-AAP coupled assays, which resulted in color formation. Kinetic studies revealed a sigmoidal relationship between the velocity over the substrate concentration. I found that there was a significant difference between the WT enzyme compared to both mutants, and across the different substrates. *In silico* molecular docking simulations were also carried out to elucidate the way the substrates fit into the active site of the enzymes, along with a proposed mechanism to support their catalytic turnover. All in all, ES6 and ES7 show promise in the biodegradation of unnatural substrates.

In my study, mutants ES6 (G120S) and ES7 (V247F/D297N/K314E) showed significant dehalogenation activity in comparison to the WT P450$_{cam}$. The natural substrate of P450$_{cam}$ is camphor, however, by mutating the enzyme, we were able to accommodate similarly structured and larger substrates within its active site. Certain residues have an important role in the stability and catalytic activity of P450$_{cam}$. Thus, rational mutations around the active site can be beneficial to ensure the integrity of the enzyme and increase its efficiency. For example, C357 is crucial for the catalytic activity, and mutations there have resulted in complete loss of activity (Murugan & Mazumdar, 2005; Yoshioka et al., 2001). Mutations on L358, which is adjacent to C357, also had the same detrimental effect (Batabyal et al., 2013). Residues involved in the H-bonding network and proton delivery, such as D186, D251, L178, T101, T185 and T252, are important for the completion of the catalytic cycle (Gerber & Sligar, 1994; Manna & Mazumdar, 2006; Martinis et al., 1989; Schlichting, 2000). In ES6 and ES7, none of these crucial residues was mutated. Surprisingly, some of the mutated residues (G120S and K314E) were not present near the active site at all, indicating that distant alternations do play a role in the substrate

selectivity. Moreover, G120S is located at the proximal end of P450$_{cam}$ and specifically at the binding site of PdX (near C helix). PdX is responsible for shuttling electrons from PdR to P450$_{cam}$, thus it has an effector role during catalysis (Batabyal et al., 2016; S. S. Pochapsky et al., 2003; Tosha et al., 2003; Tyson et al., 1972). Spectroscopic studies have shown that transitions between the substrate free (open) and substrate bound (closed) form of the enzyme result from the disorder of the B' helix and displacements in F and G helices upon PdX binding. PdX has also shown to favor the open conformation (Hiruma et al., 2013; Y.-T. Lee et al., 2010; Tripathi et al., 2013). So, mutations located in these helices may play an effector role, similar to PdX.

In the future, additional colorimetric assays can be done with other polychlorinated pollutants that have a structure similar to camphor, such as chlordane, dechlorane plus, aldrin etc. New mutants can be generated by site-directed mutagenesis or other mutants from the library of ES1-ES7 can also be tested against these substrates. Since most of the time the substrates never reach saturation during the steady-state kinetics, the PdX to PdR to P450 ratio and the substrate concentration could be adjusted so that the typical hyperbolic curve can be formed. The metabolites of the substrates can also be determined and quantified through chloride ion release assays and GC-MS studies. Moreover, X-ray crystallography and NMR studies can be used to determine the crystal structure of the enzymes when they are bound to the selected substrates. That way, the first step of the proposed dehalogenation mechanism, which is the oxidation of the C=C bond, can be used to understand the enzyme's specificity and help operate in new substrates.

4.2. Dialkoxybenzene compounds

In this project, I used abdominal honey bee extract and tested the ability of the endogenous P450s to degrade the potential miticides 1-allyloxy-4-propoxy benzene (**3c**{*3,6*}), 1,4-dipropoxy benzene (**3c**{*3,3*}) and 1,4-diallyloxy benzene (**3c**{*6,6*}). Treated (1 mM **3c**{*3,6*}) and untreated bee extracts were tested and compared with each other and with the selected substrates. I monitored the formation of the dealkylated products through 4-AAP coupled assays, which resulted in color formation. Kinetic studies revealed that the rate of product formation did not rise upon the increase of the substrate concentration.

Interestingly, the untreated extracts had much higher rates of product formation than the treated ones. GC-MS assays were carried out to determine and quantitate the dealkylated products. Compound **3c**{*3,6*} got metabolized to 1-hydroxy-4-propoxybenzene (**2c**{*3*}), 1-hydroxy-4-allyloxybenzene (**2c**{*6*}) and hydroquinone (HQ), while **3c**{*3,3*} and **3c**{*6,6*} to **2c**{*3*} and **2c**{*6*} respectively. A dealkylation mechanism was also proposed. All in all, these substrates, and especially **3c**{*3,6*}, show promise as potential varroa control agents.

Cytochrome P450 is the key enzyme for xenobiotic resistance in *A. mellifera* (Gong & Diao, 2017). Midgut and malpighian tubules of honey bee abdomens have been studied in forager and nurse bees and a variety of P450 genes were discovered (Vannette et al., 2015). The malpighian tubules had genes expressed belonging to the CYP314A1, CYP6AS5, CYP6AS11, CYP6AS13, CYP6AS15, CYP6AS16P, CYP6BD1, CYPAS10 and CYP9Q2 families. Midgut P450s responsible for detoxification were CYP6AS16P, CYP6BD1, CYP9Q1, CYP9Q1, CYP9Q2 and CYP9Q3 (Vannette et al., 2015; Mao et al., 2011).

It is important to mention that differential expression of cytochromes P450 has been noticed between foragers, nurses, workers, larvae and queens. This also includes differences between the head, thorax, and abdomen and between the different tissues of each body part (Chaimanee et al., 2016; Christen et al., 2019; Gregorc et al., 2012; Tomé et al., 2020; Yao et al., 2018; Zaworra & Nauen, 2019). Both the treated and untreated samples were from nurse or forager bees collected and frozen back in 2018 but analyzed after 2 years. Also, it is uncertain whether these populations were infested with varroa or when exactly they were frozen post-treatment. Typically, mite-exposed and/or treated populations experience an up-regulation of P450s (Alptekin et al., 2016; Gregorc et al., 2012; Johnson et al., 2012; Mao et al., 2011, 2013; Tomé et al., 2020; Yao et al., 2018), however, I noticed the activity was surprisingly increased for the untreated bees. Nonetheless, down-regulation of P450s has been observed in honey bees before. CYP9Q3 was found to be repressed by bifenthrin (insecticide) (Mao et al., 2011). CYP306A1 and CYP4G11 were repressed in workers by coumaphos, with the first one also being repressed by Apiguard (thymol) too (Boncristiani et al., 2012; Chaimanee et al., 2016). In my studies, both groups showed color formation without the addition of the substrate, indicating the

presence of endogenous phenols within the bee extract. Since there was some background color interfering with the coupled assay, it was important to shift the focus to the GC-MS experiments. Thus, to confirm that the dealkylation was indeed caused by CYP450s, controls without NADPH and with 1-phenylimidazole (competitive inhibitor) were run and showed no activity, confirming the initial hypothesis.

In the future, gene transcription studies can be used to look for P450s being expressed in the fat body of honey bees, in either exposed or not exposed populations. Most bee abdominal tissues have undergone transcriptome profiling through PCR, however, the fat body hasn't been investigated yet. Similar studies can also be done on the mites, along with colorimetric and GC-MS assays to test varroa's degradation ability towards these substrates. For my experiments, I used the whole abdomen and did not isolate a specific tissue nor purified the bee extract, which could be another reason for background color formation in the coupled assay. Also, a study that tested microsomes from the abdomens of worker bees, found the presence of an endogenous P450 inhibitor within the venom sac, which was identified to be phospholipase A2 (Zaworra & Nauen, 2019). Thus, the removal of the venom gland sting complex is advised for future studies. It is also advised to use the same type of bee (forager or nurse) and produce larger quantities of bee extract (ideally from the same batch) to prevent variability in the 4-AAP colorimetric assay. Moreover, synthesized fluorescent probes, such as biotin labels, can be used to identify the target site of the dialkoxybenzenes in the mites. Organophosphate (e.g. chlorpyrifos, coumaphos) and carbamate (e.g. aldicarb) insecticides are known to target acetylcholinesterase (AChE) (Pohanka, 2011), an enzyme responsible for neurotransmission. A current group member, Soniya Dawdani, has shown through confocal imaging studies using fluorescent probes, that **3c**{*3,6*} targets the central nervous system of the mite, however, AChE isn't its target site of **3c**{*3,6*} (Dawdani, 2021). Finally, the persistence, formulation and release method of the dialkoxybenzene compounds needs to be studied to ensure their safety towards honey bees, other animals and humans, thus, further toxicological risk assessments need to be performed.

References

Agilent Technologies. (2015). *QuikChange Site-Directed Mutagenesis Kit—Instruction Manual*.

Ahmed, S., & Brattsten, L. B. (1986). *Molecular Aspects of Insect-Plant Associations*. Plenum Press.

Ahn, S.-J., Vogel, H., & Heckel, D. G. (2012). Comparative analysis of the UDP-glycosyltransferase multigene family in insects. *Insect Biochemistry and Molecular Biology*, *42*(2), 133–147. https://doi.org/10.1016/j.ibmb.2011.11.006

Akhtar, Y., Isman, M. B., Paduraru, P. M., Nagabandi, S., Nair, R., & Plettner, E. (2007). Screening of Dialkoxybenzenes and Disubstituted Cyclopentene Derivatives against the Cabbage Looper, Trichoplusia ni, for the Discovery of New Feeding and Oviposition Deterrents. *Journal of Agricultural and Food Chemistry*, *55*(25), 10323–10330. https://doi.org/10.1021/jf071636d

Akhtar, Y., Yu, Y., Isman, M. B., & Plettner, E. (2010). Dialkoxybenzene and Dialkoxyallylbenzene Feeding and Oviposition Deterrents against the Cabbage Looper, Trichoplusia ni: Potential Insect Behavior Control Agents. *Journal of Agricultural and Food Chemistry*, *58*(8), 4983–4991. https://doi.org/10.1021/jf9045123

Al Naggar, Y., Codling, G., Vogt, A., Naiem, E., Mona, M., Seif, A., & Giesy, J. P. (2015). Organophosphorus insecticides in honey, pollen and bees (Apis mellifera L.) and their potential hazard to bee colonies in Egypt. *Ecotoxicology and Environmental Safety*, *114*, 1–8. https://doi.org/10.1016/j.ecoenv.2014.12.039

Alawi, Dr. M. (2002). Regional Distribution of Organochlorine Pesticides in Human Breast Milk from Jordan. *Fresenius Environmental Bulletin*, *11*, 1023–1029.

Alptekin, S., Bass, C., Nicholls, C., Paine, M. J. I., Clark, S. J., Field, L., & Moores, G. D. (2016). Induced thiacloprid insensitivity in honeybees (Apis mellifera L.) is associated with up-regulation of detoxification genes. *Insect Molecular Biology*, *25*(2), 171–180. https://doi.org/10.1111/imb.12211

Amellal, N., Portal, J.-M., Vogel, T., & Berthelin, J. (2001). *Distribution and location of polycyclic aromatic hydrocarbons (PAHs) and PAH-degrading bacteria within polluted soil aggregates*. *12*, 49–57.

Ardalani, H., Vidkjær, N. H., Laursen, B. B., Kryger, P., & Fomsgaard, I. S. (2021). Dietary quercetin impacts the concentration of pesticides in honey bees. *Chemosphere*, *262*, 127848. https://doi.org/10.1016/j.chemosphere.2020.127848

Argikar, U. A., & Remmel, R. P. (2009). Effect of Aging on Glucuronidation of Valproic Acid in Human Liver Microsomes and the Role of UDP-Glucuronosyltransferase UGT1A4, UGT1A8, and UGT1A10. *Drug Metabolism and Disposition*, *37*(1), 229–236. https://doi.org/10.1124/dmd.108.022426

Asciutto, E. K., Dang, M., Pochapsky, S. S., Madura, J. D., & Pochapsky, T. C. (2011). Experimentally restrained molecular dynamics simulations for characterizing the open states of cytochrome P450cam. *Biochemistry*, *50*(10), 1664–1671. https://doi.org/10.1021/bi101820d

ASTDR. (1989). Toxicological profile for heptachlor/heptachlor epoxide. *U.S. Environmental Protection Agency*.

Atkins, W. M., & Sligar, S. G. (1990). Tyrosine-96 as a natural spectroscopic probe of the cytochrome P-450cam active site. *Biochemistry*, *29*(5), 1271–1275. https://doi.org/10.1021/bi00457a024

ATSDR. (2007). Public Health Statement on heptachlor and heptachlor epoxide. *U.S. Department of Health and Human Services*.

Auclair, K., Moënne-Loccoz, P., & Ortiz de Montellano, P. R. (2001). Roles of the Proximal Heme Thiolate Ligand in Cytochrome P450 cam. *Journal of the American Chemical Society*, *123*(21), 4877–4885. https://doi.org/10.1021/ja0040262

Axelrod, J. (1955). THE ENZYMATIC DEAMINATION OF AMPHETAMINE (BENZEDRINE). *Journal of Biological Chemistry*, *214*(2), 753–763. https://doi.org/10.1016/S0021-9258(18)70924-1

Batabyal, D., Lewis-Ballester, A., Yeh, S.-R., & Poulos, T. L. (2016). A Comparative Analysis of the Effector Role of Redox Partner Binding in Bacterial P450s. *Biochemistry*, *55*(47), 6517–6523. https://doi.org/10.1021/acs.biochem.6b00913

Batabyal, D., Li, H., & Poulos, T. L. (2013). Synergistic Effects of Mutations in Cytochrome P450cam Designed to Mimic CYP101D1. *Biochemistry*, *52*(32), 5396–5402. https://doi.org/10.1021/bi400676d

Behera, R. K., & Mazumdar, S. (2008). Roles of two surface residues near the access channel in the substrate recognition by cytochrome P450cam. *Biophysical Chemistry*, *135*(1–3), 1–6. https://doi.org/10.1016/j.bpc.2008.02.016

Bell, S. G., Chen, X., Sowden, R. J., Xu, F., Williams, J. N., Wong, L.-L., & Rao, Z. (2003). Molecular Recognition in (+)-α-Pinene Oxidation by Cytochrome P450. *Journal of the American Chemical Society*, *125*(3), 705–714. https://doi.org/10.1021/ja028460a

Bell, S. G., Orton, E., Boyd, H., Stevenson, J.-A., Riddle, A., Campbell, S., & Wong, L.-L. (2003). Engineering cytochrome P450cam into an alkane hydroxylase. *Dalton Transactions*, *11*, 2133–2140. https://doi.org/10.1039/B300869J

Bell, S. G., Sowden, R. J., & Wong, L.-L. (2001). Engineering the haem monooxygenase cytochrome P450cam for monoterpene oxidation. *Chemical Communications*, *7*, 635–636. https://doi.org/10.1039/B100290M

Bell, S. G., Stevenson, J.-A., Boyd, H. D., Campbell, S., Riddle, A. D., Orton, E. L., & Wong, L.-L. (2002). Butane and propane oxidation by engineered cytochrome P450cam. *Chemical Communications*, *5*, 490–491. https://doi.org/10.1039/B110957J

Benjamini, Y., & Hochberg, Y. (1995). Controlling the False Discovery Rate: A Practical and Powerful Approach to Multiple Testing. *Journal of the Royal Statistical Society. Series B (Methodological)*, *57*(1), 289–300.

Bennett, R. N., & Wallsgrove, R. M. (1994). Secondary metabolites in plant defence mechanisms. *New Phytologist*, *127*(4), 617–633. https://doi.org/10.1111/j.1469-8137.1994.tb02968.x

Berenbaum, M. R., & Johnson, R. M. (2015). Xenobiotic detoxification pathways in honey bees. *Current Opinion in Insect Science*, *10*, 51–58. https://doi.org/10.1016/j.cois.2015.03.005

Bhattacharya, A., Sood, P., & Citovsky, V. (2010). The roles of plant phenolics in defence and communication during Agrobacterium and Rhizobium infection. *Molecular Plant Pathology*, *11*(5), 705–719. https://doi.org/10.1111/j.1364-3703.2010.00625.x

Bogdanov, S. (2015). Beeswax: Quality issues today. *Bee World*, *85*, 46–50. https://doi.org/10.1080/0005772X.2004.11099623

Bollag, J.-M., Myers, C. J., & Minard, R. D. (1992). Biological and chemical interactions of pesticides with soil organic matter. *Science of The Total Environment*, *123–124*, 205–217. https://doi.org/10.1016/0048-9697(92)90146-J

Boncristiani, H., Underwood, R., Schwarz, R., Evans, J. D., Pettis, J., & vanEngelsdorp, D. (2012). Direct effect of acaricides on pathogen loads and gene expression levels in honey bees Apis mellifera. *Journal of Insect Physiology*, *58*(5), 613–620. https://doi.org/10.1016/j.jinsphys.2011.12.011

Bowen-Walker, P. L., & Gunn, A. (2001). The effect of the ectoparasitic mite, Varroa destructor on adult worker honeybee (Apis mellifera) emergence weights, water, protein, carbohydrate, and lipid levels. *Entomologia Experimentalis et Applicata*, *101*(3), 207–217. https://doi.org/10.1046/j.1570-7458.2001.00905.x

Bowen-Walker, P. L., Martin, S. J., & Gunn, A. (1999). The Transmission of Deformed Wing Virus between Honeybees (Apis melliferaL.) by the Ectoparasitic MiteVarroa jacobsoniOud. *Journal of Invertebrate Pathology*, *73*(1), 101–106. https://doi.org/10.1006/jipa.1998.4807

Bradford, M. M. (1976). A rapid and sensitive method for the quantitation of microgram quantities of protein utilizing the principle of protein-dye binding. *Analytical Biochemistry*, *72*(1), 248–254. https://doi.org/10.1016/0003-2697(76)90527-3

Buss, D. S., & Callaghan, A. (2008). Interaction of pesticides with p-glycoprotein and other ABC proteins: A survey of the possible importance to insecticide, herbicide and fungicide resistance. *Pesticide Biochemistry and Physiology*, *90*(3), 141–153. https://doi.org/10.1016/j.pestbp.2007.12.001

Calderone, N. W. (2012). Insect Pollinated Crops, Insect Pollinators and US Agriculture: Trend Analysis of Aggregate Data for the Period 1992–2009. *PLOS ONE*, *7*(5), e37235. https://doi.org/10.1371/journal.pone.0037235

Campbell, C. D., Walgenbach, J. F., & Kennedy, G. G. (1991). Effect of Parasitoids on Lepidopterous Pests in Insecticide-Treated and Untreated Tomatoes in Western North Carolina. *Journal of Economic Entomology*, *84*(6), 1662–1667. https://doi.org/10.1093/jee/84.6.1662

Cappiello, A., Famiglini, G., Palma, P., Termopoli, V., Lavezzi, A. M., & Matturri, L. (2014). Determination of selected endocrine disrupting compounds in human fetal and newborn tissues by GC-MS. *Analytical and Bioanalytical Chemistry*, *406*(12), 2779–2788. https://doi.org/10.1007/s00216-014-7692-0

Carvalho, S. M., Belzunces, L. P., Carvalho, G. A., Brunet, J.-L., & Badiou-Beneteau, A. (2013). Enzymatic biomarkers as tools to assess environmental quality: A case study of exposure of the honeybee Apis mellifera to insecticides. *Environmental Toxicology and Chemistry*, *32*(9), 2117–2124. https://doi.org/10.1002/etc.2288

Çelik, A., Speight, R. E., & Turner, N. J. (2005). Identification of broad specificity P450CAM variants by primary screening against indole as substrate. *Chemical Communications*, *29*, 3652–3654. https://doi.org/10.1039/B506156C

Cerrillo, I., Granada, A., López-Espinosa, M.-J., Olmos, B., Jiménez, M., Caño, A., Olea, N., & Fátima Olea-Serrano, M. (2005). Endosulfan and its metabolites in fertile women, placenta, cord blood, and human milk. *Environmental Research*, *98*(2), 233–239. https://doi.org/10.1016/j.envres.2004.08.008

Chaimanee, V., Evans, J. D., Chen, Y., Jackson, C., & Pettis, J. S. (2016). Sperm viability and gene expression in honey bee queens (Apis mellifera) following exposure to the neonicotinoid insecticide imidacloprid and the organophosphate acaricide coumaphos. *Journal of Insect Physiology*, *89*, 1–8. https://doi.org/10.1016/j.jinsphys.2016.03.004

Christen, V., Joho, Y., Vogel, M., & Fent, K. (2019). Transcriptional and physiological effects of the pyrethroid deltamethrin and the organophosphate dimethoate in the brain of honey bees (Apis mellifera). *Environmental Pollution*, *244*, 247–256. https://doi.org/10.1016/j.envpol.2018.10.030

Claudianos, C., Ranson, H., Johnson, R. M., Biswas, S., Schuler, M. A., Berenbaum, M. R., Feyereisen, R., & Oakeshott, J. G. (2006). A deficit of detoxification enzymes: Pesticide sensitivity and environmental response in the honeybee. *Insect Molecular Biology*, *15*(5), 615–636. https://doi.org/10.1111/j.1365-2583.2006.00672.x

Colthart, A. M., Tietz, D. R., Ni, Y., Friedman, J. L., Dang, M., & Pochapsky, T. C. (2016). Detection of substrate-dependent conformational changes in the P450 fold by nuclear magnetic resonance. *Scientific Reports*, *6*, 22035. https://doi.org/10.1038/srep22035

Compton, S. J., & Jones, C. G. (1985). Mechanism of dye response and interference in the Bradford protein assay. *Analytical Biochemistry*, *151*(2), 369–374. https://doi.org/10.1016/0003-2697(85)90190-3

Cornell, W. D., Cieplak, P., Bayly, C. I., Gould, I. R., Merz, K. M., Ferguson, D. M., Spellmeyer, D. C., Fox, T., Caldwell, J. W., & Kollman, P. A. (1995). A Second Generation Force Field for the Simulation of Proteins, Nucleic Acids, and Organic Molecules. *Journal of the American Chemical Society*, *117*(19), 5179–5197. https://doi.org/10.1021/ja00124a002

Daiber, A., Shoun, H., & Ullrich, V. (2008). Nitric Oxide Reductase (P450nor) from Fusarium oxysporum. In *The Smallest Biomolecules: Diatomics and their Interactions with Heme Proteins* (pp. 354–377). Elsevier. https://doi.org/10.1016/B978-044452839-1.50015-2

Davydov, R., Makris, T. M., Kofman, V., Werst, D. E., Sligar, S. G., & Hoffman, B. M. (2001). Hydroxylation of Camphor by Reduced Oxy-Cytochrome P450cam: Mechanistic Implications of EPR and ENDOR Studies of Catalytic Intermediates in Native and Mutant Enzymes. *Journal of the American Chemical Society*, *123*(7), 1403–1415. https://doi.org/10.1021/ja0035831

Dawdani, S. (2021). *Evaluating the Effects of 1-allyloxy-4-propoxybenzene on the Parasitic Mite Varroa Destructor and Synthesis of Fluorescent Probes to Visualize the Binding Location(s) of the Active Compound in the Mite* [M.Sc. thesis]. Simon Fraser University, Canada.

Dawson, J. H., & Sono, Masanori. (1987). Cytochrome P-450 and chloroperoxidase: Thiolate-ligated heme enzymes. Spectroscopic determination of their active-site structures and mechanistic implications of thiolate ligation. *Chemical Reviews*, *87*(5), 1255–1276. https://doi.org/10.1021/cr00081a015

De Moraes, C., Lewis, W. J., Pare, P., Alborn, H., & Tumlinson, J. (1998). Herbivore-infested plants selectively attract parasitoids. *Nature*, *393*, 570–573. https://doi.org/10.1038/31219

Dean, R. B., & Dixon, W. J. (1951). Simplified Statistics for Small Numbers of Observations. *Analytical Chemistry*, *23*(4), 636–638. https://doi.org/10.1021/ac60052a025

Degtyarenko, K., & Kulikova, T. A. (2001). Evolution of bioinorganic motifs in P450-containing systems. *Biochemical Society Transactions*, *29*, 139–147. https://doi.org/10.1042/BST0290139

Delle Site, A. (2001). Factors Affecting Sorption of Organic Compounds in Natural Sorbent/Water Systems and Sorption Coefficients for Selected Pollutants. A Review. *Journal of Physical and Chemical Reference Data*, *30*(1), 187–439. https://doi.org/10.1063/1.1347984

Denisov, I. G., Makris, T. M., Sligar, S. G., & Schlichting, I. (2005). Structure and Chemistry of Cytochrome P450. *Chemical Reviews*, *105*(6), 2253–2278. https://doi.org/10.1021/cr0307143

Derecka, K., Blythe, M. J., Malla, S., Genereux, D. P., Guffanti, A., Pavan, P., Moles, A., Snart, C., Ryder, T., Ortori, C. A., Barrett, D. A., Schuster, E., & Stöger, R. (2013). Transient Exposure to Low Levels of Insecticide Affects Metabolic Networks of Honeybee Larvae. *PLOS ONE*, *8*(7), e68191. https://doi.org/10.1371/journal.pone.0068191

Dermauw, W., & Van Leeuwen, T. (2014). The ABC gene family in arthropods: Comparative genomics and role in insecticide transport and resistance. *Insect Biochemistry and Molecular Biology*, *45*, 89–110. https://doi.org/10.1016/j.ibmb.2013.11.001

Dixon, W. (1953). *Processing Data for Outliers*. https://doi.org/10.2307/3001634

Doolotkeldieva, T., Bobusheva, S., & Konurbaeva, M. (2021). The Improving Conditions for the Aerobic Bacteria Performing the Degradation of Obsolete Pesticides in Polluted Soils. *Air, Soil and Water Research*, *14*, 1178622120982590. https://doi.org/10.1177/1178622120982590

Dörfler, U., Schneider, P., & Scheunert, I. (1991). Volatilization rates of pesticides from soil and plant surfaces under controlled conditions. *Toxicological & Environmental Chemistry*, *31*(1), 87–95. https://doi.org/10.1080/02772249109357676

Dörr, J. M., Scheidelaar, S., Koorengevel, M. C., Dominguez, J. J., Schäfer, M., van Walree, C. A., & Killian, J. A. (2016). The styrene–maleic acid copolymer: A versatile tool in membrane research. *European Biophysics Journal*, *45*, 3–21. https://doi.org/10.1007/s00249-015-1093-y

Dube, A., Zbytniewski, R., Kowalkowski, T., Cukrowska, E., & Buszewski, B. (2001). Adsorption and Migration of Heavy Metals in Soil. *Undefined*. https://www.semanticscholar.org/paper/Adsorption-and-Migration-of-Heavy-Metals-in-Soil-Dube-Zbytniewski/1b79a592bbd63327c2a4e37282ad3d099fa1294f

Ebrahimi, P. (2012). *Partition, sorption and structure activity relation study of dialkoxybenzenes that modulate insect behavior*. Simon Fraser University, Canada.

Ebrahimi, P., & Plettner, E. (2014). Biodegradation of 1-allyloxy-4-propoxybenzene by selected strains of Pseudomonas putida. *Biodegradation*, *25*(1), 31–39. https://doi.org/10.1007/s10532-013-9638-1

Ebrahimi, P., Spooner, J., Weinberg, N., & Plettner, E. (2013). Partition, sorption and structure activity relation study of dialkoxybenzenes that modulate insect behavior. *Chemosphere*, *93*(1), 54–60. https://doi.org/10.1016/j.chemosphere.2013.04.065

ECETOC. (2003). Aquatic hazard assessment II. *Technical Report No. 91*.

Eliash, N., Singh, N. K., Kamer, Y., Pinnelli, G. R., Plettner, E., & Soroker, V. (2014). Can We Disrupt the Sensing of Honey Bees by the Bee Parasite Varroa destructor? *PLOS ONE*, *9*(9), e106889. https://doi.org/10.1371/journal.pone.0106889

Emerson, E. (1943). THE CONDENSATION OF AMINOANTIPYRINE. II. A NEW COLOR TEST FOR PHENOLIC COMPOUNDS. *The Journal of Organic Chemistry*, *08*(5), 417–428. https://doi.org/10.1021/jo01193a004

England, P. A., Rouch, D. A., Westlake, A. C. G., Bell, S. G., Nickerson, D. P., Webberley, M., Flitsch, S. L., & Wong, L. L. (1996). Aliphatic vs aromatic C-H bond activation of phenylcyclohexane catalysed by cytochrome P450cam. *CHEMICAL COMMUNICATIONS*, *3*. https://ora.ox.ac.uk/objects/uuid:9263beda-28d6-43f6-a093-e47f13340432

Enhui, Z., Na, C., MengYun, L., Jia, L., Dan, L., Yongsheng, Y., Ying, Z., & DeFu, H. (2016). Isomers and their metabolites of endosulfan induced cytotoxicity and oxidative damage in SH-SY5Y cells. *Environmental Toxicology*, *31*(4), 496–504. https://doi.org/10.1002/tox.22066

Ernst, O., & Zor, T. (2010). Linearization of the Bradford Protein Assay. *Journal of Visualized Experiments : JoVE*, *38*, 1918. https://doi.org/10.3791/1918

Fowler, S. M., England, P. A., Westlake, A. C. G., Rouch, D. R., Nickerson, D. P., Blunt, C., Braybrook, D., West, S., Wong, L.-L., & Flitsch, S. L. (1994). Cytochrome P-450cam monooxygenase can be redesigned to catalyse the regioselective aromatic hydroxylation of diphenylmethane. *Journal of the Chemical Society, Chemical Communications*, *24*, 2761–2762. https://doi.org/10.1039/C39940002761

Galinato, M. G. I., Spolitak, T., Ballou, D. P., & Lehnert, N. (2011). Elucidating the Role of the Proximal Cysteine Hydrogen Bonding Network in Ferric Cytochrome P450cam and corresponding mutants using Magnetic Circular Dichroism Spectroscopy. *Biochemistry*, *50*(6), 1053–1069. https://doi.org/10.1021/bi101911y

Gannon, N., & Bigger, J. H. (1958). *The conversion of aldrin and heptachlor to their epoxides in soil*. *51*, 1–2.

Gannon, N., & Decker, G. C. (1958). *The conversion of heptachlor to its epoxide on plants*. *51*, 3–7.

Genersch, E. (2010). Honey bee pathology: Current threats to honey bees and beekeeping. *Applied Microbiology and Biotechnology*, *87*(1), 87–97. https://doi.org/10.1007/s00253-010-2573-8

Gerber, N. C., & Sligar, S. G. (1994). A role for Asp-251 in cytochrome P-450cam oxygen activation. *Journal of Biological Chemistry*, *269*(6), 4260–4266. https://doi.org/10.1016/S0021-9258(17)41772-8

Gilbert, L. I. (2012). *Insect molecular biology and biochemistry*. Elsevier/Academic Press.

Gong, Y., & Diao, Q. (2017). Current knowledge of detoxification mechanisms of xenobiotic in honey bees. *Ecotoxicology*, *26*(1), 1–12. https://doi.org/10.1007/s10646-016-1742-7

Gotoh, O. (1992). Substrate recognition sites in cytochrome P450 family 2 (CYP2) proteins inferred from comparative analyses of amino acid and coding nucleotide sequences. *Journal of Biological Chemistry*, *267*(1), 83–90. https://doi.org/10.1016/S0021-9258(18)48462-1

Gott, R., Kunkel, G., Zobel, E., Lovett, B., & Hawthorne, D. (2017). Implicating ABC Transporters in Insecticide Resistance: Research Strategies and a Decision Framework. *Journal of Economic Entomology*, *110*. https://doi.org/10.1093/jee/tox041

Gregorc, A., Evans, J. D., Scharf, M., & Ellis, J. D. (2012). Gene expression in honey bee (Apis mellifera) larvae exposed to pesticides and Varroa mites (Varroa destructor). *Journal of Insect Physiology*, *58*(8), 1042–1049. https://doi.org/10.1016/j.jinsphys.2012.03.015

Grout, T. G., & Richards, G. I. (1992). Susceptibility ofEuseius addoensis addoensis (Acari: Phytoseiidae) to field-weathered residues of insecticides used on citrus. *Experimental and Applied Acarology*, *15*(3), 199–204. https://doi.org/10.1007/BF01195791

Groves, J. T. (2014). ENZYMATIC C–H BOND ACTIVATION. *Nature Chemistry*, *6*(2), 89–91. https://doi.org/10.1038/nchem.1855

Groves, J. T., & McClusky, G. A. (1976). Aliphatic hydroxylation via oxygen rebound. Oxygen transfer catalyzed by iron. *Journal of the American Chemical Society*, *98*(3), 859–861. https://doi.org/10.1021/ja00419a049

Groves, J. T., McClusky, G. A., White, R. E., & Coon, M. J. (1978). Aliphatic hydroxylation by highly purified liver microsomal cytochrome P-450. Evidence for a carbon radical intermediate. *Biochemical and Biophysical Research Communications*, *81*(1), 154–160. https://doi.org/10.1016/0006-291X(78)91643-1

Guengerich, F. P., & Yoshimoto, F. K. (2018). Formation and Cleavage of C–C Bonds by Enzymatic Oxidation–Reduction Reactions. *Chemical Reviews*, *118*(14), 6573–6655. https://doi.org/10.1021/acs.chemrev.8b00031

Hannemann, F., Bichet, A., Ewen, K. M., & Bernhardt, R. (2007). Cytochrome P450 systems—Biological variations of electron transport chains. *Biochimica et Biophysica Acta (BBA) - General Subjects*, *1770*(3), 330–344. https://doi.org/10.1016/j.bbagen.2006.07.017

Harford-Cross, C. F., Carmichael, A. B., Allan, F. K., England, P. A., Rouch, D. A., & Wong, L. L. (2000). Protein engineering of cytochrome p450(cam) (CYP101) for the oxidation of polycyclic aromatic hydrocarbons. *Protein Engineering*, *13*(2), 121–128. https://doi.org/10.1093/protein/13.2.121

Harris, J. R., Stoddard, G. E., Bateman, G. Q., Shupe, J. L., Greenwood, D. A., Harris, L. E., Bahler, T. L., & Lieberman, F. V. (1956). Pesticides in Animal Feeds, Effects of Feeding Dieldrin- and Heptachlor-Treated Alfalfa Hay to Dairy Cows. *Journal of Agricultural and Food Chemistry*, *4*(8), 694–696. https://doi.org/10.1021/jf60066a004

Hayashi, T., Harada, K., Sakurai, K., Shimada, H., & Hirota, S. (2009). A Role of the Heme-7-Propionate Side Chain in Cytochrome P450cam as a Gate for Regulating the Access of Water Molecules to the Substrate-Binding Site. *Journal of the American Chemical Society*, *131*(4), 1398–1400. https://doi.org/10.1021/ja807420k

Hays, A.-M. A., Dunn, A. R., Chiu, R., Gray, H. B., Stout, C. D., & Goodin, D. B. (2004). Conformational States of Cytochrome P450cam Revealed by Trapping of Synthetic Molecular Wires. *Journal of Molecular Biology*, *344*(2), 455–469. https://doi.org/10.1016/j.jmb.2004.09.046

Hernandez-Ortega, A., Vinaixa, M., Zebec, Z., Takano, E., & Scrutton, N. S. (2018). A Toolbox for Diverse Oxyfunctionalisation of Monoterpenes. *Scientific Reports*, *8*, 14396. https://doi.org/10.1038/s41598-018-32816-1

Hiruma, Y., Hass, M. A. S., Kikui, Y., Liu, W.-M., Ölmez, B., Skinner, S. P., Blok, A., Kloosterman, A., Koteishi, H., Löhr, F., Schwalbe, H., Nojiri, M., & Ubbink, M. (2013). The Structure of the Cytochrome P450cam–Putidaredoxin Complex Determined by Paramagnetic NMR Spectroscopy and Crystallography. *Journal of Molecular Biology*, *425*(22), 4353–4365. https://doi.org/10.1016/j.jmb.2013.07.006

Hoa, G. H. B., & Marden, M. C. (1982). The Pressure Dependence of the Spin Equilibrium in Camphor-Bound Ferric Cytochrome P-450. *European Journal of Biochemistry*, *124*(2), 311–315. https://doi.org/10.1111/j.1432-1033.1982.tb06593.x

Hoffmann, G., Bonsch, K., Greiner-Stoffele, T., & Ballschmiter, M. (2011). Changing the substrate specificity of P450cam towards diphenylmethane by semi-rational enzyme engineering. *Protein Engineering Design and Selection*, *24*(5), 439–446. https://doi.org/10.1093/protein/gzq119

Hogue, C. (2011). ENDOSULFAN BANNED WORLDWIDE: PERSISTENT POLLUTANTS: Certain uses of pesticide can continue until 2017. *Chemical & Engineering News Archive*, *89*, 15. https://doi.org/10.1021/cen-v089n019.p015a

Hough-Goldstein, J., & Keil, C. (1991). Prospects for Integrated Control of the Colorado Potato Beetle (Coleoptera: Chrysomelidae) Using Perillus Bioculatus (Hemiptera: Pentatomidae) and Various Pesticides. *Journal of Economic Entomology*, *84*, 1645–1651. https://doi.org/10.1093/jee/84.6.1645

Høyer, A. P., Grandjean, P., Jørgensen, T., Brock, J. W., & Hartvig, H. B. (1998). Organochlorine exposure and risk of breast cancer. *Lancet (London, England)*, *352*(9143), 1816–1820. https://doi.org/10.1016/s0140-6736(98)04504-8

Hsu, P.-Y., Tsai, A.-L., Kulmacz, R. J., & Wang, L.-H. (1999). Expression, Purification, and Spectroscopic Characterization of Human Thromboxane Synthase *. *Journal of Biological Chemistry*, *274*(2), 762–769. https://doi.org/10.1074/jbc.274.2.762

Huber, W. (1993). Ecotoxicological relevance of atrazine in aquatic systems. *Environmental Toxicology and Chemistry*, *12*(10), 1865–1881. https://doi.org/10.1002/etc.5620121014

Hussain, S., Arshad, M., Saleem, M., & Khalid, A. (2007). Biodegradation of α- and β-endosulfan by soil bacteria. *Biodegradation*, *18*(6), 731–740. https://doi.org/10.1007/s10532-007-9102-1

Hussain, S., Arshad, M., Saleem, M., & Zahir, Z. A. (2007). Screening of soil fungi for in vitro degradation of endosulfan. *World Journal of Microbiology and Biotechnology*, *23*(7), 939–945. https://doi.org/10.1007/s11274-006-9317-z

IBTB. (2021). *CYtochrome P450 Engineering Database*. Retrieved August 10, 2021, from https://cyped.biocatnet.de/sequence-browser

Isman, M. (2002). Insect antifeedants. *Pesticide Outlook*, *13*(4), 152–157. https://doi.org/10.1039/B206507J

Iwasa, T., Motoyama, N., Ambrose, J. T., & Roe, R. M. (2004). Mechanism for the differential toxicity of neonicotinoid insecticides in the honey bee, Apis mellifera. *Crop Protection*, *23*(5), 371–378. https://doi.org/10.1016/j.cropro.2003.08.018

Jaworska, J. S., Hunter, R. S., & Schultz, T. W. (1995). Quantitative structure-toxicity relationships and volume fraction analyses for selected esters. *Archives of Environmental Contamination and Toxicology*, *29*(1), 86–93. https://doi.org/10.1007/BF00213091

Jefcoate, C. R. (1978). Measurement of substrate and inhibitor binding to microsomal cytochrome P-450 by optical-difference spectroscopy. In S. Fleischer & L. Packer (Eds.), *Methods in Enzymology* (Vol. 52, pp. 258–279). Academic Press. https://doi.org/10.1016/S0076-6879(78)52029-6

Jiménez Torres, C., Ortiz, I., San-Martin, P., & Hernandez, I. (2016). Biodegradation of malathion, α- and β-endosulfan by bacterial strains isolated from agricultural soil in Veracruz, Mexico. *Journal of Environmental Science and Health, Part B*, *51*, 1–7. https://doi.org/10.1080/03601234.2016.1211906

Johnson, R. M., Mao, W., Pollock, H. S., Niu, G., Schuler, M. A., & Berenbaum, M. R. (2012). Ecologically Appropriate Xenobiotics Induce Cytochrome P450s in Apis mellifera. *PLOS ONE*, *7*(2), e31051. https://doi.org/10.1371/journal.pone.0031051

Jones, J. P., O'Hare, E. J., & Wong, L.-L. (2000). The oxidation of polychlorinated benzenes by genetically engineered cytochrome P450cam: Potential applications in bioremediation. *Chemical Communications*, *3*, 247–248. https://doi.org/10.1039/A909536E

Jung, C. (2011). The mystery of cytochrome P450 Compound I. *Biochimica et Biophysica Acta (BBA) - Proteins and Proteomics*, *1814*(1), 46–57. https://doi.org/10.1016/j.bbapap.2010.06.007

Kammoonah, S. (2016). *Oxidation of 3-Chloroindole and Biodegradation of Dialkoxybenzenes with Cytochrome P450cam (CYP101A1)* [M.Sc. thesis]. Simon Fraser University, Canada.

Kammoonah, S., Prasad, B., Balaraman, P., Mundhada, H., Schwaneberg, U., & Plettner, E. (2018). Selecting of a cytochrome P450cam SeSaM library with 3-chloroindole and endosulfan – Identification of mutants that dehalogenate 3-chloroindole. *Biochimica et Biophysica Acta (BBA) - Proteins and Proteomics*, *1866*(1), 68–79. https://doi.org/10.1016/j.bbapap.2017.09.006

Kataoka, R., Takagi, K., & Sakakibara, F. (2010). A new endosulfan-degrading fungus, Mortierella species, isolated from a soil contaminated with organochlorine pesticides. *Journal of Pesticide Science*, *35*(3). https://doi.org/10.1584/jpestics.g10-10

Kelly, B. C., & Gobas, F. A. P. C. (2003). An Arctic Terrestrial Food-Chain Bioaccumulation Model for Persistent Organic Pollutants. *Environmental Science & Technology*, *37*(13), 2966–2974. https://doi.org/10.1021/es021035x

Kim, K.-R., & Oh, D.-K. (2013). Production of hydroxy fatty acids by microbial fatty acid-hydroxylation enzymes. *Biotechnology Advances*, *31*(8), 1473–1485. https://doi.org/10.1016/j.biotechadv.2013.07.004

Klein, A.-M., Vaissière, B. E., Cane, J. H., Steffan-Dewenter, I., Cunningham, S. A., Kremen, C., & Tscharntke, T. (2007). Importance of pollinators in changing landscapes for world crops. *Proceedings of the Royal Society B: Biological Sciences*, *274*(1608), 303–313. https://doi.org/10.1098/rspb.2006.3721

Klibanov, A. M., Alberti, B. N., Morris, E. D., & Felshin, L. M. (1980). Enzymatic removal of toxic phenols and anilines from waste waters. *J. Appl. Biochem.; (United States)*, *2:5*. https://www.osti.gov/biblio/6449569-enzymatic-removal-toxic-phenols-anilines-from-waste-waters

Kruskal, W. H., & Wallis, W. A. (1952). Use of Ranks in One-Criterion Variance Analysis. *Journal of the American Statistical Association*, *47*(260), 583–621. https://doi.org/10.1080/01621459.1952.10483441

Kullman, S. W., & Matsumura, F. (1996). Metabolic pathways utilized by Phanerochaete chrysosporium for degradation of the cyclodiene pesticide endosulfan. *Applied and Environmental Microbiology*, *62*(2), 593–600.

Labute, P. (2008). The generalized Born/volume integral implicit solvent model: Estimation of the free energy of hydration using London dispersion instead of atomic surface area. *Journal of Computational Chemistry*, *29*(10), 1693–1698. https://doi.org/10.1002/jcc.20933

Labute, P. (2009). Protonate3D: Assignment of ionization states and hydrogen coordinates to macromolecular structures. *Proteins*, *75*(1), 187–205. https://doi.org/10.1002/prot.22234

Lee, S. C., Knowles, T. J., Postis, V. L. G., Jamshad, M., Parslow, R. A., Lin, Y.-P., Goldman, A., Sridhar, P., Overduin, M., Muench, S. P., & Dafforn, T. R. (2016). A method for detergent-free isolation of membrane proteins in their local lipid environment. *Nature Protocols*, *11*(7), 1149–1162. https://doi.org/10.1038/nprot.2016.070

Lee, Y.-T., Glazer, E. C., Wilson, R. F., Stout, C. D., & Goodin, D. B. (2011). Three clusters of conformational states in P450cam reveal a multi-step pathway for closing of the substrate access channel. *Biochemistry*, *50*(5), 693–703. https://doi.org/10.1021/bi101726d

Lee, Y.-T., Wilson, R. F., Rupniewski, I., & Goodin, D. B. (2010). P450cam Visits an Open Conformation in the Absence of Substrate. *Biochemistry*, *49*(16), 3412–3419. https://doi.org/10.1021/bi100183g

Lefever, M. R., & Wackett, L. P. (1994). Oxidation of Low Molecular Weight Chloroalkanes by Cytochrome P450CAM. *Biochemical and Biophysical Research Communications*, *201*(1), 373–378. https://doi.org/10.1006/bbrc.1994.1711

Lehotay, S. J., Harman-Fetcho, J. A., & McConnell, L. L. (1998). Agricultural pesticide residues in oysters and water from two chesapeake bay tributaries. *Marine Pollution Bulletin*, *37*(1–2), 32–44. https://doi.org/10.1016/S0025-326X(98)00129-5

Leo, A., Hansch, C., & Elkins, D. (1971). Partition coefficients and their uses. *Chemical Reviews*, *71*(6), 525–616. https://doi.org/10.1021/cr60274a001

Li, Z., Jiang, Y., Guengerich, F. P., Ma, L., Li, S., & Zhang, W. (2020). Engineering cytochrome P450 enzyme systems for biomedical and biotechnological applications. *The Journal of Biological Chemistry*, *295*(3), 833–849. https://doi.org/10.1074/jbc.REV119.008758

Lichtenstein, E. P., & Schulz, K. R. (1960). *Epoxidation of aldrin and heptachlor in soils as influenced by autoclaving, moisture, and soil type*. *53*, 192–197.

Loida, P. J., & Sligar, S. G. (1993). Engineering cytochrome P-450cam to increase the stereospecificity and coupling of aliphatic hydroxylation. *Protein Engineering, Design and Selection*, *6*(2), 207–212. https://doi.org/10.1093/protein/6.2.207

Lozano, A., Hernando, M. D., Uclés, S., Hakme, E., & Fernández-Alba, A. R. (2019). Identification and measurement of veterinary drug residues in beehive products. *Food Chemistry*, *274*, 61–70. https://doi.org/10.1016/j.foodchem.2018.08.055

Luek, J. L., Dickhut, R. M., Cochran, M. A., Falconer, R. L., & Kylin, H. (2017). Persistent organic pollutants in the Atlantic and southern oceans and oceanic atmosphere. *Science of The Total Environment*, *583*, 64–71. https://doi.org/10.1016/j.scitotenv.2016.12.189

Luthra, A., Denisov, I. G., & Sligar, S. G. (2011). Spectroscopic features of cytochrome P450 reaction intermediates. *Archives of Biochemistry and Biophysics*, *507*(1), 26–35. https://doi.org/10.1016/j.abb.2010.12.008

Mabey, W. R., Smith, J. H., Podoll, R. T., Johnson, H. L., Mill, T., Chou, T. W., Gates, J., Partridge, I. W., Jaber, H., & Vandenberg, D. (1982). Aquatic fate process data for organic priority pollutants. *U.S. Environmental Protection Agency*.

Mann, H. B., & Whitney, D. R. (1947). On a Test of Whether one of Two Random Variables is Stochastically Larger than the Other. *The Annals of Mathematical Statistics*, *18*(1), 50–60.

Manna, S. K., & Mazumdar, S. (2006). Role of Threonine 101 on the Stability of the Heme Active Site of Cytochrome P450cam: Multiwavelength Circular Dichroism Studies [†]. *Biochemistry*, *45*(42), 12715–12722. https://doi.org/10.1021/bi060848l

Manna, S. K., & Mazumdar, S. (2010). Tuning the substrate specificity by engineering the active site of cytochrome P450cam: A rational approach. *Dalton Transactions*, *39*(12), 3115–3123. https://doi.org/10.1039/B922885C

Mao, W., Rupasinghe, S. G., Johnson, R. M., Zangerl, A. R., Schuler, M. A., & Berenbaum, M. R. (2009). Quercetin-metabolizing CYP6AS enzymes of the pollinator Apis mellifera (Hymenoptera: Apidae). *Comparative Biochemistry and Physiology Part B: Biochemistry and Molecular Biology*, *154*(4), 427–434. https://doi.org/10.1016/j.cbpb.2009.08.008

Mao, W., Schuler, M. A., & Berenbaum, M. R. (2011). CYP9Q-mediated detoxification of acaricides in the honey bee (Apis mellifera). *Proceedings of the National Academy of Sciences*, *108*(31), 12657–12662. https://doi.org/10.1073/pnas.1109535108

Mao, W., Schuler, M. A., & Berenbaum, M. R. (2013). Honey constituents up-regulate detoxification and immunity genes in the western honey bee Apis mellifera. *Proceedings of the National Academy of Sciences*, *110*(22), 8842–8846. https://doi.org/10.1073/pnas.1303884110

Martinis, S. A., Atkins, W. M., Stayton, P. S., & Sligar, S. G. (1989). A conserved residue of cytochrome P-450 is involved in heme-oxygen stability and activation. *Journal of the American Chemical Society*, *111*(26), 9252–9253. https://doi.org/10.1021/ja00208a031

Mayhew, M. P., Roitberg, A. E., Tewari, Y., Holden, M. J., Vanderah, D. J., & Vilker, V. L. (2002). Benzocycloarene hydroxylation by P450 biocatalysis. *New Journal of Chemistry*, *26*(1), 35–42. https://doi.org/10.1039/B107584P

McDonnell, A. M., & Dang, C. H. (2013). Basic Review of the Cytochrome P450 System. *Journal of the Advanced Practitioner in Oncology*, *4*(4), 263–268.

McLean, K. J., Sabri, M., Marshall, K. R., Lawson, R. J., Lewis, D. G., Clift, D., Balding, P. R., Dunford, A. J., Warman, A. J., McVey, J. P., Quinn, A.-M., Sutcliffe, M. J., Scrutton, N. S., & Munro, A. W. (2005). Biodiversity of cytochrome P450 redox systems. *Biochemical Society Transactions*, *33*(4), 796–801. https://doi.org/10.1042/BST0330796

Meesters, R. J. W., Duisken, M., & Hollender, J. (2007). Study on the cytochrome P450-mediated oxidative metabolism of the terpene alcohol linalool: Indication of biological epoxidation. *Xenobiotica*, *37*(6), 604–617. https://doi.org/10.3109/00498250701393191

Mill, T., Mabey, W. R., Bomberger, D. C., Chou, T. W., Hendry, D. G., & Smith, J. H. (1982). Laboratory protocols for evaluating the fate of organic chemicals in air and water. *U.S. Environmental Protection Agency*.

Mondet, F., Rau, A., Klopp, C., Rohmer, M., Severac, D., Le Conte, Y., & Alaux, C. (2018). Transcriptome profiling of the honeybee parasite Varroa destructor provides new biological insights into the mite adult life cycle. *BMC Genomics*, *19*(1), 328. https://doi.org/10.1186/s12864-018-4668-z

Montellano, P. R. O. de (Ed.). (2005). *Cytochrome P450: Structure, Mechanism, and Biochemistry* (3rd ed.). Springer US. https://doi.org/10.1007/b139087

Morales, M. M., Gómez Ramos, M. J., Parrilla Vázquez, P., Díaz Galiano, F. J., García Valverde, M., Gámiz López, V., Manuel Flores, J., & Fernández-Alba, A. R. (2020). Distribution of chemical residues in the beehive compartments and their transfer to the honeybee brood. *Science of The Total Environment*, *710*, 136288. https://doi.org/10.1016/j.scitotenv.2019.136288

Morawski, B., Quan, S., & Arnold, F. H. (2001). Functional expression and stabilization of horseradish peroxidase by directed evolution in Saccharomyces cerevisiae. *Biotechnology and Bioengineering*, *76*(2), 99–107. https://doi.org/10.1002/bit.1149

Morishima, I., Kurono, M., & Shiro, Y. (1986). Presence of endogenous calcium ion in horseradish peroxidase. Elucidation of metal-binding site by substitutions of divalent and lanthanide ions for calcium and use of metal-induced NMR (1H and 113Cd) resonances. *Journal of Biological Chemistry*, *261*(20), 9391–9399. https://doi.org/10.1016/S0021-9258(18)67667-7

Moser, V. C. (2001). Neurotoxicological Outcomes of Perinatal Heptachlor Exposure in the Rat. *Toxicological Sciences*, *60*(2), 315–326. https://doi.org/10.1093/toxsci/60.2.315

Mukherjee, I., & Mittal, A. (2005). Bioremediation of Endosulfan Using Aspergillus terreus and Cladosporium oxysporum. *Bulletin of Environmental Contamination and Toxicology*, *75*, 1034–1040. https://doi.org/10.1007/s00128-005-0853-2

Mullin, C. A., Frazier, M., Frazier, J. L., Ashcraft, S., Simonds, R., vanEngelsdorp, D., & Pettis, J. S. (2010). High Levels of Miticides and Agrochemicals in North American Apiaries: Implications for Honey Bee Health. *PLOS ONE*, *5*(3), e9754. https://doi.org/10.1371/journal.pone.0009754

Munro, A. W., Girvan, H. M., & McLean, K. J. (2007). Cytochrome P450–redox partner fusion enzymes. *Biochimica et Biophysica Acta (BBA) - General Subjects*, *1770*(3), 345–359. https://doi.org/10.1016/j.bbagen.2006.08.018

Murugan, R., & Mazumdar, S. (2005). Structure and Redox Properties of the Haem Centre in the C357M Mutant of Cytochrome P450cam. *ChemBioChem*, *6*(7), 1204–1211. https://doi.org/10.1002/cbic.200400399

Nagano, S., & Poulos, T. L. (2005). Crystallographic Study on the Dioxygen Complex of Wild-type and Mutant Cytochrome P450cam: IMPLICATIONS FOR THE DIOXYGEN ACTIVATION MECHANISM. *Journal of Biological Chemistry*, *280*(36), 31659–31663. https://doi.org/10.1074/jbc.M505261200

NCI. (1977). Bioassay of heptachlor for possible carcinogenicity. *Carcinogenesis Technical Report Series*.

Nelson, D. R. (2009). The Cytochrome P450 Homepage. *Human Genomics*, *4*(1), 59. https://doi.org/10.1186/1479-7364-4-1-59

Noltmann, E. A., Gubler, C. J., & Kuby, S. A. (1961). Glucose 6-Phosphate Dehydrogenase (Zwischenferment). *Journal of Biological Chemistry*, *236*(5), 1225–1230. https://doi.org/10.1016/S0021-9258(18)64153-5

Nomura, T., Kushiro, T., Yokota, T., Kamiya, Y., Bishop, G. J., & Yamaguchi, S. (2005). The Last Reaction Producing Brassinolide Is Catalyzed by Cytochrome P-450s, CYP85A3 in Tomato and CYP85A2 in Arabidopsis. *Journal of Biological Chemistry*, *280*(18), 17873–17879. https://doi.org/10.1074/jbc.M414592200

Omura, T., & Sato, R. (1964). The Carbon Monoxide-binding Pigment of Liver Microsomes. *Journal of Biological Chemistry*, *239*(7), 2370–2378. https://doi.org/10.1016/S0021-9258(20)82244-3

Orantes-Bermejo, F. J., Pajuelo, A. G., Megías, M. M., & Fernández-Píñar, C. T. (2010). Pesticide residues in beeswax and beebread samples collected from honey bee colonies (*Apis mellifera* L.) in Spain. Possible implications for bee losses. *Journal of Apicultural Research*, *49*(3), 243–250. https://doi.org/10.3896/IBRA.1.49.3.03

OuYang, B., Pochapsky, S. S., Pagani, G. M., & Pochapsky, T. C. (2006). Specific Effects of Potassium Ion Binding on Wild-Type and L358P Cytochrome P450cam. *Biochemistry*, *45*(48), 14379–14388. https://doi.org/10.1021/bi0617355

Paduraru, P. M., Popoff, R. T. W., Nair, R., Gries, R., Gries, G., & Plettner, E. (2008). Synthesis of Substituted Alkoxy Benzene Minilibraries, for the Discovery of New Insect Olfaction or Gustation Inhibitors. *Journal of Combinatorial Chemistry*, *10*(1), 123–134. https://doi.org/10.1021/cc700139y

Peterson, J. A. (1971). Camphor binding by Pseudomonas putida cytochrome P-450. *Archives of Biochemistry and Biophysics*, *144*(2), 678–693. https://doi.org/10.1016/0003-9861(71)90375-4

Peterson, J. A., & Graham, S. E. (1998). A close family resemblance: The importance of structure in understanding cytochromes P450. *Structure*, *6*(9), 1079–1085. https://doi.org/10.1016/S0969-2126(98)00109-9

Pikuleva, I. (2006). Cholesterol-metabolizing cytochromes P450. *Drug Metabolism and Disposition: The Biological Fate of Chemicals*, *34*, 513–520. https://doi.org/10.1124/dmd.105.008789

Plettner, E., & Gries, R. (2010). Agonists and Antagonists of Antennal Responses of Gypsy Moth (Lymantria dispar) to the Pheromone (+)-Disparlure and Other Odorants. *Journal of Agricultural and Food Chemistry*, *58*(6), 3708–3719. https://doi.org/10.1021/jf904139e

PMRA. (2011). *Discontinuation of Endosulfan*.

Pochapsky, S. S., Pochapsky, T. C., & Wei, J. W. (2003). A Model for Effector Activity in a Highly Specific Biological Electron Transfer Complex: The Cytochrome P450cam −Putidaredoxin Couple. *Biochemistry*, *42*(19), 5649–5656. https://doi.org/10.1021/bi034263s

Pochapsky, T. (1996). A structure-based model for cytochrome P450cam-pufidaredoxin interactions. *Biochimie*, *78*(8–9), 723–733.

Pohanka, M. (2011). CHOLINESTERASES, A TARGET OF PHARMACOLOGY AND TOXICOLOGY. *Biomedical Papers*, *155*(3), 219–223. https://doi.org/10.5507/bp.2011.036

Pokethitiyook, P., & Poolpak, T. (2012). Heptachlor and Its Metabolite: Accumulation and Degradation in Sediment. In R. P. Soundararajan (Ed.), *Pesticides—Recent Trends in Pesticide Residue Assay*. InTech. https://doi.org/10.5772/48741

Poulos, T. L., Finzel, B. C., Gunsalus, I. C., Wagner, G. C., & Kraut, J. (1985). The 2.6-A crystal structure of Pseudomonas putida cytochrome P-450. *Journal of Biological Chemistry*, *260*(30), 16122–16130. https://doi.org/10.1016/S0021-9258(17)36209-9

Poulos, T. L., Finzel, B. C., & Howard, A. J. (1987). High-resolution crystal structure of cytochrome P450cam. *Journal of Molecular Biology*, *195*(3), 687–700. https://doi.org/10.1016/0022-2836(87)90190-2

Pozo, K., Harner, T., Wania, F., Muir, D. C. G., Jones, K. C., & Barrie, L. A. (2006). Toward a Global Network for Persistent Organic Pollutants in Air: Results from the GAPS Study. *Environmental Science & Technology*, *40*(16), 4867–4873. https://doi.org/10.1021/es060447t

Prasad, B. (2013). *The Borneol Cycle of Cytochrome P450cam and Evolution of the Enzyme for New Applications* [Ph.D thesis]. Simon Fraser University, Canada.

Price, N., & Stevens, L. (1999). *Fundamentals of Enzymology: Cell and Molecular Biology of Catalytic Proteins* (3rd edition). Oxford University Press.

Primo, C. D., Hoa, G. H. B., Douzou, P., & Sligar, S. (1990). Effect of the tyrosine 96 hydrogen bond on the inactivation of cytochrome P-450cam induced by hydrostatic pressure. *European Journal of Biochemistry*, *193*(2), 383–386. https://doi.org/10.1111/j.1432-1033.1990.tb19350.x

Purnomo, A. S., Putra, S. R., Shimizu, K., & Kondo, R. (2014). Biodegradation of heptachlor and heptachlor epoxide-contaminated soils by white-rot fungal inocula. *Environmental Science and Pollution Research*, *21*(19), 11305–11312. https://doi.org/10.1007/s11356-014-3026-1

Ramsey, S. D., Ochoa, R., Bauchan, G., Gulbronson, C., Mowery, J. D., Cohen, A., Lim, D., Joklik, J., Cicero, J. M., Ellis, J. D., Hawthorne, D., & vanEngelsdorp, D. (2019). Varroa destructor feeds primarily on honey bee fat body tissue and not hemolymph. *Proceedings of the National Academy of Sciences of the United States of America*, *116*(5), 1792–1801. https://doi.org/10.1073/pnas.1818371116

Rehman, A. (2021). *Cytochrome P450cam (CYP101A1) Mutants to Study Dehalogenation of Endosulfan: A Persistent Organic Pollutant, and Oxidation of β-phellandrene: A Monoterpene* [Ph.D thesis]. Simon Fraser University, Canada.

Rittle, J., & Green, M. T. (2010). Cytochrome P450 Compound I: Capture, Characterization, and C-H Bond Activation Kinetics. *Science*, *330*(6006), 933–937. https://doi.org/10.1126/science.1193478

Roberts, G. A., Grogan, G., Greter, A., Flitsch, S. L., & Turner, N. J. (2002). Identification of a New Class of Cytochrome P450 from a Rhodococcus sp. *Journal of Bacteriology*, *184*(14), 3898–3908. https://doi.org/10.1128/JB.184.14.3898-3908.2002

Rorabacher, D. B. (1991). Statistical treatment for rejection of deviant values: Critical values of Dixon's "Q" parameter and related subrange ratios at the 95% confidence level. *Analytical Chemistry*, *63*(2), 139–146. https://doi.org/10.1021/ac00002a010

Rui, L., Pochapsky, S. S., & Pochapsky, T. C. (2006). Comparison of the complexes formed by cytochrome P450cam with cytochrome b5 and putidaredoxin, two effectors of camphor hydroxylase activity. *Biochemistry*, *45*(12), 3887–3897. https://doi.org/10.1021/bi052318f

Sakaki, T. (2012). Practical Application of Cytochrome P450. *Biological and Pharmaceutical Bulletin*, *35*(6), 844–849. https://doi.org/10.1248/bpb.35.844

Sakurai, K. (2009). *Studies on roles of the amino acid residues in the vicinity of the active site in cytochrome P450cam* [Ph.D thesis]. Osaka University, Japan.

Samsonov, Y. N., Makarov, V. I., & Koutsenogii, K. P. (1998). Physicochemical model and kinetics of pesticide constituent evaporation out of multi-ingredient polydisperse aerosols. *Pesticide Science*, *52*(3), 292–302. https://doi.org/10.1002/(SICI)1096-9063(199803)52:3<292::AID-PS725>3.0.CO;2-A

Schaller, C. P. (2006). *Coordination chemistry*. Retrieved July 18, 2021, from https://employees.csbsju.edu/cschaller/Reactivity/coordchem/coordchem%20ligandfield.htm

Schlichting, I. (2000). The Catalytic Pathway of Cytochrome P450cam at Atomic Resolution. *Science*, *287*(5458), 1615–1622. https://doi.org/10.1126/science.287.5458.1615

Schmehl, D. R., Teal, P. E. A., Frazier, J. L., & Grozinger, C. M. (2014). Genomic analysis of the interaction between pesticide exposure and nutrition in honey bees (Apis mellifera). *Journal of Insect Physiology*, *71*, 177–190. https://doi.org/10.1016/j.jinsphys.2014.10.002

Schmidt, W. F., Hapeman, C. J., Fettinger, J. C., Rice, C. P., & Bilboulian, S. (1997). Structure and Asymmetry in the Isomeric Conversion of β- to α-Endosulfan. *Journal of Agricultural and Food Chemistry*, *45*(4), 1023–1026. https://doi.org/10.1021/jf970020t

Scippo, M.-L., Argiris, C., Van De Weerdt, C., Muller, M., Willemsen, P., Martial, J., & Maghuin-Rogister, G. (2004). Recombinant human estrogen, androgen and progesterone receptors for detection of potential endocrine disruptors. *Analytical and Bioanalytical Chemistry*, *378*(3), 664–669. https://doi.org/10.1007/s00216-003-2251-0

Sedmak, J. J., & Grossberg, S. E. (1977). A rapid, sensitive, and versatile assay for protein using Coomassie brilliant blue G250. *Analytical Biochemistry*, *79*(1), 544–552. https://doi.org/10.1016/0003-2697(77)90428-6

Sehlmeyer, S., Wang, L., Langel, D., Heckel, D. G., Mohagheghi, H., Petschenka, G., & Ober, D. (2010). Flavin-Dependent Monooxygenases as a Detoxification Mechanism in Insects: New Insights from the Arctiids (Lepidoptera). *PLOS ONE*, *5*(5), e10435. https://doi.org/10.1371/journal.pone.0010435

Sen, S., Manna, S. K., & Mazumdar, S. (2011). Interaction of gammaxene with site specific mutants of cytochrome P450cam. *INDIAN J CHEM*, 50A, 438-446.

Sevrioukova, I. F., & Poulos, T. L. (2011). Structural Biology of Redox Partner Interactions in P450cam Monooxygenase: A Fresh Look at an Old System. *Archives of Biochemistry and Biophysics*, *507*(1), 66–74. https://doi.org/10.1016/j.abb.2010.08.022

Shen, L., & Wania, F. (2005). Compilation, Evaluation, and Selection of Physical−Chemical Property Data for Organochlorine Pesticides. *Journal of Chemical & Engineering Data*, *50*(3), 742–768. https://doi.org/10.1021/je049693f

Shen, L., Wania, F., Lei, Y. D., Teixeira, C., Muir, D. C. G., & Bidleman, T. F. (2005). Atmospheric Distribution and Long-Range Transport Behavior of Organochlorine Pesticides in North America. *Environmental Science & Technology*, *39*(2), 409–420. https://doi.org/10.1021/es049489c

Sibbesen, O., Voss, J. J. D., & Montellano, P. R. O. de. (1996). Putidaredoxin Reductase-Putidaredoxin-Cytochrome P450cam Triple Fusion Protein: CONSTRUCTION OF A SELF-SUFFICIENT ESCHERICHIA COLI CATALYTIC SYSTEM *. *Journal of Biological Chemistry*, *271*(37), 22462–22469. https://doi.org/10.1074/jbc.271.37.22462

Singh, N. K., Eliash, N., Kamer, Y., Zaidman, I., Plettner, E., & Soroker, V. (2015). The effect of DEET on chemosensing of the honey bee and its parasite Varroa destructor. *Apidologie*, *46*(3), 380–391. https://doi.org/10.1007/s13592-014-0330-1

Singh, N. K., Eliash, N., & Raj, N. (2020). Effect of the insect feeding deterrent 1-allyloxy-4- propoxybenzene on olfactory responses and host choice of Varroa destructor. *Apidologie*, *51*, 1133–1142.

Sligar, S. G., Debrunner, P. G., Lipscomb, J. D., Namtvedt, M. J., & Gunsalus, I. C. (1974). A Role of the Putidaredoxin COOH-Terminus in P-450cam (Cytochrome m) Hydroxylations. *Proceedings of the National Academy of Sciences of the United States of America*, *71*(10), 3906–3910.

Smirnova, I. A., Ädelroth, P., & Brzezinski, P. (2018). Extraction and liposome reconstitution of membrane proteins with their native lipids without the use of detergents. *Scientific Reports*, *8*(1), 14950. https://doi.org/10.1038/s41598-018-33208-1

Snyder, R., Witz, G., & Goldstein, B. D. (1993). The toxicology of benzene. *Environmental Health Perspectives*, *100*, 293–306.

Sono, M., Roach, M. P., Coulter, E. D., & Dawson, J. H. (1996). Heme-Containing Oxygenases. *Chemical Reviews*, *96*(7), 2841–2888. https://doi.org/10.1021/cr9500500

Sowden, R. J., Yasmin, S., Rees, N. H., Bell, S. G., & Wong, L.-L. (2005). Biotransformation of the sesquiterpene (+)-valencene by cytochrome P450cam and P450BM-3. *Organic & Biomolecular Chemistry*, *3*(1), 57–64. https://doi.org/10.1039/B413068E

Spaans, S. K., Weusthuis, R. A., van der Oost, J., & Kengen, S. W. M. (2015). NADPH-generating systems in bacteria and archaea. *Frontiers in Microbiology*, *6*, 742. https://doi.org/10.3389/fmicb.2015.00742

Spector, T. (1978). Refinement of the coomassie blue method of protein quantitation. A simple and linear spectrophotometric assay for less than or equal to 0.5 to 50 microgram of protein. *Analytical Biochemistry*, *86*(1), 142–146. https://doi.org/10.1016/0003-2697(78)90327-5

Speight, R., Hancock, F., Winkel, C., Bevinakatti, H., Sarkar, M., Flitsch, S., & Turner, N. (2004). Rapid identification of cytochrome P450 cam variants by in vivo screening of active site libraries. *Tetrahedron Asymmetry*, *15*, 2829–2831. https://doi.org/10.1016/j.tetasy.2004.06.053

Stevenson, J.-A., Bearpark, J. K., & Wong, L.-L. (1998). Engineering molecular recognition in alkane oxidation catalysed by cytochrome P450cam. *New Journal of Chemistry*, *22*(6), 551–552. https://doi.org/10.1039/A801637B

Stevenson, J.-A., Westlake, A. C. G., Whittock, C., & Wong, L.-L. (1996). The Catalytic Oxidation of Linear and Branched Alkanes by Cytochrome P450 cam. *Journal of the American Chemical Society*, *118*(50), 12846–12847. https://doi.org/10.1021/ja963087q

Stockholm Convention. (2001). *Stockholm Convention on Persistent Organic Pollutants*. https://treaties.un.org/doc/Treaties/2001/05/20010522%2012-55%20PM/Ch_XXVII_15p.pdf

Stoll, S., Lee, Y.-T., Zhang, M., Wilson, R. F., Britt, R. D., & Goodin, D. B. (2012). Double electron–electron resonance shows cytochrome P450cam undergoes a conformational change in solution upon binding substrate. *Proceedings of the National Academy of Sciences of the United States of America*, *109*(32), 12888–12893. https://doi.org/10.1073/pnas.1207123109

Streit, B. (1992). Bioaccumulation processes in ecosystems. *Experientia*, *48*(10), 955–970. https://doi.org/10.1007/BF01919142

Student. (1908). The Probable Error of a Mean. *Biometrika*, *6*(1), 1–25. https://doi.org/10.2307/2331554

Stuetz, W., Prapamontol, T., Erhardt, J. G., & Classen, H. G. (2001). Organochlorine pesticide residues in human milk of a Hmong hill tribe living in Northern Thailand. *Science of The Total Environment*, *273*(1–3), 53–60. https://doi.org/10.1016/S0048-9697(00)00842-1

Sutherland, T. D., Horne, I., Harcourt, R. L., Russell, R. J., & Oakeshott, J. G. (2002). Isolation and characterization of a Mycobacterium strain that metabolizes the insecticide endosulfan. *Journal of Applied Microbiology*, *93*(3), 380–389. https://doi.org/10.1046/j.1365-2672.2002.01728.x

Tavanti, M., Parmeggiani, F., Castellanos, J. R. G., Mattevi, A., & Turner, N. J. (2017). One-Pot Biocatalytic Double Oxidation of α-Isophorone for the Synthesis of Ketoisophorone. *ChemCatChem*, *9*(17), 3338–3348. https://doi.org/10.1002/cctc.201700620

Teklu, B. M., Retta, N., & Van den Brink, P. J. (2016). Sensitivity of Ethiopian aquatic macroinvertebrates to the pesticides endosulfan and diazinon, compared to literature data. *Ecotoxicology*, *25*(6), 1226–1233. https://doi.org/10.1007/s10646-016-1676-0

Tomé, H. V. V., Schmehl, D. R., Wedde, A. E., Godoy, R. S. M., Ravaiano, S. V., Guedes, R. N. C., Martins, G. F., & Ellis, J. D. (2020). Frequently encountered pesticides can cause multiple disorders in developing worker honey bees. *Environmental Pollution*, *256*, 113420. https://doi.org/10.1016/j.envpol.2019.113420

Tosha, T., Yoshioka, S., Takahashi, S., Ishimori, K., Shimada, H., & Morishima, I. (2003). NMR Study on the Structural Changes of Cytochrome P450cam upon the Complex Formation with Putidaredoxin. *Journal of Biological Chemistry*, *278*(41), 39809–39821. https://doi.org/10.1074/jbc.M304265200

Tripathi, S., Li, H., & Poulos, T. L. (2013). Structural Basis for Effector Control and Redox Partner Recognition in Cytochrome P450. *Science*, *340*(6137), 1227–1230. https://doi.org/10.1126/science.1235797

Tyson, C. A., Lipscomb, J. D., & Gunsalus, I. C. (1972). The Roles of Putidaredoxin and P450cam in Methylene Hydroxylation. *Journal of Biological Chemistry*, *247*(18), 5777–5784. https://doi.org/10.1016/S0021-9258(19)44826-6

Urlacher, V. B., & Girhard, M. (2012). Cytochrome P450 monooxygenases: An update on perspectives for synthetic application. *Trends in Biotechnology*, *30*(1), 26–36. https://doi.org/10.1016/j.tibtech.2011.06.012

US EPA. (2010, November). *Endosulfan Phase-out | Pesticides*. https://archive.epa.gov/pesticides/reregistration/web/html/endosulfan-agreement.html#agreement

USEPA. (1980). Ambient water quality criteria for heptachlor. *U.S. Environmental Protection Agency*.

Vannette, R. L., Mohamed, A., & Johnson, B. R. (2015). Forager bees (Apis mellifera) highly express immune and detoxification genes in tissues associated with nectar processing. *Scientific Reports*, *5*, 16224.

Varadaraju, C., Tamilselvan, G., Enoch, I. V. M. V., & Selvakumar, P. M. (2018). Phenol Sensing Studies by 4-Aminoantipyrine Method-A Review. *Organic & Medicinal Chemistry International Journal*, *5*(2), 555657. https://doi.org/10.19080/OMCIJ.2018.05.555657

Volkamer, A., Griewel, A., Grombacher, T., & Rarey, M. (2010). Analyzing the Topology of Active Sites: On the Prediction of Pockets and Subpockets. *Journal of Chemical Information and Modeling*, *50*(11), 2041–2052. https://doi.org/10.1021/ci100241y

von Grafenstein, S., Fuchs, J. E., Huber, M. M., Bassi, A., Lacetera, A., Ruzsanyi, V., Troppmair, J., Amann, A., & Liedl, K. R. (2014). Precursors for cytochrome P450 profiling breath tests from an *in silico* screening approach. *Journal of Breath Research*, *8*(4), 046001. https://doi.org/10.1088/1752-7155/8/4/046001

Walker, A., Moon, Y.-H., & Welch, S. J. (1992). Influence of temperature, soil moisture and soil characteristics on the persistence of alachlor. *Pesticide Science*, *35*(2), 109–116. https://doi.org/10.1002/ps.2780350203

Walsh, M. E., Kyritsis, P., Eady, N. A., Hill, H. A., & Wong, L. L. (2000). Catalytic reductive dehalogenation of hexachloroethane by molecular variants of cytochrome P450cam (CYP101). *European Journal of Biochemistry*, *267*(18), 5815–5820. https://doi.org/10.1046/j.1432-1327.2000.01666.x

Wan, M., Kuo, J.-N., McPherson, B., & Pasternak, J. (2006). Agricultural Pesticide Residues in Farm Ditches of the Lower Fraser Valley, British Columbia, Canada. *Journal of Environmental Science and Health, Part B: Pesticides, Food Contaminants, and Agricultural Wastes*, *41*(5), 647–669. https://doi.org/10.1080/03601230600701817

Ward, E. M., Schulte, P., Grajewski, B., Andersen, A., Patterson, D. G., Turner, W., Jellum, E., Deddens, J. A., Friedland, J., Roeleveld, N., Waters, M., Butler, M. A., DiPietro, E., & Needham, L. L. (2000). Serum Organochlorine Levels and Breast Cancer: A Nested Case-Control Study of Norwegian Women. *Cancer Epidemiology and Prevention Biomarkers*, *9*(12), 1357–1367.

Wauchope, R. D., Buttler, T. M., Hornsby, A. G., Augustijn-Beckers, P. W., & Burt, J. P. (1992). The SCS/ARS/CES pesticide properties database for environmental decision-making. *Reviews of Environmental Contamination and Toxicology*, *123*, 1–155.

Wauchope, R. D., Yeh, S., Linders, J. B. H. J., Kloskowski, R., Tanaka, K., Rubin, B., Katayama, A., Kördel, W., Gerstl, Z., Lane, M., & Unsworth, J. B. (2002). Pesticide soil sorption parameters: Theory, measurement, uses, limitations and reliability. *Pest Management Science*, *58*(5), 419–445. https://doi.org/10.1002/ps.489

Weber, E. (2012). Apis mellifera: The Domestication and Spread of European Honey Bees for Agriculture in North America. *University of Michigan Undergraduate Research Journal, 9*, 20-23.

Weber, J., Halsall, C. J., Muir, D. C. G., Teixeira, C., Burniston, D. A., Strachan, W. M. J., Hung, H., Mackay, N., Arnold, D., & Kylin, H. (2006). Endosulfan and γ-HCH in the Arctic: An Assessment of Surface Seawater Concentrations and Air−Sea Exchange. *Environmental Science & Technology*, *40*(24), 7570–7576. https://doi.org/10.1021/es061591h

Weinstock, G. M., Robinson, G. E., Gibbs, R. A., Weinstock, G. M., Weinstock, G. M., Robinson, G. E., Worley, K. C., Evans, J. D., Maleszka, R., Robertson, H. M., Weaver, D. B., Beye, M., Bork, P., Elsik, C. G., Evans, J. D., Hartfelder, K., Hunt, G. J., Robertson, H. M., Robinson, G. E., … (2006). Insights into social insects from the genome of the honeybee Apis mellifera. *Nature*, *443*(7114), 931–949. https://doi.org/10.1038/nature05260

Weiss, M. J., McLeod, P., Schatz, B. G., & Hanson, B. K. (1991). Potential for Insecticidal Management of Flea Beetle (Coleoptera: Chrysomelidae) on Canola. *Journal of Economic Entomology*, *84*(5), 1597–1603. https://doi.org/10.1093/jee/84.5.1597

Wessel, N., Rousseau, S., Caisey, X., Quiniou, F., & Akcha, F. (2007). Investigating the relationship between embryotoxic and genotoxic effects of benzo[a]pyrene, 17α-ethinylestradiol and endosulfan on Crassostrea gigas embryos. *Aquatic Toxicology*, *85*(2), 133–142. https://doi.org/10.1016/j.aquatox.2007.08.007

Whitehouse, C. J. C., Bell, S. G., & Wong, L.-L. (2012). P450(BM3) (CYP102A1): Connecting the dots. *Chem. Soc. Rev.*, *41*(3), 1218–1260. https://doi.org/10.1039/C1CS15192D

WHO. (2004). Heptachlor and Heptachlor Epoxide in Drinking-water. *WHO/SDE/WSH/03.04/99*.

Williams, R. T. (1947). *Detoxication mechanisms: The metabolism of drugs and allied organic compounds* (1st ed.). Chapman & Hall.

Wong, T. S., Tee, K. L., Hauer, B., & Schwaneberg, U. (2004). Sequence saturation mutagenesis (SeSaM): A novel method for directed evolution. *Nucleic Acids Research*, *32*(3), e26. https://doi.org/10.1093/nar/gnh028

Xiao, P., Mori, T., Kamei, I., & Kondo, R. (2011). Metabolism of organochlorine pesticide heptachlor and its metabolite heptachlor epoxide by white rot fungi, belonging to genus Phlebia. *FEMS Microbiology Letters*, *314*(2), 140–146. https://doi.org/10.1111/j.1574-6968.2010.02152.x

Xu, F., Bell, S. G., Lednik, J., Insley, A., Rao, Z., & Wong, L.-L. (2005). The Heme Monooxygenase Cytochrome P450cam Can Be Engineered to Oxidize Ethane to Ethanol. *Angewandte Chemie*, *117*(26), 4097–4100. https://doi.org/10.1002/ange.200462630

Xu, F., Bell, S. G., Rao, Z., & Wong, L.-L. (2007). Structure-activity correlations in pentachlorobenzene oxidation by engineered cytochrome P450cam. *Protein Engineering Design and Selection*, *20*(10), 473–480. https://doi.org/10.1093/protein/gzm028

Xu, J., Strange, J. P., Welker, D. L., & James, R. R. (2013). Detoxification and stress response genes expressed in a western North American bumble bee, Bombus huntii(Hymenoptera: Apidae). *BMC Genomics*, *14*(1), 874. https://doi.org/10.1186/1471-2164-14-874

Xu, L.-H., & Du, Y.-L. (2018). Rational and semi-rational engineering of cytochrome P450s for biotechnological applications. *Synthetic and Systems Biotechnology*, *3*(4), 283–290. https://doi.org/10.1016/j.synbio.2018.10.001

Yao, J., Zhu, Y. C., & Adamczyk, J. (2018). Responses of Honey Bees to Lethal and Sublethal Doses of Formulated Clothianidin Alone and Mixtures. *Journal of Economic Entomology*, *111*(4), 1517–1525. https://doi.org/10.1093/jee/toy140

Yoshioka, S., Takahashi, S., Hori, H., Ishimori, K., & Morishima, I. (2001). Proximal cysteine residue is essential for the enzymatic activities of cytochrome P450cam. *European Journal of Biochemistry*, *268*(2), 252–259. https://doi.org/10.1046/j.1432-1033.2001.01872.x

Yu, Q.-Y., Lu, C., Li, W.-L., Xiang, Z.-H., & Zhang, Z. (2009). Annotation and expression of carboxylesterases in the silkworm, Bombyx mori. *BMC Genomics*, *10*(1), 553. https://doi.org/10.1186/1471-2164-10-553

Zaworra, M., & Nauen, R. (2019). New approaches to old problems: Removal of phospholipase A2 results in highly active microsomal membranes from the honey bee, Apis mellifera. *Pesticide Biochemistry and Physiology*, *161*, 68–76. https://doi.org/10.1016/j.pestbp.2019.04.014

Zhang, W., Pochapsky, S. S., Pochapsky, T. C., & Jain, N. U. (2008). Solution NMR structure of putidaredoxin-cytochrome P450cam complex via a combined residual dipolar coupling-spin labeling approach suggests a role for Trp106 of putidaredoxin in complex formation. *Journal of Molecular Biology*, *384*(2), 349–363. https://doi.org/10.1016/j.jmb.2008.09.037

Zheng, T., Holford, T. R., Tessari, J., Mayne, S. T., Zahm, S. H., Owens, P. H., Zhang, B., Ward, B., Carter, D., Zhang, Y., Zhang, W., Dubrow, R., & Boyle, P. (2000). Oxychlordane and trans-nonachlor in breast adipose tissue and risk of female breast cancer. *Journal of Epidemiology and Biostatistics*, *5*(3), 153–160.

Appendix A.

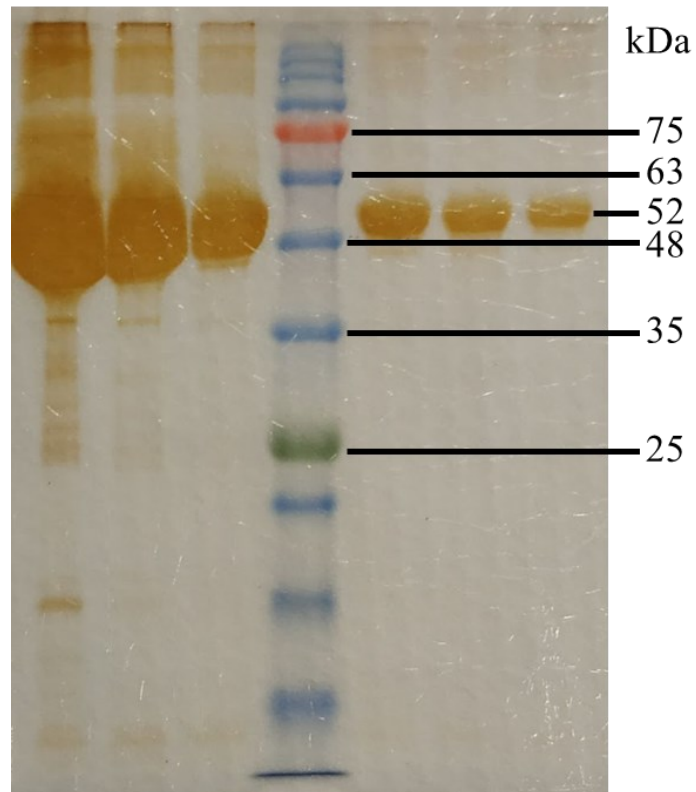## Supplementary material for Chapter 2

Figure A.1. **Cytochrome P450 purification - fragments (47 kDa protein + 5 kDa His-tag) from Nickel column. The first three lanes is unpurified protein, fourth lane is the prestained protein ladder (marker), and the other three lanes is the purified protein (52 kDa).**
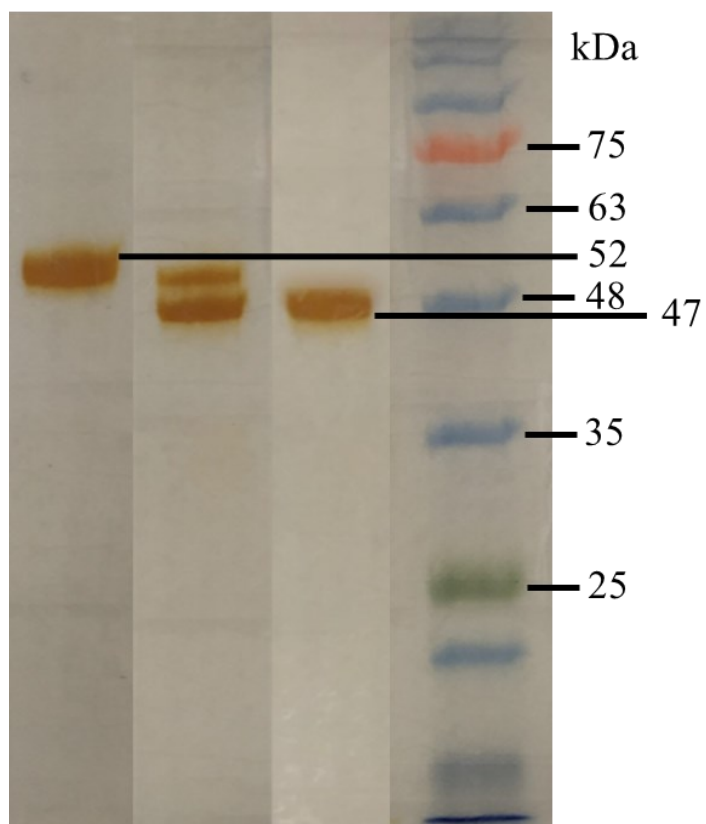
Figure A.2. **Cytochrome P450 cleaved with Factor Xa protease. First lane is the uncleaved protein (52 kDa), second lane is incomplete cleavage after 24 hours, third lane is the fully cleaved protein (47 kDa) after ~32-36 hours and forth lane is the prestained protein ladder (marker).**
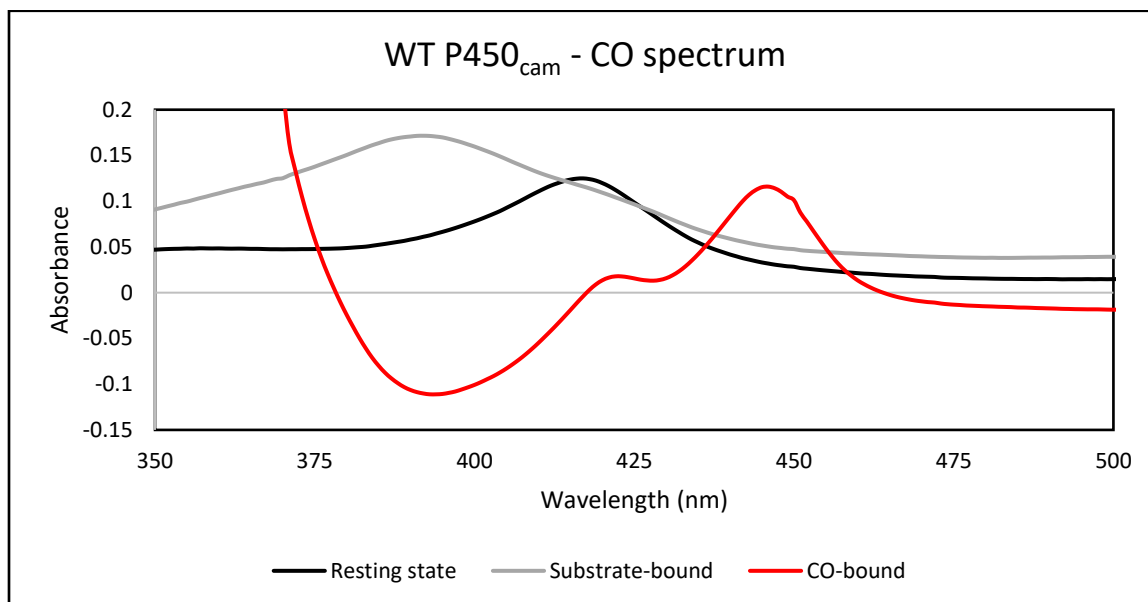

Figure A.3. **Example of carbon monoxide spectrum with WT P450cam.**

Table A.1. Dixon's Q parameter and related subrange ratios for different confidence levels (Rorabacher, 1991).

N	Qcrit 90% CL	Qcrit 95% CL	Qcrit 99% CL
3	0.941	0.970	0.994
4	0.765	0.829	0.926
5	0.642	0.710	0.821

Table A.2. Experimental Q value (Q_{exp}) for WT P450$_{cam}$. N/A is not applicable.

Substrates/ Concentration	50 μM	100 μM	200 μM	300 μM	400 μM	500 μM
ES diol	N/A	N/A	N/A	N/A	N/A	N/A
ES lactone	N/A	N/A	0.019	0.667	0.309	0.951
ES ether	N/A	N/A	0.845	0.876	0.734	0.464
ES sulfate	N/A	N/A	0.376	0.184	0.818	0.507
ES α:β	N/A	N/A	N/A	0.167	0.431	0.056
Heptachlor	N/A	N/A	0.737	0.291	0.229	0.509

Table A.3. Experimental Q value (Q_{exp}) for ES6. N/A is not applicable.

Substrates/ Concentration	50 μM	100 μM	200 μM	300 μM	400 μM	500 μM
ES diol	N/A	0.190	0.704	0.619	0.676	0.424
ES lactone	N/A	N/A	0.678	0.656	0.537	0.288
ES ether	0.486	0.361	0.064	0.394	0.208	0.990
ES sulfate	0.048	0.118	0.938	0.280	0.134	0.213
ES α:β	0.891	0.189	0.511	0.851	0.840	0.566
Heptachlor	0.115	0.054	0.826	0.678	0.811	0.634

Table A.4. Experimental Q value (Q_{exp}) for ES7. N/A is not applicable.

Substrates/ Concentration	50 μM	100 μM	200 μM	300 μM	400 μM	500 μM
ES diol	N/A	0.175	0.812	0.684	0.544	0.486
ES lactone	N/A	N/A	0.235	0.927	0.582	0.087
ES ether	0.342	0.978	0.226	0.532	0.523	0.438
ES sulfate	0.589	0.957	0.383	0.830	0.011	0.494
ES α:β	0.745	0.266	0.546	0.377	0.477	0.715
Heptachlor	0.452	0.110	0.675	0.679	0.290	0.009

Table A.5. Conformational energies (E_{conf}) for WT P450$_{cam}$, ES6 and ES7.

Substrate	E_{conf} (kcal/mol)		
	WT P450$_{cam}$	ES6	ES7
ES diol	148.0	139.1	136.4
ES lactone	101.8	95.26	96.40
ES ether	138.1	150.0	141.5
ES sulfate	205.3	181.8	170.3
ES α:β	116.9	126.5	116.9
Heptachlor	155.1	169.9	149.8

polar — sidechain acceptor — solvent residue — nonconserved
acidic — sidechain donor — metal complex — nonpresent
basic — backbone acceptor — solvent contact — inconsistent
greasy — backbone donor — metal/ion contact — arene-arene
proximity — ligand — receptor — arene-H
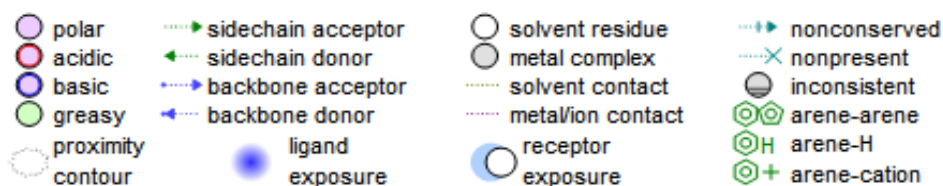contour — exposure — exposure — arene-cation

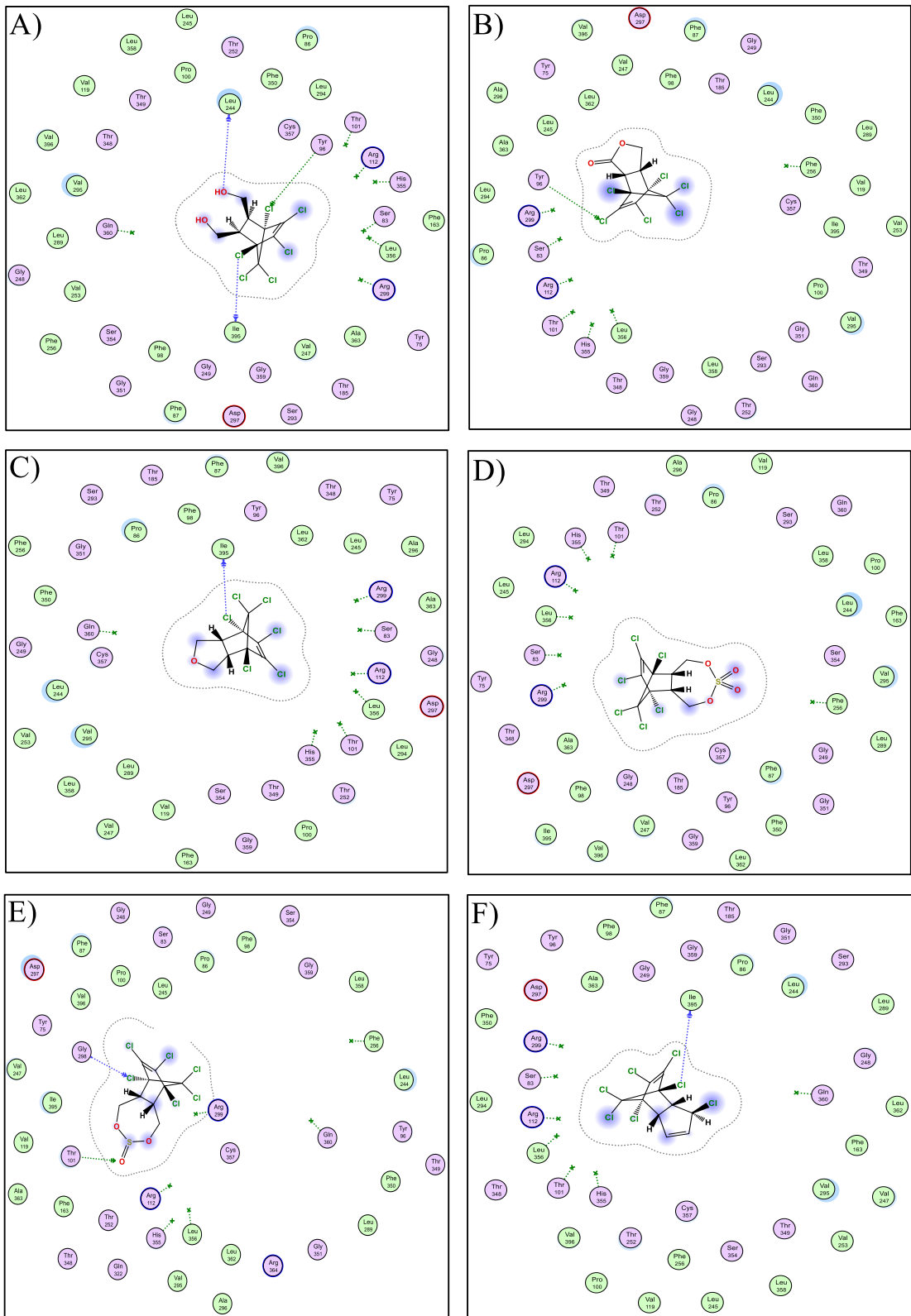**Figure A.4.** Ligand interaction indicators.

Figure A.5. Ligand interactions between WT and the substrates. A) ES diol, B) ES lactone, C) ES ether, D) ES sulfate, E) ES α:β and F) Heptachlor.

Figure A.6. Ligand interactions between ES6 and the substrates. A) ES diol, B) ES lactone, C) ES ether, D) ES sulfate, E) ES α:β and F) Heptachlor.

Figure A.7. Ligand interactions between ES7 and the substrates. A) ES diol, B) ES lactone, C) ES ether, D) ES sulfate, E) ES α:β and F) Heptachlor.
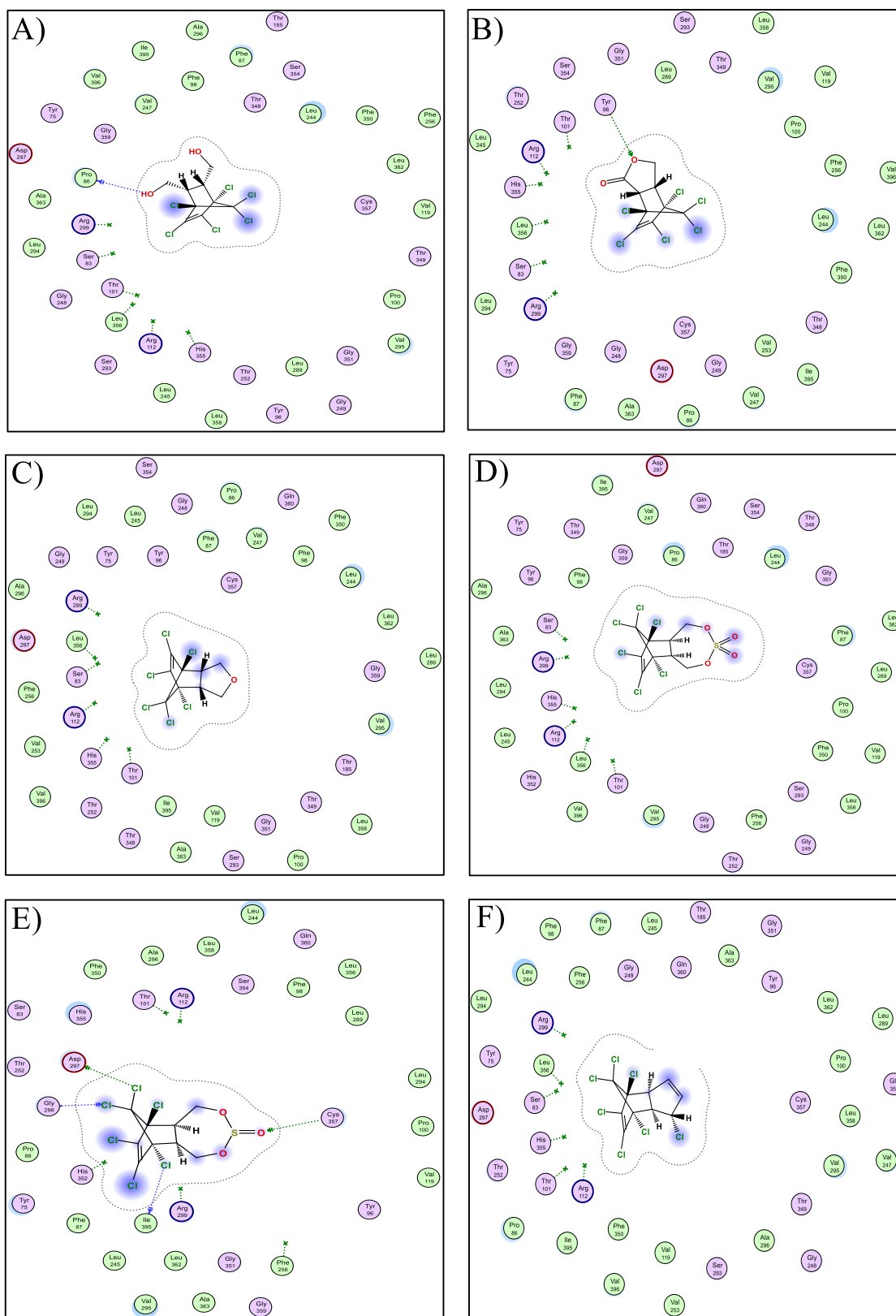
Table A.6.   Amino acid abbreviations and letter codes.

| Amino acid	1 letter code	3 letter codes	Amino acid	1 letter code	3 letter codes
Alanine	A	Ala	**Methionine**	M	Met
Cysteine	C	Cys	**Asparagine**	N	Asn
Aspartic acid	D	Asp	**Proline**	P	Pro
Glutamic acid	E	Glu	**Glutamine**	Q	Gln
Phenylalanine	F	Phe	**Arginine**	R	Arg
Glycine	G	Gly	**Serine**	S	Ser
Histidine	H	His	**Threonine**	T	Thr
Isoleucine	I	Ile	**Valine**	V	Val
Lysine	K	Lysine	**Tryptophan**	W	Trp
Leucine	L	Leucine	**Tyrosine**	Y	Tyr

Appendix B.

Supplementary material for Chapter 3
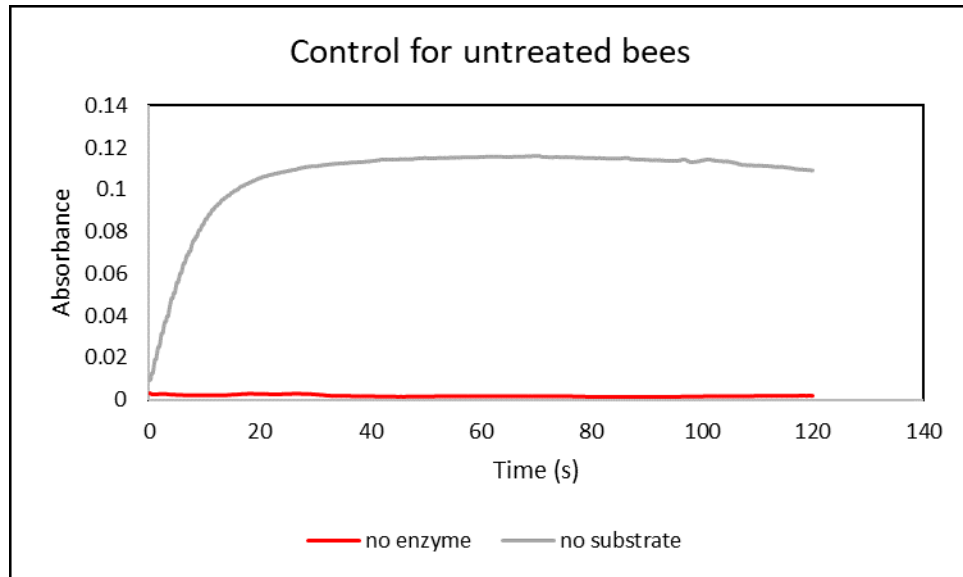
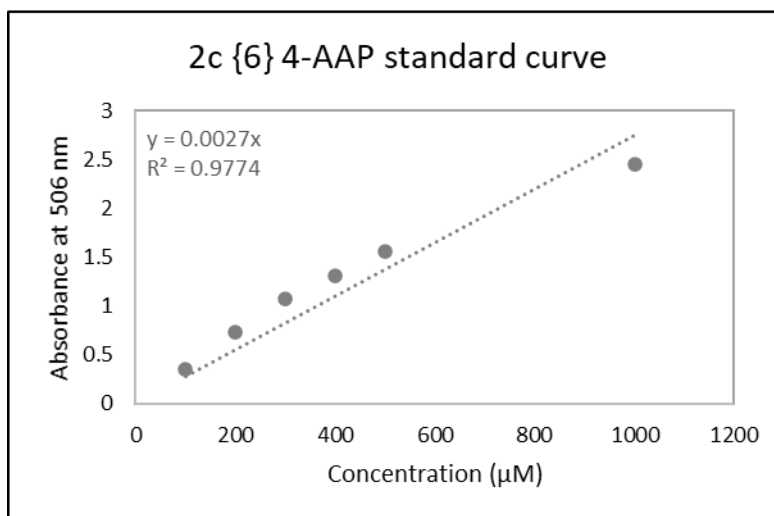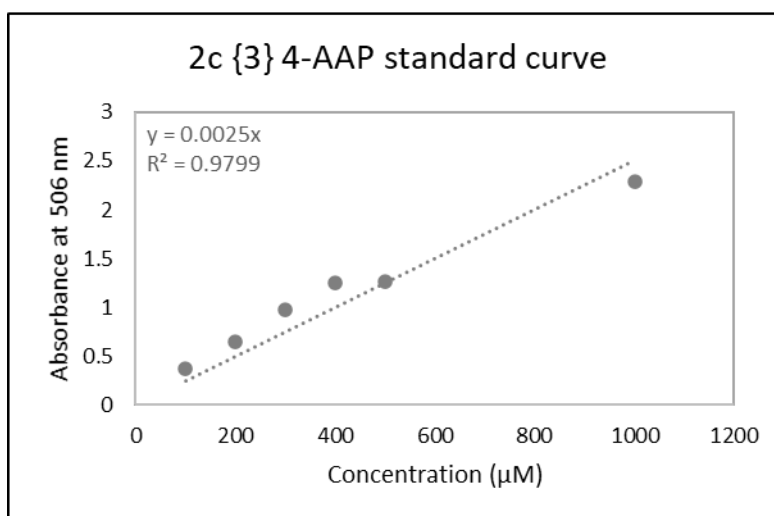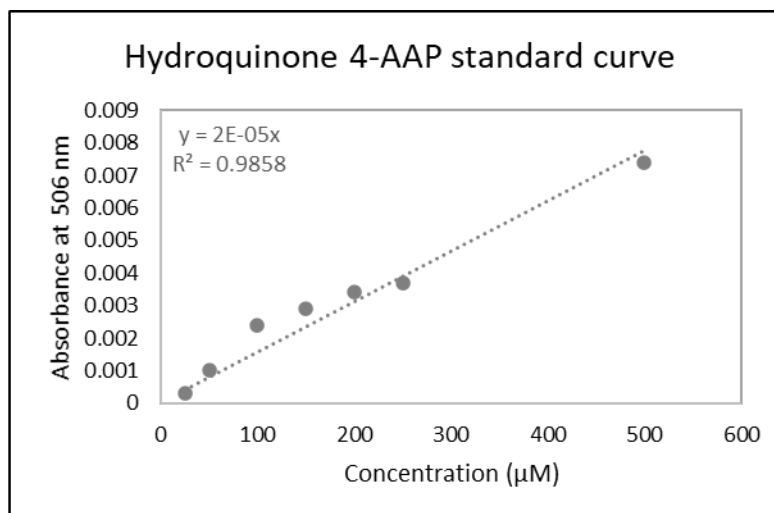**Figure B.1.   Control without enzyme and without substrate for the untreated bees.**

Figre B.2. **4-AAP assay standard curves for the dealkylated products.**

Table B.1. Retention times (RT) and molecular weight (MW) of the dialkoxybenzene compounds and their dealkylated products.

Compound	RT (min)	MW (g/mol)
HQ	9.282	110
2c{*3*}	10.964	152
2c{*6*}	10.946	150
3c{*3,6*}	12.479	192
3c{*3,3*}	12.561	194
3c{*6,6*}	12.394	190

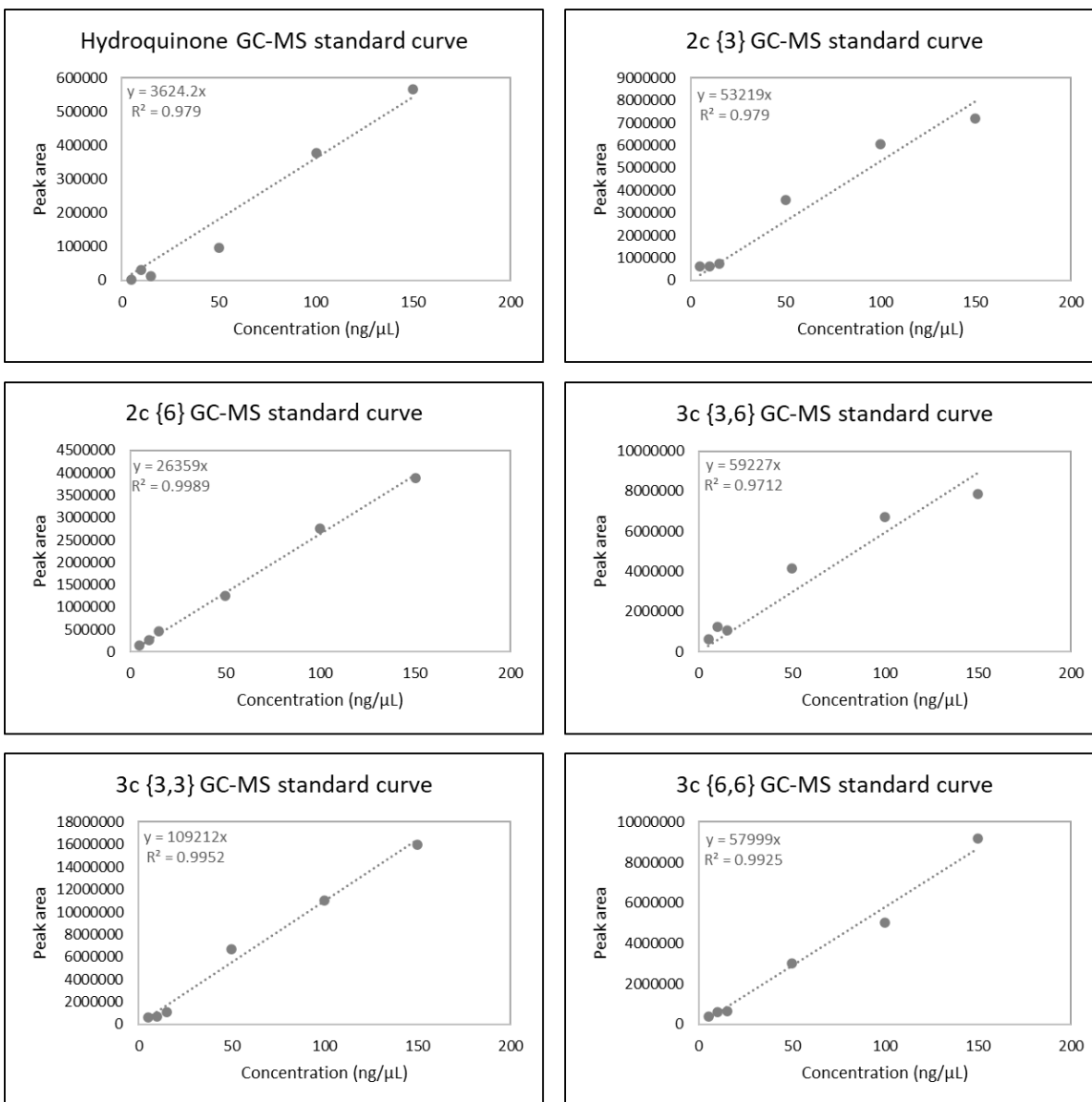**Figure B.3.** **GC-MS assay standard curves for the the dialkoxybenzene compounds and their dealkylated products.**

Table B.2. GC-MS peak area and concentration (ng/µL) for 3c{3,6} and its products. N/D is not detected.

Assay conc. (µM)	Area 3c{3,6}	3c{3,6} conc. (ng/µL)	Area 2c{3}	2c{3} conc. (ng/µL)	Area 2c{6}	2c{6} conc. (ng/µL)	Area HQ	HQ conc. (ng/µL)
10	20707	0.3496	189	0.0036	180	0.0068	196	0.0541
15	39262	0.6629	235	0.0044	145	0.0055	296	0.0817
20	82607	1.3948	95	0.0018	67	0.0025	242	0.0668
50	87538	1.4780	61	0.0011	51	0.0019	N/D	N/D
100	279402	4.7175	90	0.0017	85	0.0032	N/D	N/D
150	478132	8.0729	120	0.0023	97	0.0037	N/D	N/D

Table B.3. GC-MS peak area and concentration (ng/µL) for 3c{3,3} and its products. N/D is not detected.

Assay conc. (µM)	Area 3c{3,3}	3c{3,3} conc. (ng/µL)	Area 2c{3}	2c{3} conc. (ng/µL)	Area 2c{6}	2c{6} conc. (ng/µL)	Area HQ	HQ conc. (ng/µL)
10	24339	0.223	76	0.0014	N/D	N/D	N/D	N/D
15	54384	0.498	24	0.0005	N/D	N/D	N/D	N/D
20	39736	0.364	48	0.0009	N/D	N/D	N/D	N/D
50	220250	2.017	34	0.0006	N/D	N/D	N/D	N/D
100	451369	4.133	58	0.0011	N/D	N/D	N/D	N/D
150	959421	8.785	37	0.0007	N/D	N/D	N/D	N/D

Table B.4. GC-MS peak area and concentration (ng/µL) for 3c{6,6} and its products. N/D is not detected.

Assay conc. (µM)	Area 3c{6,6}	3c{6,6} conc. (ng/µL)	Area 2c{3}	2c{3} conc. (ng/µL)	Area 2c{6}	2c{6} conc. (ng/µL)	Area HQ	HQ conc. (ng/µL)
10	1605	0.028	N/D	N/D	387	0.0147	N/D	N/D
15	1661	0.029	N/D	N/D	183	0.0069	N/D	N/D
20	10362	0.179	N/D	N/D	138	0.0052	N/D	N/D
50	39128	0.675	N/D	N/D	271	0.0103	N/D	N/D
100	110205	1.900	N/D	N/D	93	0.0035	N/D	N/D
150	115331	1.988	N/D	N/D	23	0.0009	N/D	N/D

Table B.5. GC-MS peak area, concentration (ng/µL) and recovery yield for HQ, 2c{3} and 2c{6}.

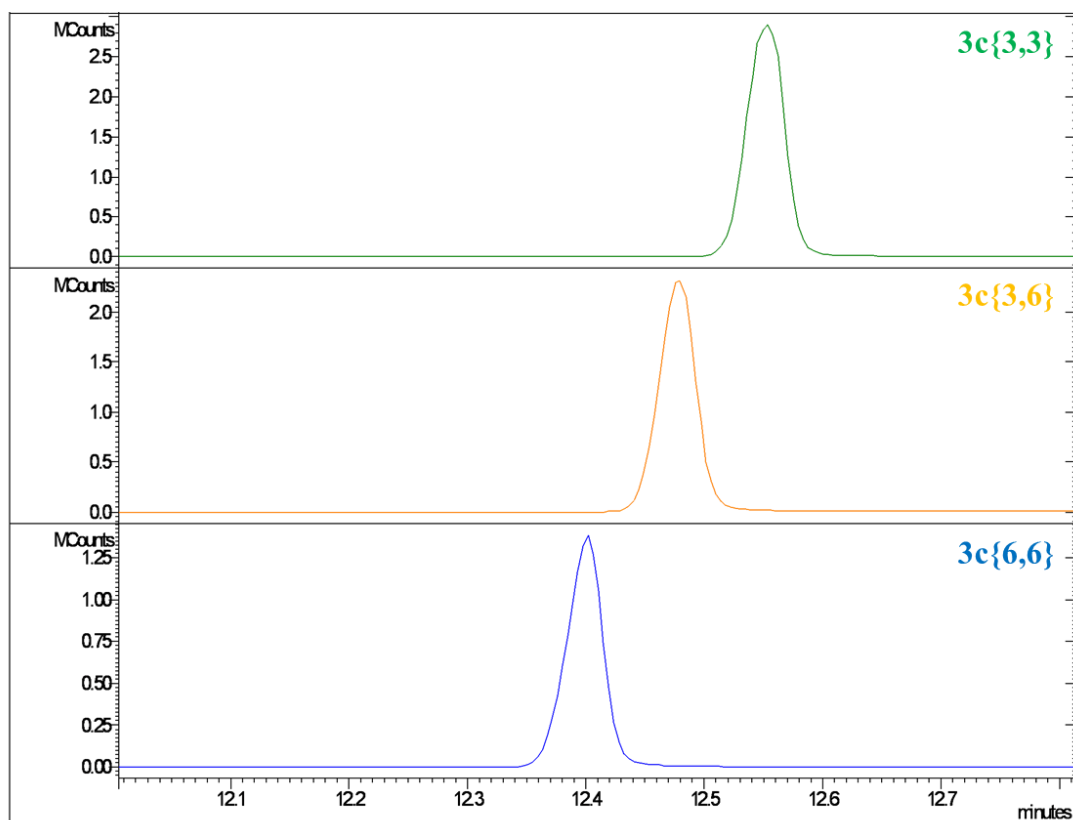| Controls	Area	Concentration (ng/µL)	Added (nmol)	Recovered (nmol)	Lost (nmol)	Recovery yield (%)
HQ 50 µM	137	0.04	25	0.2	24.8	0.7
HQ 200 µM	1535	0.42	100	1.9	98.1	1.9
2c{3} 50 µM	72393	1.36	25	4.5	20.5	17.9
2c{3} 200 µM	477953	8.98	100	29.5	70.5	29.5
2c{6} 50 µM	25204	0.96	25	3.2	21.8	12.7
2c{6} 200 µM	248918	9.44	100	31.5	68.5	31.5

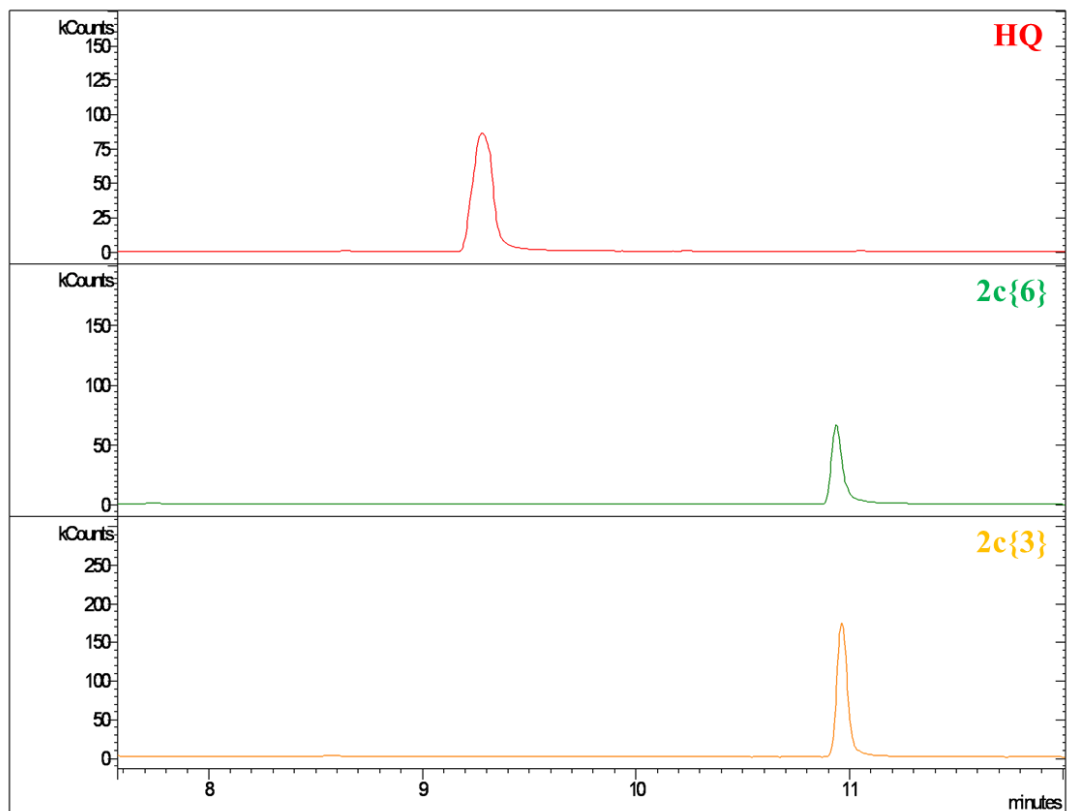**Figure B.4.   Chromatograph for compounds 3c{3,6}, 3c{3,3} and 3c{6,6}.**

Figure B.5.   Chromatograph for HQ, 2c{3} and 2c{6} products.